Defining early $CD8^+$ T cell responses during acute and chronic viral infection using single-cell RNA-seq analysis

by

Nyambura Irungu Kahia

A thesis submitted to the Faculty of Graduate Studies of The University of Manitoba in partial fulfilment of the requirements of the degree of

Master of Science

Department of Immunology

University of Manitoba

Winnipeg, Manitoba

Dedication

I dedicate this thesis to myself for my determination to see it through until the end. This thesis is a true testament to my perseverance and commitment.

I would like to express my deepest gratitude to my stretcher-bearers. Their unwavering belief in me helped me get to the finish line. Kathleen Glover, Rilwan Azeez, and Kristy Caroll, thank you for being there for me every step of the way. I am forever grateful.

Table of Contents

Acknowledgements

I am grateful to all who have contributed to the successful completion of this thesis.

First, I thank God through whom all things are possible. I thank my supervisor Dr. Janilyn Arsenio, for her invaluable guidance, support, and encouragement throughout my research project. I am grateful for the time and effort she put into helping me develop my research skills, providing critical feedback, and inspiring me to strive for excellence.

I thank my thesis advisory committee: Dr. Lyle McKinnon and Dr. Thomas Murooka, for their support and valuable feedback, which were instrumental in shaping my research project.

I thank the faculty of Department of Immunology for teaching courses that improved my understanding of my research project. I thank all the administrative assistants who facilitated the progression and successful completion of my program.

I thank my colleagues and friends in the Department of Immunology and Manitoba Centre for Proteomics and Systems Biology, for their insightful discussions, constructive criticism, and support during my research work. My sincere gratitude goes to my family and close friends for their unwavering love, support, and encouragement throughout my academic journey. Their constant motivation and belief in me kept me going even when the going got tough.

I am grateful for the financial support provided by my supervisor though her Canada Research Chairs funding, Research Manitoba and Rady Faculty of Health Sciences, which allowed me to pursue my research project.

I am grateful to all those who have contributed to the successful completion of this thesis. Your support and encouragement have been instrumental in my academic and professional development.

Abstract

CD8$^+$ T cells are key in mediating immune responses to viral infections. Viral infections can be acute, in which the infection is resolved, or chronic, in which antigen persists in the body. Several studies have illustrated that CD8$^+$ T cells adopt distinct functional states in each infection type. In acute infections, naïve CD8$^+$T cells become activated, undergo vigorous clonal expansion and differentiate into cytotoxic CD8$^+$ T cells (CTLs). CTLs induce apoptosis of virus-infected cells by releasing cytolytic molecules such as granzymes, defensins and perforins. Following resolution of the infection, majority of CTLs undergo apoptosis, whereas 5-10% are maintained as memory CD8$^+$ T cells. In chronic infections, activated CD8$^+$ T cells adopt an altered state known as exhaustion. Exhausted CD8$^+$ T cells lose effector functions and show high expression of inhibitory receptors such as PD-1. Several studies have characterized CD8$^+$ T cell exhaustion at late time-points after a persistent infection has already been established. Recent studies have begun to demonstrate that CD8$^+$ T cell exhaustion may be specified during earlier phases of a developing chronic infection (1), as early as after the first cell division following T cell activation. However, these studies do not address the effect of biological sex on early CD8$^+$ T cell responses to chronic infection. Sex differences in infectious diseases susceptibility and outcomes are well-appreciated. However, the cellular and molecular mechanisms underlying sex differences are understudied. The role of sex bias in the development of CD8$^+$ T cell exhaustion and in the molecular programs underlying CD8$^+$ T cell responses to acute and chronic viral infections remains undefined. This study, therefore, set out to investigate early and sex-based differences in the transcriptional profiles of CD8$^+$ T cells that underlie their responses to acute versus chronic viral infection.

The mouse model of acute and chronic lymphocytic choriomeningitis virus infection was used to comparatively analyze single antigen-specific $CD8^+$ T cell transcriptional signatures during acute versus chronic infection at multiple time-points post-infection. Next sequencing (NGS) was coupled with bioinformatics-based approaches to analyze our single-cell RNA sequencing (scRNA-seq) data. Our results reveal an early transcriptional divergence of $CD8^+$ T cells responding to acute versus chronic viral infection. We show that there are sex-specific differences in the transcription profiles of single $CD8^+$ T cells responding to acute versus chronic viral infection at an early time-point and at the clonal expansion phase after primary infection. We demonstrate sex differences in the expression of pro-inflammatory cytokine expression as well as in the clonal expansion of antigen-specific $CD8^+$ T cells between the two infection types. We further identify potential sex-specific candidate regulators of $CD8^+$ T cell differentiation. These findings suggest that the molecular mechanisms governing $CD8^+$ T cell responses to acute versus chronic viral infection are differentially regulated between males and females, which can occur during early phases of infection. Overall, the findings in this thesis uncover novel insights into how and when sex differences in $CD8^+$ T cell immunity to acute and chronic viral infection arises and provides the foundation for future sex-based mechanistic studies of $CD8^+$ T cell differentiation.

List of Figures

List of Abbreviations

T cell Receptors (TCRs)

Major Histocompatibility Complex class I (MHC-I)

Major Histocompatibility Complex class II (MHC-II)

Medullary thymic epithelial cells (mTECs)

Antigen presenting cells (APCs)

Interleukin-2 (IL-2)

Interleukin-1(IL-12)

Interleukin-7 receptor α (IL-7Rα)

Interferon-γ (IFN-γ)

Interferon-γ receptor (IFN-γR)

T-box transcription factor TBX21(T-bet)

Interferon regulatory factor 4 (IRF4)

T cell Factor 1 (TCF-1)

Cytotoxic T lymphocytes (CTLs)

Tumor Necrosis Factor α (TNF-α)

TNF-α receptor (TNFR2)

Memory precursor effector cells (MPECs)

Killer cell lectin-like receptor G1 (KLRG1)

Eomesodermin (Eomes)

Lymphocytic choriomeningitis virus (LCMV)

Programmed cell death 1 (PD-1)

Lymphocyte-activation gene 3 (*lag3*)

T cell immunoglobulin and mucin-domain containing-3 (Tim-3)

Inhibitory receptors (IR)

Single-cell RNA sequencing (scRNA-seq)

Next Generation Sequencing (NGS)

Systemic lupus erythematosus (SLE)

X chromosome inactivation (XCI)

Estradiol (E2)

Dihydrotestosterone (DHT)

X-inactive specific transcript (XIST)

C-X-C chemokine receptor type 3 (CXCR3)

Pattern recognition receptors (PRRs)

Plasmacytoid dendritic cells (pDCs)

Estrogens receptors (ER)

Androgen receptors (AR)

Progesterone receptors (PR)

Carboxyfluorescein diacetate succinimidyl ester (CFSE)

Hours post-infection (hpi)

Days post-infection (dpi)

Intravenously(i.v)

Intraperitoneally (i.p)

Plaque-forming units (pfu)

Gel-emulsion (GEM)

Differentially expressed genes (DEGs)

Integrin-Associated Protein (IAP)

Female donor cells-to-female recipients (F-F)

Male donor cells-to male recipients (M-M)

Animal Care Committee (ACC)

Supramolecular activation clusters (SMACs)

central SMAC (cSMAC)

peripheral SMAC (pSMAC)

lymphocyte function-associated antigen (LFA-1)

distal SMAC (dSMAC)

1 Introduction

1.1 $CD8^+$ T cell Development

$CD8^+$ T cells play a crucial role in cell-mediated immunity by recognizing and eliminating tumor cells or cells infected with intracellular pathogens such bacteria and virus. The development of $CD8^+$ T cells is a complex process that involves various stages of differentiation and selection. $CD8^+$ T cells develop from common lymphoid progenitor stem cells of the red bone marrow. Under the influence of chemotactic agents and thymic factors such as thymotaxin, thymosin and thymopoietin, progenitor T cells leave the bone marrow for the thymus where they undergo maturation. During thymic maturation, T cells progress through distinct stages characterized by expression of antigen receptor genes, CD4 and CD8 co-receptor molecules, and distinct location in the thymus. The earliest immigrants to the thymus do not express T cell Receptors (TCRs), CD4 or CD8 molecules. Thymocytes, which are developing T cells in the thymus, initially populate the outer cortex. Here, they undergo proliferation, rearrangement of TCR genes and surface expression of TCR, CD3, CD4 and CD8 molecules. Within the cortex, precursor T cells in undergo selection processes that further drive their maturation. Positive selection occurs in the thymic cortex, where thymic epithelial cells present self-peptides on major histocompatibility complex class I (MHC-I) molecules to T cell precursors. At the same time, bone marrow derived dendritic cells and bone marrow derived macrophages in the thymus present self-peptides on major histocompatibility complex class II (MHC-II) molecules to T cell precursors. The interaction of immature thymocytes with cortical epithelial cells and antigen presenting cells (APCs) transduces a survival and differentiation signal, protecting against cell death. Thymocytes with TCRs that

weakly bind to self-peptide-self-MHC molecules survive. Conversely, precursor T cells with TCRs that are unable to engage the peptide-MHC ligand on fail to receive a survival signal and die (2,3).

Thymocytes that survive positive selection have TCRs with varying affinities for self-antigen presented by self-MHC molecule. Most negative selection occurs in the thymic medulla and is mediated by thymic dendritic cells and medullary thymic epithelial cells (mTECs). mTECs transcribe genes that are normally expressed in peripheral tissues(3). Specialized APCs having class I and class II MHC molecules present self-antigens derived from widely expressed protein antigens including proteins restricted to specific tissues(2).

Negative selection occurs when the TCR of a thymocyte recognizes a peptide-MHC ligand with high affinity, signalling the cell for apoptosis. This process eliminates potentially self-reactive thymocytes and generates a repertoire of peripheral T cells that is tolerant to self-antigens(4), thus preventing autoimmunity. Negative selection can occur before or after positive selection and in thymocytes at all stages of development (3).

Following positive selection, developing thymocytes in the medulla mature into either $CD4^+$ or $CD8^+$ T cells. Interaction with a peptide-MHC class I ligand positively selects for MHC class-I-restricted, $CD8^+$ T cells, whereas recognition of a peptide-MHC class II ligand signals for the development of MHC class-II-restricted, $CD4^+$, helper T cells (3). After screening and maturation in the spleen, $CD8^+$ T cells leave the thymus and enter circulation as resting cells in the G0 stage of the cell cycle. Naïve $CD8^+$ T cells recirculate between the blood and lymph system, residing in secondary lymphoid organs/tissues such as the spleen and lymph nodes.

1.2 $CD8^+$ T cell Activation

$CD8^+$ T cell activation is an intricate process involving various steps such as, antigen presentation, co-stimulation, signal transduction, and regulation. Activation is initiated when $CD8^+$ T cells identify antigens presented by MHC-I molecules on the surface of APCs, tumor cells or cells infected by virus or intracellular bacteria. After interacting with infected or tumor cells, $CD8^+$ T cells navigate across the surface, converting mechanical energy into signals that activate their TCR complex. Once activated, $CD8^+$ T cells establish immunological synapses (IS) with tumor or infected cells, where their TCR and CD8 co-receptor interact with the presented peptide and the MHC-α subunit, respectively, to confirm the tumor or infected cell's nature.

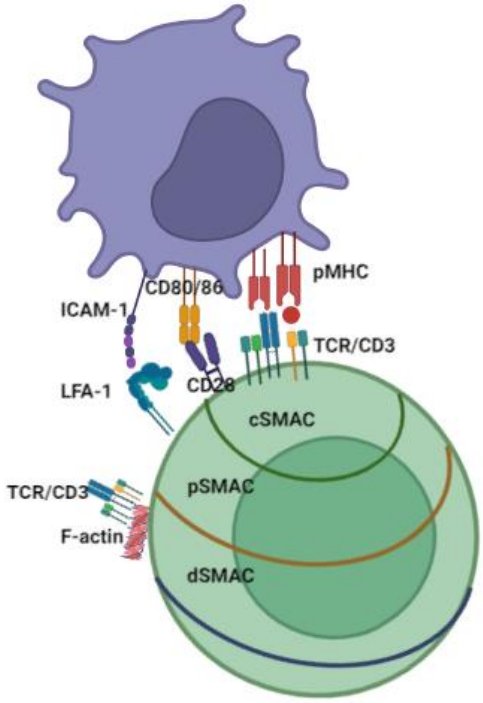

Figure 1. Immunological synapse assembly. The IS features the central supramolecular activation cluster (cSMAC) characterized by the presence of TCRs and TCR-associated proteins such as the co-stimulatory receptor CD28, the peripheral SMAC (pSMAC) enriched in the integrin LFA-1 and the distal SMAC (dSMAC) enriched in TCR-CD28 microclusters that move centripetally driven by F-actin. Image was created in Biorender.

Formation of the immunological synapse (IS) necessitates two essential components: the interaction between T-cell receptor and peptide-major histocompatibility complex, along with the accumulation of co-receptors, adhesion molecules, and signaling and cytoskeletal

elements at the contact area between the T cell and APC. Once fully formed, the IS exhibits a distinctive "bull's eye" structure characterized by concentric domains called supramolecular activation clusters (SMACs). These SMACs differ in their molecular composition and function. The central SMAC (cSMAC) is primarily enriched in TCRs and TCR-associated proteins, and it is surrounded by the peripheral SMAC (pSMAC), which is enriched in integrins like lymphocyte function-associated antigen (LFA-1) and cytoskeleton-associated proteins. Surrounding the pSMAC is the distal SMAC (dSMAC), which is enriched in F-actin as well as molecules that are excluded from the center of the IS (5) (refer to Figure 1). Before the killing mechanism is triggered, a co-stimulatory signal from the CD28 co-receptor is necessary. CD28 receptors on $CD8^+$ T cells interact with CD80/B7.1 or CD86/B7.2, which are highly expressed on APCs, macrophages and activated B cells. This secondary signal prevents $CD8^+$ T cells from responding to self-antigens, thus minimizing the risk of tissue damage and autoimmunity (6).

Assembly of the $CD8^+$ TCR complex and CD28 co-stimulation initiate a cascade of intracellular events that result in the transcription of genes driving the cell cycle. The cell enters the G_1 phase of the cell cycle, increases transcription of the *il-2* gene and the *α* chain of the high affinity IL-2 receptor (CD25). Consequently, *il-2* mRNA transcription increases, and its stabilization amplifies IL-2 production by about 100-fold in the activated T cell. IL-2, a cytokine and potent T cell mitogen, plays a critical role in regulating $CD8^+$ T cell proliferation and differentiation during the expansion phase. *In vivo* mice studies have demonstrated that blocking IL-2 signalling can lead to reduced $CD8^+$ T cell proliferation. While TCR stimulation alone can induce $CD8^+$ T cell proliferation, the absence of IL-2 signaling results in suboptimal expansion and slower progression through the cell cycle(7).

While the initial division of Ag-specific $CD8^+$ T cells following priming can be IL-2 independent, sustained exposure to IL-2 is crucial for prolonged expansion of $CD8^+$ T cells.

Deprivation of IL-2 leads to decreased cell viability, loss of CD25 expression, and reduced cellular protein content, including key regulators of the cell cycle such as cyclin D2, cyclin D3, cyclin A, cyclin B1, cyclin B2, CDK4, CDK6, CDK1, p15, and p21. *In vivo* mice studies have shown that presence of IL-2 in culture reduces the minimum threshold of TCR signaling required to initiate cell cycle entry(7). About 48 hours after activation, the naïve T cell enlarges into a blast cell followed by repeated rounds of cell division. The secretion of IL-2 and subsequent binding to CD25 induces the activated naïve T cell to proliferate and differentiate (6).

1.3 $CD8^+$ T cell Differentiation

Distinct $CD8^+$ T cell subsets with specialized functions are crucial for a robust immune response. Recent studies employing single-cell adoptive transfer and 'genetic barcoding' approaches have unveiled the remarkable ability of a single-$CD8^+$ T cell to generate diverse progeny with distinct functions(8) (9). How a single activated T lymphocyte yields different fated progenies including effector and memory, and the time at which those differentiation pathways diverge, has remained controversial in the field. Proposed models of $CD8^+$ T cell differentiation have investigated the influence of TCR signal-strength, environmental cues, and transcriptional changes on T cell differentiation.

One model, known as the separate pre-cursor model, proposes that naive T cells possess inherent programming acquired during their development in the thymus. This programming guides their differentiation into specific states upon activation. However, limited empirical evidence currently supports this model (10). On the contrary, single cell profiling studies employing 'genetic barcoding' approaches unveiled that a single $CD8^+$ T cell is multipotent, and a wide range of diversity could develop out of a single precursor cell,

including different types of effector and memory T cells under different infection conditions including *L. monocytogenes* and influenza A and tumor challenge.

An alternative possibility is the linear differentiation path model, which proposes that an activated naive $CD8^+$ T cell and progeny progress along a linear differentiation path, initially becoming effector cells, and a subset of those cells later acquiring the memory fate (11,12). According to this decreasing-potential model, effector T cells acquire diverse differentiation states based on the collective signals they encounter throughout an infection. Repetitive exposure to antigenic stimulation, along with additional signals like IL-2 and interleukin-12(IL-12), enhances effector T cell proliferation and terminal differentiation. While these cells retain their effector functions and cytolytic capacity, they lose certain properties characteristic of memory cells, including enhanced longevity, proliferative potential, and expression of interleukin-7 receptorα (IL-7Rα). This linear progression model offers a framework for the generation of a diverse spectrum of effector T cells at various differentiation states, based on the cumulative history of signals encountered during infection. This model can be viewed as one of late divergence in that diversification into distinct T cell fates occurs in later stages of the immune response(10).

The signal-strength model proposes that the strength of TCR and cytokine signals received during initial priming specifies whether the progeny of an activated naïve T cell adopts a terminal effector or memory cell fate. The generation of heterogeneous populations of effector cells is influenced by the overall strength of three key signals encountered during the early priming of T cells: antigen (signal 1), co-stimulation (signal 2), and pro-inflammatory cytokines (signal 3). When these signals combine, a robust and potent signal can promote extensive clonal expansion and play a crucial role in selecting T cells capable of forming long-lasting memory cells. However, an excessive magnitude of this strong signal can also induce

terminal differentiation of effector T cells. This model diverges from the decreasing-potential hypothesis as it allows for the early specification of different cell fates in a more varied manner, depending on the intensity of the received signals, rather than following a linear, stepwise progression driven solely by successive rounds of stimulation(10).

The asymmetric cell division model is another early divergence model which proposes that terminal effector and memory T cell fates can be can arise from a single precursor T cell, and can be identified as early as the first cell division(13). The daughter cell that inherits the immunological synapse between a T cell and an APC, receives stronger TCR and co-stimulatory signals. This enhanced signaling is attributed to close proximity to the APC and additional signals mediated by pro-inflammatory cytokines like IL-12 and IFN-γ (10).

During *Listeria monocytogenes* infection in mice, daughter cells proximal to the immunological synapse ('proximal daughter cells') and distal to the immunological synapse ('distal daughter cells') adopt different fates, owing to asymmetric cell division. The most proximal daughter cells more closely resembled short-lived effector $CD8^+$ T cells, while most distal daughter cells more closely resembled central memory $CD8^+$ T cells (TCM) (14). Recent studies have revealed that exhausted-like $CD8^+$ T cells can be identified as early as the first cell division chronic LCMV infection in mice(1,15).

Furthermore, early fate divergence in lymphocytes could be due to unequal inheritance of certain cell fate determinants by daughter cells following cell divisions. These include interferon-γ receptor (IFN-γR), IL-2Rα and the transcription factors such as T-box transcription factor TBX21(T-bet), interferon regulatory factor 4 (IRF4) and T cell Factor 1 (TCF-1) (16).
The above models are not mutually exclusive and can be integrated in the understanding of $CD8^+$ T cell differentiation.

1.4 Role of $CD8^+$ T cells in viral infections

An effective response to viral infection requires the differentiation of a naïve $CD8^+$ T cell into a heterogeneous pool of $CD8^+$ T cell subsets with distinct functions. Viral infections may be acute, in which the infection is resolved, or chronic, where viral antigens persist in the body, thus the infection is not cleared. Several studies have illustrated that $CD8^+$ T cells adopt distinct functional states in each infection type(17,18).

1.4.1 $CD8^+$ T cell response in acute infection

During acute viral infections, naïve $CD8^+$ T cells in secondary lymphoid organs are activated when their TCRs recognize foreign viral antigens presented by class I MHC molecules on APCs like macrophages and dendritic cells (DCs). In addition to TCR stimulation, the activation of naïve $CD8^+$ T cells requires co-stimulation via CD28 signaling and production of pro-inflammatory cytokine (18). Once activated, $CD8^+$ T cells undergo vigorous clonal expansion and differentiate into short-lived effector $CD8^+$ T cells, also known as terminal effectors or cytotoxic T lymphocytes (CTLs). These effector cells induce apoptosis of virus-infected cells by releasing cytolytic molecules like granzymes, defensins and perforins. Perforins create pores in the membrane of the target cell allowing granzymes to enter the infected cell. Granzymes cleave proteins inside the cell, effectively shutting down production of viral proteins and ultimately resulting in apoptosis of the target cell (19).

In addition to eliminating virus-infected cells by releasing cytolytic molecules, CTLs secrete cytokines, interferon-γ (IFN-γ) and Tumor Necrosis Factor α (TNF-α). These cytokines not only restrict viral replication in infected cells but also induce anti-viral responses in neighbouring cells. Typically, antiviral $CD8^+$ T cells produce cytokines in a hierarchical manner,

with the majority producing IFN-γ, and a subset of those producing TNF-α (20). IFN-γ signalling via the IFN-γ receptor (IFNγR) directly inhibits viral replication and enhances the expression of MHC class I proteins on infected cells. Increased MHC Class I expression on infected cells amplifies the likelihood of recognition as target cells for cytotoxic attack(21). TNF-α exerts its effects through the predominant TNF-α receptor 2(TNFR2), which is expressed on immune cells, including $CD8^+$ T cells. The interaction between TNF-α and TNFR2 provides early costimulatory signals during $CD8^+$ T cell activation. Furthermore, TNF-α signalling induces the expression of granzyme B in $CD8^+$ T cells, when a co-stimulation signal from with CD28/CD86 interactions is provided simultaneously, thereby reinforcing the cytotoxic activity (20). Once the pathogen is cleared, there is a contraction phase where most (about 90-95%) of effector $CD8^+$ T cells undergo apoptosis, while a small population (5-10%) survives and transitions into memory T cells. Memory $CD8^+$ T cells are sustained long-term via homeostatic proliferation and respond more vigorously than naïve cells upon re-infection.

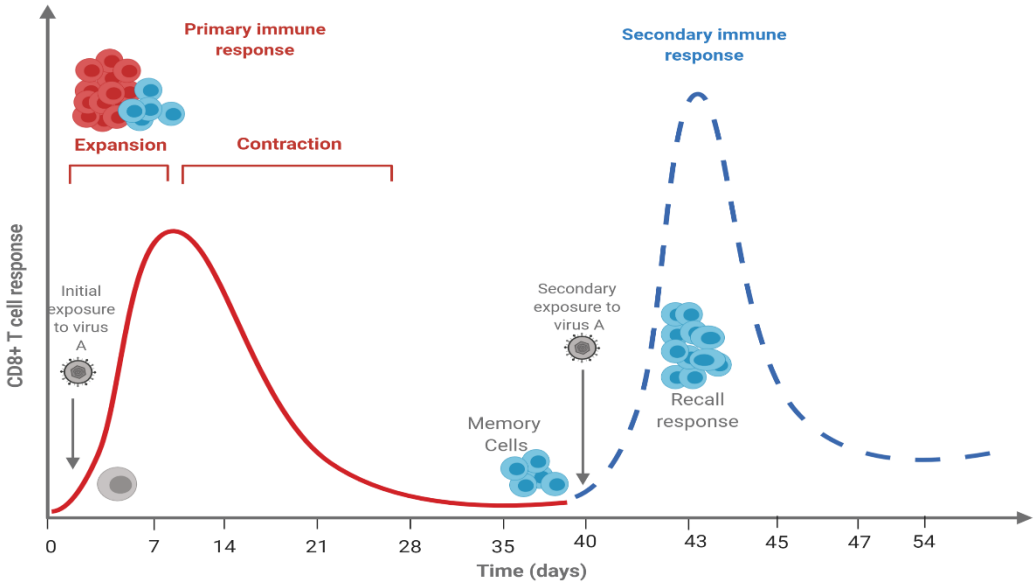

Figure 2. $CD8^+$ T cell response kinetics during an acute viral infection. Image was created in Biorender

Memory $CD8^+$ T cells include circulating effector (T_{EM}) and central (T_{CM}) memory cells and non-circulating tissue resident memory (T_{RM}) $CD8^+$ T cells. $CD8^+$ T cell differentiation from naïve into effector and memory subsets is critical for effective clearance of the pathogen and establishment of long-lasting immunity against re-infection(19). This differentiation process involves various changes at the transcriptional, epigenetic and metabolic level (22). While the cytotoxic functions of $CD8^+$ T cells are crucial in eliminating viruses, excessive killing of host cells can lead to immunopathological damage, and sometimes death (23). Effector and memory $CD8^+$ T cell subsets can be distinguished based on differential expression of specific cell surface markers and key transcription factors. Certain transcription factors play a significant role in determining whether $CD8^+$ T lymphocytes differentiate into either an effector or memory $CD8^+$ T cells. Memory precursor effector cells (MPECs), can be identified based on their high expression levels of surface markers such as CD127, IL-7Rα, CD27, CD28, CD62L, CXCR3 and their decreased expression of killer cell lectin-like receptor G1 (KLRG1). By contrast, short-lived effector CD8 T cells display high expression of KLRG1 and low expression of IL-7Rα (24).

In-depth research in the past decade has identified key transcription factors that regulate the differentiation of effector and memory T cells. A fascinating emerging concept suggests that pairs of transcription factors operate in opposing ways to determine whether $CD8^+$ T lymphocytes adopt a terminal-effector or memory fate. For example, high levels of transcription factor T-bet foster the differentiation of effector $CD8^+$ T cells toward the terminally differentiated state characterized by high expression of KLRG1. On the other hand, the transcription factor Eomesodermin (Eomes), which is highly homologous to T-bet, particularly in the DNA-binding domain, appears to induce the development of memory $CD8^+$

T cells rather than KLRG1^{hi} effector CD8^{+} T cells(25). Intricate mechanisms underlie the differentiation of CD8^{+} T cells into either effector or memory T cell subsets, and may be dependent on whether the pathogen is cleared as seen in acute infections, or persists, as is the case in chronic infections.

1.4.2 CD8^{+} T cell response in chronic infection

Initial stages of CD8^{+} T cell expansion are similar in acute and chronic viral infections. However, in chronic infections such as HIV and HCV, CD8^{+} T cells lose their effector functions and become exhausted. In 1993, Moskophidis *et al*., described exhaustion as the deletion of antigen-specific CTLs during LCMV infection (26). Building on this, others later showed that CTLs recognizing certain viral epitopes were deleted while other epitope responses persisted in the host with diminished antiviral function (27,28). Together, these works demonstrated that a polyclonal T cell repertoire could give rise to different cell fates, thereby suggesting that different manifestations of CD8^{+} T cell exhaustion could exist. The lymphocytic choriomeningitis virus (LCMV) model system provided well-established and controlled approaches to understanding T cell exhaustion. The system has been extensively used in biological research and is associated with fundamental discoveries in viral immunology.

1.4.2.1 CD8^{+} T cell exhaustion

Fundamental qualities of T cell exhaustion were established in the LCMV model of chronic viral infection (26–28). CD8^{+} T cell exhaustion is a gradual process that develops over the first three weeks of a chronic infection(29). In early stages, exhausted CD8^{+} T cells lose effector cytokine production starting with IL-2 followed by TNF-α and IFN-γ(30). Additionally,

the cytotoxic capacity of these cells is impaired, as they show reduced killing activity *in vivo* but can kill target cells *in vitro*(31). Loss of effector functions is subsequently accompanied by high expression of inhibitory surface receptors such as programmed cell death 1 (PD-1), Lymphocyte-activation gene 3 (*lag3*), T cell immunoglobulin and mucin-domain containing-3 (Tim-3), CD244 and CD160. Additionally, exhausted $CD8^+$ T cells are characterized by dysregulated metabolism, poor memory recall response and impaired homeostatic proliferation(32–34). Altogether, loss of proliferative and cytotoxic functions, allow for long-term persistence of antigen in chronic infections(35). In acute infections, inhibitory receptors (IR) are expressed by effector $CD8^+$ T cells where they function to attenuate excessive T cell activation to limit immunopathology or autoimmunity, followed by a decrease once the infection is resolved. After pathogen clearance, IR expression decreases and subsequent resting memory $CD8^+$ T cells often have low IR expression. However, in chronic infections and cancer, exhausted $CD8^+$ T cells consistently express multiple IRs simultaneously, at high levels after initial activation (32).

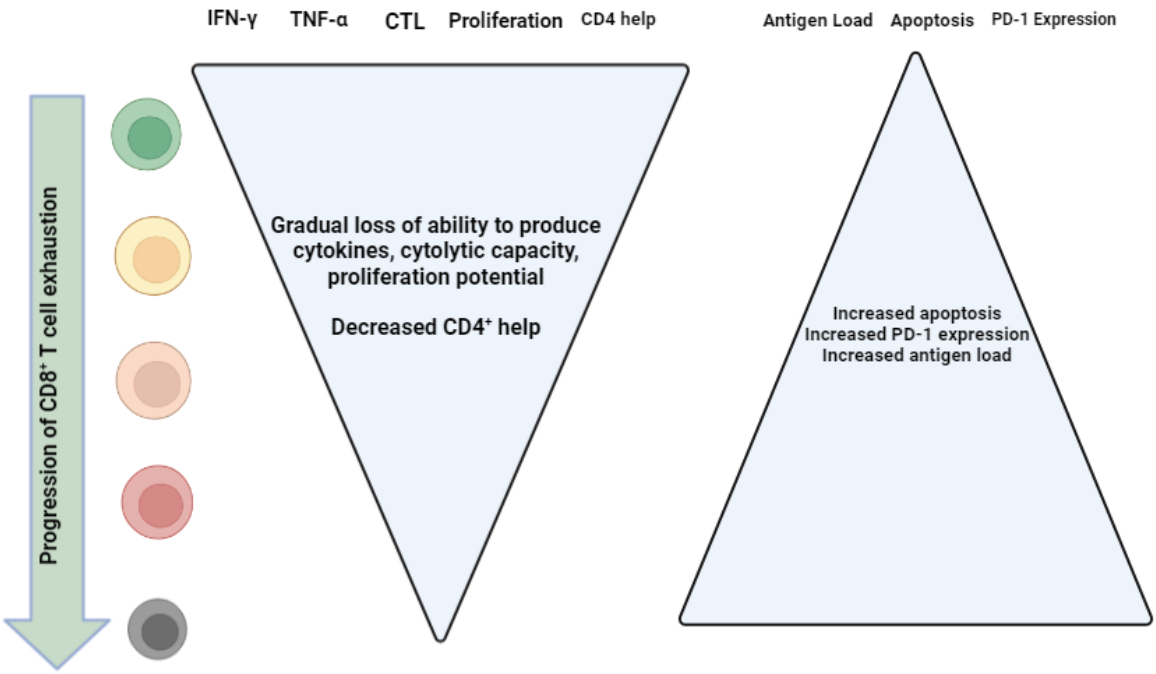

Figure 3. Canonical characteristics of $CD8^+$ T cell exhaustion. Image was created in Biorender.

By comparing functional and exhausted T cells through microarray analysis, Barber *et al*. were the first to show that PD-1 is upregulated during the short-lived effector response in acute infection, but remained elevated in exhausted T cells from chronic LCMV(36). They also provided evidence that blocking PD-1 binding to its ligands PD-L1 and PD-L2 could improve T cell function. Specifically, antibody blockade of the ligand increased T cell proliferation, increased frequency of IFN-γ producing cells as well and enhanced viral control(36).

Several other studies established PD-1 as a ubiquitous marker of T cell exhaustion and provided key insights into the regulation of PD-1 in several human chronic viral infections including HIV, HCV and HBV(33,37,38). In particular, PD-1 was upregulated on HIV-specific $CD8^+$ and $CD4^+$ T cells, and levels of PD-1 expression correlated with markers of HIV disease progression such as plasma viral load. (25,39,40). HCV studies showed that PD-1 was expressed early on most HCV-specific T cell responses, and that PD-1 expression dissipated in resolvers but not in chronic HCV settings. This was observed in both peripheral and

intrahepatic $CD8^+$ T cell compartments.(41,42). Flow cytometry experiments using high affinity antibodies for PD-1 discovered that expression of PD-1 is not uniform across the pool of $CD8^+$ T cells in chronic infection. There exists a sub-population of cells that expresses only intermediate levels(43). This pool of intermediately exhausted cells (PD-1int) were distinct from terminally exhausted cells (PD-1high) in that they responded better to anti-PDL1 treatment by expanding and re-acquiring effector functions(43).

The pool of exhausted $CD8^+$ T cells in LCMV infections is heterogeneous, consisting of subsets with distinct functional properties and developmental potential. For instance, up to seven different inhibitory receptors are expressed in various combinations on exhausted $CD8^+$ T cells. Higher diversity and density of inhibitory receptors on the cell surface correlates with severity of exhaustion in LCMV infections. Progenitor or precursor Tex cells are characterized by intermediate expression of PD-1 while terminally exhausted $CD8^+$ T cells are defined by heightened expression of inhibitory receptors such as PD-1, LAG-3, TIM-3, TIGIT, 2B4 and CD160 (1,32). Additionally, the cognate ligands for many of these IRs are upregulated on APCs, tumor cells, and other cells during chronic infections and cancer(32). The differentiation between terminally exhausted and precursor exhausted T cells based on their specific inhibitory receptor profiles provides valuable insights into the progressive stages of T cell exhaustion. However, better biomarkers for $CD8^+$T cell exhaustion are needed, beyond the presence of inhibitory receptors due to their complex heterogeneity in expression. Moreover, the mechanism of the induction of exhaustion remains understudied, along with the possible roles of the inhibitory receptors in maintaining, promoting, or defining the exhausted phenotype.

Characteristic features of exhausted T cells were mainly identified using bulk transcriptional measurements. Advanced mass cytometry and single-cell transcriptomics

have enabled better elucidation of the exhausted T cell pool in chronic infections(44–46). In 2007, Wherry *et al.* published the first systems-level analysis of exhausted T cells in chronic LCMV which revealed distinct transcriptional differences between effector and memory cells from acute infection and exhausted cells from chronic infection with LCMV (29). In 2022, by using LCMV model of $CD8^+$ T cell differentiation in combination with single-cell transcriptional and epigenetic analyses to investigate the developmental trajectories of effector $CD8^+$ T cells (Teff), memory $CD8^+$ T cells (Tmem) and exhausted $CD8^+$ T cells (Tex) cells, the same group identified shared and distinct transcriptional and epigenetic programs underlying these cellular identities. For instance, they identified a T_{ex} subset expressing Natural Killer (NK) receptors in both chronic and acute LCMV infections, which they designated Exh-KLR. Although these Exh-KLR $CD8^+$ T cell subsets in LCMV-Arm (Acute) and LCMV-Cl13(chronic) infection shared similar biological circuits, including a requirement for *Zeb2*, these subsets were otherwise largely distinct cell types(47)**.**

Exhausted T cells had a unique transcriptional signature beyond high PD-1 expression and could be distinguished from other signatures of impaired T cell function like anergy (29,47). Distinct transcriptional features associated with $CD8^+$ T cell exhaustion can be identified at the peak of infection(47) and as early the first-cell division following activation (1). Some regulatory factors are differentially expressed in exhausted $CD8^+$ T cells include inhibitory & surface receptors (*pdcd1, ctla4, lag3*), molecules associated with homing and migration (*Ccl5, Cxcr3*), survival and proliferation *(Bcl2, Casp3*) as well as metabolism (*Acas2l, Pdha1)*(29,47). Exhausted T cells also express key transcription factors such as *Blimp-1* and NFAT (29,31).

Exhausted $CD8^+$ T cells exhibit heterogeneity and can be categorized into at least three distinct states. The progenitor or precursor state is characterized by elevated expression of

TCF-1, SLAMF6, and CXCR5, intermediate expression of PD-1 while showing low levels T-bet and Eomes. The second intermediate or transitory phase is marked by high levels of T-bet, CX3CR1, TIM3, intermediate expression of PD-1 and reduced levels of Eomes. Lastly, in addition to the heightened expression inhibitory receptors such as PD-1, LAG-3, TIM-3, TIGIT, 2B4 and CD160, terminally exhausted $CD8^+$ T cells are defined by high levels of Eomes and diminished levels of T-bet (1,32).

Transcriptional profiling of $CD8^+$ T cells with high and low antigen stimulation revealed TOX as a major transcription factor required for the acquisition of an exhausted phenotype in $CD8^+$ T cells following chronic antigenic stimulation (48). TOX is induced by calcineurin and NFAT2 and operates in a feed-forward loop in which it becomes calcineurin-independent and sustained in terminally differentiated Tex cells(49). Further, Alfei *et al.*, showed that TOX is indispensable in generation of the exhausted phenotype affecting expression of IFN-*γ* and T cell homing. Genetic ablation of TOX restores effector secretion of INF-*γ* and TNF-α (50). Moreover, network analysis of exhaustion-associated transcriptional changes pointed towards altered pathways and proposed additional regulators of exhaustion such as the transcription factors T-bet, Eomes, and Helios(51). The heterogeneity of exhausted T cells, categorized into progenitor, intermediate, and terminally exhausted states, highlights the complexity of this phenomenon. The identification of key transcription factors, such as TOX, and the exploration of transcriptional and epigenetic programs provide valuable insights understanding the induction and maintenance mechanisms underlying the $CD8^+$ T cell exhaustion.

1.5 Sex-based differences in viral infections

Sex is a biological variable that influences disease incidences and outcomes (52,53). Sex can be described as female, male, or intersex based on a composite of sex chromosomes (e.g., 46XXor 46XY), gonads (e.g., ovaries or testes), and gonadal hormones (e.g., estrogens or androgens)(53). Males are typically more susceptible to infections by various pathogens as evidenced by higher prevalence rates of leishmaniasis and tuberculosisreported in males compared to females (54). Similarly, in viral infections including HIV, Influenza Virus (avian H7N9), MERS-COV and Hepatitis B, males exhibit incidence rates compared to their female counterparts. Additionally, males infected with hepatitis C virus and HIV exhibit higher viral loads than their female counterparts (55,56), suggesting that females can limit pathogen growth more effectively. On the other hand, at comparable viral loads, symptoms of infection are often significantly worse in females compared with males. This can be seen in influenza infections during which females experience more severe disease than males (57). As discussed in (58), sex differences are observed in pathogen load, incidence, prevalence and severity of disease in humans following viral infection.

Table 1. Sex Differences in severity of viral infections

Male Bias	Female Bias
Coxsackievirus	Influenza Viruses
Ebolavirus	HIV
Hantaviruses	
Hepatitis B virus	
MERS-CoV	
SARS-CoV	
SARS-CoV 2	

Table 1 above outlines sex differences in severity of viral infections referring to hospitalization or disease state progression as reported by (58)**.** Severe symptoms can be attributed to stronger innate and adaptive immune responses observed in females (59). Stronger immune responses confer better protection against infections and increase vaccine efficacy. However, enhanced immune responses in females can be pathological and are a risk factor for the development of autoimmune diseases. Higher prevalence of rheumatoid arthritis, multiple sclerosis and systemic lupus erythematosus (SLE) have been reported in females than males, with SLE being the most sex-disparate (60).

1.6 Sex-based differences in $CD8^+$ T cell responses

Sexual dimorphism in infectious disease outcomes can be attributed to differences in the immune response during infection, including the $CD8^+$ T cell response. For example, using microarray analysis Patel *et al.*, showed that female $CD8^+$T cells exhibit enhanced upregulation of antiviral and pro-inflammatory genes after *in vitro* stimulation with PMA–ionomycin (57). This observation may explain why females are less vulnerable to intracellular pathogens yet respond with more inflammation. A recent study involving murine infections with vaccinia virus and *Listeria monocytogenes* demonstrated that male and female $CD8^+$ T cells respond differently to intracellular pathogens. Female $CD8^+$ T cells were shown to have an inherent propensity to undergo effector cell differentiation post-infection with both pathogens while male $CD8^+$ T cells were more likely to become memory precursor effector cells (61), suggesting that females have an enhanced ability to clear intracellular pathogens in this study.

The mechanisms that underlie differences in $CD8^+$ T cell responses between the sexes are complex and can involve immunological, hormonal, and (epi-) genetic factors. These

factors may be cell-intrinsic or influenced by environmental differences between males and females.

Cell-intrinsic factors may include variations in gene expression and epigenetic modifications between the male and female $CD8^+$ T cells. Additionally, signaling pathways that affect the activation, differentiation, and function of $CD8^+$ T cells may be regulated in a sex-specific manner.

Alterations in gene expressions between males and females can be attributed to genes linked to sex chromosomes. In humans, sex chromosomes are heterologous in males (XY) and homologous in females (XX). Many genes on the X chromosome regulate immune function and play an important role in modulating sex-differences during infection(52). The human X chromosome contains over 1,100 annotated genes that include a significant number of immune related genes, such as interleukin 2 (IL-2) receptor-γ chain, IL-3 receptor-α chain, IL-13 receptor-α chains, Toll-like receptor 7 (TLR7), TLR8, GATA1, IL-1 receptor-associated kinase 1 (IRAK1), CD40 ligand and FOXP3. These genes code for proteins ranging from PRRs (for example, TLR7 and TLR8) to cytokine receptors (for example, IL2RG and IL13RA2) and transcriptional factors (for example, FOXP3) (52,62). X-linked genes are determinants of sex-specific immune responses. Females have two X chromosomes (XX) while males have one (XY). Therefore, to equalize gene expression between sexes, females undergo a process called X chromosome inactivation (XCI). During XCI, one copy of a gene is silenced to ensure only a single copy functions in each sex. A copy on either X chromosome is randomly chosen to be transcriptionally silenced. The X-inactive specific transcript (XIST) gene initiates XCI. Approximately 15% of X genes in humans and 3% in mice escape X inactivation and are found in higher copy number in females than males (52). In this regard, immune-associated genes that map to the X chromosome are of keen interest because they can affect the nature and

intensity of immune responses between the sexes, depending on whether they escape XCI. Reactivation of the usually silent second X chromosome in females promotes sex differences in the immune system. As an example, C-X-C chemokine receptor type 3 (CXCR3) is an important immune-related gene that maps to the X chromosome (57). CXCR3 is expressed by activated $CD4^+$ T cells, $CD8^+$ T cells, macrophages, dendritic cells, and other immune cells(57). This inducible chemokine receptor is critical for migration of effector $CD8^+$ T cells into tissues(63). Studies have shown that CXCR3 escapes XCI in T cells when activated *in vitro* as well as during *in vivo* infection with *L. Mexicana* (64). Given that CXCR3 is involved in $CD8^+$ T cell migration, differentiation, and activation, the increased protein expression observed following escape of X-chromosome inactivation could potentially result in enhanced immune response in females leading to significant biological consequences in infectious disease. Other immune related X-linked genes that escape XCI can result in heightened immune responses in females. The Y chromosome also contains numerous regulatory response genes that can influence susceptibility of males to viral infections(52).

Innate responses that influence $CD8^+$ T cell differentiation can contribute to sex-based differences in $CD8^+$ T cell responses. For example, detection of nucleic acids by pattern recognition receptors (PRRs) differs between the sexes(52). *TLR7* gene is encoded on the X chromosome and can escape X inactivation leading to higher TLR7 expression in females compared to males (65). Increased TLR7 signalling on APCs such as plasmacytoid dendritic cells (pDCs) can enhance recognition of ssRNA viral antigens leading to stronger secondary $CD8^+$ T cell activation in females. Innate immune responses are critical co-stimulatory signals for $CD8^+$ T cells in the response to viral infection and can contribute to sex-based differences in $CD8^+$ T cell responses.

Hormone mediated effects between males and females can also affect $CD8^+$ T cell differentiation and function(59,66). Sex hormones can act directly on $CD8^+$ T cells through receptor signalling or indirectly by shaping the tissue niches they reside in. Lymphocytes and myeloid cells express estrogens receptors (ER), androgen receptors (AR), and progesterone receptors (PR). Sex steroid receptors act as nuclear transcription factors through different ligand-dependent or ligand-independent mechanisms. Sex hormones can act both locally and systemically, exerting a variety of immunological effects on adaptive immunity and $CD8^+$ T cells in particular.

Estrogen can affect the maturation, differentiation, and function of T cells. Studies have shown that human and murine $CD8^+$ T cells express both ERα and Erβ, the two ER subtypes for classical oestrogen signalling (66,67). In rodents, estradiol (E2) signaling through Er*α* and not *ERβ* was shown to be necessary for effective differentiation of $CD8^+$ T cells(68). Additionally, *in vitro* co-culture studies involving antigen-specific T cells and 17β-estradiol showed that E2 treatment differentially affects anti-tumor effector functions of female and male $CD8^+$ T cells. Female, but not male $CD8^+$ T cells, exhibit increased production of effector molecules. Specifically, female $CD8^+$ T cells showed significant increase in IFNγ and granzyme B production as the hormone dosage increased (69). Levels of estrogen, for example, 17β-estradiol (E2), are variable during the menstrual cycle, high during pregnancy and low after menopause in females (52). Hormonal changes during the menstrual cycle, act directly or indirectly to regulate $CD8^+$ T cells cytotoxic activity during viral infections. A recent human study investigating the effects of sex hormones on $CD8^+$ T cells in female genital tract showed that estradiol directly suppressed cytotoxic activity, in particular the production of perforin and granzymes by the endometrial (EM) $CD8^+$ T cells. Interestingly, incubation of polarized endometrial epithelial cells with progesterone (P) increased TGFβ secretion (70). TGFβ has

previously been implicated as a potent cytokine capable of suppressing T cell effector function by downregulating granzyme, perforin, and interferon encoding genes(71). These findings demonstrate that E2 acts directly on $CD8^+$ T cell to suppress cytotoxic activity while P acts indirectly through induction of TGFβ production.

On the other hand, androgens including dihydrotestosterone (DHT) and testosterone have been shown to generally supress immune activity(52). For example, exposure to testosterone *in vivo* can dampen innate immune responses such as NK cell activity and TLR signalling in macrophages(52). AR expression has been identified on the majority of innate and adaptive immune cells suggesting that androgens directly modulate the function and development of immune cells. $CD8^+$ T cells express the classical cytoplasmic AR and other membrane-bound androgen receptors (mAR) such as the zinc transporter ZIP9 (69). Androgen signalling can affect T cell maturation, proliferation, differentiation and cytokine production in mice and adult males, directly or indirectly. However, the effects of androgen signalling on T cells are context dependent, and driven by cellular and molecular mechanisms. For example, a recent bladder cancer study using multiple *in vivo* genetic models, high-dimensional flow cytometry, coupled with sex-disaggregated single-cell transcriptomic analysis of tumor-infiltrating $CD8^+$T cells ($CD8^+$TILs) showed that androgen directly regulates differentiation of activated $CD8^+$ T cells. In particular, androgen signaling steers male $CD8^+$ TILs towards exhaustion in a T cell–intrinsic manner such that that loss of AR in $CD8^+$ T cells alone, improved $CD8^+$ T cell effector functions, rendering male mice equally protected against cancer as female mice (72).

Sex-based differences in $CD8^+$ T cell responses play a crucial role in influencing disease outcomes and immune responses to various pathogens. Further research is warranted to

unravel the intricate mechanisms the immunological, hormonal, and (epi-) genetic factors underlying these differences.

1.7 The Lymphocytic Choriomeningitis Virus (LCMV) model

The LCMV system for viral infections has been utilized extensively in immunology studies yielding significant discoveries of T cell differentiation, function, and exhaustion. An understanding of T cell exhaustion and successful immune checkpoint blockade (ICB) therapy to restore T cell function was first described using the Clone 13 variant of LCMV selected from the Armstrong 53b parental strain. LCMV is a prototypic virus of the family *Arenavidae*. The LCMV genome consists of two negative-sense single-stranded RNA segments, designated L and S. Both segments contain two viral genes in an ambisense coding strategy, with some genes encoded in sense and others in antisense (73,74). The two segments, termed L (7.2 kb) and S (3.4 kb) are separated by a unique hairpin structure. The L segment contains the viral RNA dependent RNA polymerase (L) and a small RING finger protein (Z). The S segment contains the nucleoprotein (NP) and glycoprotein polyprotein precursor (GP0) that is cleaved post-translationally into SSP (signal peptide), GP1 and GP2. (73,75). Tetramers of GP-1 and GP-2 make up the spikes on the virion envelope. GP-1 mediates virus interaction with host cell surface receptor affecting entry into cells(74).

LCMV is a valuable model for a broad range of in-depth infection and immune response studies. Several well-characterized viral strains that differ in their replicative capacity, host range (cell tropism, mouse strain and age), and experimental routes of infection (intracranial versus intraperitoneal (i.p.) or intravenous (i.v.) in mice which may be used to elicit different infection outcomes of study (76). For example, inbred mouse strains including C57BL/6, BALB/c, SWR/J, A/J, 129, C3H, and all but one collaborative cross (CC) mouse strain exhibit

immunosuppressed T cell responses, high PD-1, and viral titers leading to persistent infection following intravenous injection with LCMV-CL13. In contrast, FVB/N, NZB, PL/J, SL/J, and CC NZO mice challenged intravenously with LCMV-CL13 have a robust T cell response, high viral titres, PD-1, and Lag3 markers on T cells(77). The LCMV-ARM strain was isolated from a monkey undergoing a LCMV infection (73). Inoculation of LCMV-Arm in its natural host *Mus musculus* leads to an acute infection, with virus eliminated within 7-10 days after infection. LCMV-CL13 is a genetic variant of the parent LCMV-Arm virus that was isolated from the spleen of carrier mice which sustained a persistent LCMV infection since birth, due to suppression of LCMV-specific CTL responses (78).

The genome of LCMV-CL13 is distinct from its parental strain by five out of the out of 10,600 nucleotides, which cause two amino acid variations. Amino acid residue 260 on the glycoprotein encoded on the S segment is mutated from phenylalanine to leucine and amino acid 1079 of the RNA polymerase encoded on the L segment is mutated from lysine to glutamine (79,80). Research has demonstrated that either of the mutations in the viral polymerase or glycoprotein genes can account for the biological phenotype of the persistent infection(78). α-Dystroglycan (α-DG) is the cellular receptor for LCMV expressed on various cells including immune cells such as dendritic cells and macrophages. α-DG is a peripheral protein that can complex with β-DG, a trans-membrane protein, upon activation(81). α-DG on immune cells can interact with various extracellular matrix (ECM) components such as laminin and collagen associated with the stroma of lymphoid tissues via processes that involve integrin signalling. The cell-matrix interactions play a direct role in the positioning and/or migration of leukocytes within lymphoid tissues(82). The mutation in the GP of LCMV-CL13 was shown to increase the affinity of GP for α-DG up to 100-fold and increase LCMV-CL13 binding over LCMV-ARM binding(81,83–85). The mutation of amino acid 1079 of the RNA

polymerase of LCMV-CL13 increases the replication rate of the chronic strain and increases early viremia(86).

The marginal zone (MZ) and white pulp (WP) of the spleen have increased expression of αDG that binds laminin, and higher numbers macrophages and DCs (82,84). Fluorescent microscopy of LCMV-infected spleens demonstrated the co-localization of LCMV-CL13 with the MZ and WP of the spleen, while LCMV-Arm virus was restricted to primarily to the red pulp (RP) of the spleen during LCMV-ARM infection. Mutations in the GP complex of LCMV CL13 cause the virus strain to acquire a higher affinity for binding α-DG, and as a consequence has a different cellular tropism than LCMV-Arm, the parental strain(83,85). The higher affinity of LCMV CL13 for α-DG confers higher infectivity, particularly in infecting CD11c+ splenic DCs, the interdigitating DCs in T cell areas, and nests of cells near the MZ, that primarily express α-DG (87,88). *In vivo* mouse studies demonstrated that receptor–virus interaction on DCs is an essential step in the initiation of virus-induced immunosuppression and persistent infection(87). LCMV-CL13 and other persistent LCMV strains have also been shown to have higher infectivity of pDCs (86). In contrast, LCMV-ARM primarily infects F4/80+ macrophages and some DCs, but to a lesser extent than LCMV-CL13(87). Notably, the mutations in LCMV-CL13 confer greater infectivity of fibroblastic reticular cells (FRCs) compared to LCMV-Arm(89). FRCs are part of a complex microstructure within lymphoid organs that support and organize the migration, recruitment and activation of lymphocytes(89,90). Infection of the intricate conduit network dampens early $CD8^+$ T cell responses to prevent T-cell mediated immunopathology contributing to viral persistence in the spleen(89).

For my project, I used the LCMV model to comparatively analyze antigen-specific CD8+ T cell differentiation during acute (LCMV-Arm) vs. chronic (LCMV-CL13) infection. I use the LCMV-Clone13 (chronic) and LCMV-Armstrong 53b (acute) (LCMV-Arm) strains, as they were

readily available for propagation from our collaborator. Additionally, C57BL/6 mice were selected to explore CTL responses to LCMV-CL13 and LCMV-Arm because of their well published established genetic and immunologic profiles in the context of LCMV studies.

The TCRs of the transgenic cells (P14 $CD8^+$ T cells) used in this model recognize the gp33-41 peptide, a shared epitope expressed by both LCMV-Arm and LCMV-CL13. The experimental model system involves the adoptive cell transfer of $CD45.1^+$ P14 $CD8^+$ T cells into recipient CD45.2 C57BL/6 mice. CD45.1/2 are congenic markers that are used to detect donor and recipient cells. P14 donor cells are homozygous for the CD45.1 allele and this feature distinguishes them from recipient (CD45.2) cells.

1.8 Application of single-cell RNA seq analysis in studying $CD8^+$T cell differentiation

$CD8^+$ T cell differentiation towards effector, memory or exhausted cell fates is a complex process that is specified in part, by the expression of transcription factors and other signaling molecules. Gene expression profiling studies have played a crucial role in enhancing our comprehension of the molecular mechanisms that guide the differentiation of $CD8^+$ T cells. However, these studies were based on bulk RNA sequencing of T cell populations that measured the average gene expression across a combined pool of $CD8^+$ T cells, masking rare cell types or subpopulations with distinct gene expression patterns. As a result, it was impossible to distinguish variations in gene expression between individual effector, exhausted and memory $CD8^+$ T cells (18). Single-cell RNA sequencing (scRNA-seq) technology has revolutionized our understanding of the heterogeneity and dynamics of $CD8^+$ T cell differentiation. This technology enables the identification of individual cells, and the quantification of their gene expression profiles, providing unprecedented resolution and

sensitivity to detect rare cell types and subpopulations, which was not previously possible using bulk RNA-sequencing. Additionally, scRNA-seq enables the detailed characterization and visualization of developmental trajectories in cell differentiation. The unique advantage of scRNA-seq lies in its ability to capture the asynchronous development of individual $CD8^+$ T cells. Mathematical models or artificial intelligence algorithms can be used to reconstruct the underlying dynamic process by connecting the different cell states and ordering along a potential differentiation path.

Several studies have used scRNA-seq to investigate the transcriptional changes that occur during effector, memory, and exhausted $CD8^+$ T cell differentiation(14,15,29,47,91). This study builds upon Dr. Arsenio's previous work that employed scRNA-seq analysis to identify novel early cell fate regulators of $CD8^+$ T cell responses to LCMV-Arm in mice. Unsupervised t-distributed Stochastic Neighborhood Embedding (tSNE) clustering analysis identified distinct differences in transcription profiles of "effector-like" or "memory-like" cell fates as early as after the first cell division following *in vivo* LCMV-Arm. 89 genes were identified to be novel early regulators of $CD8^+$ T cell differentiation. For my project, I applied similar experimental and scRNA-seq analysis approaches as previously used (14,91) to identify potential early regulators of exhaustion formation in the context of a chronic LCMV infection.

2 Thesis Summary

2.1 Rationale

While several studies characterize exhaustion after this state has developed, it remains less clear how and when exhaustion is specified. It is known that diverse cellular fates (effector and memory) can be generated from a single antigen specific $CD8^+$ T cell. Cell fate diversification can occur as early as after the first cell division after *in vivo* acute-resolving infection. However, it remains less defined if exhaustion may develop during early phases of a developing chronic infection, and what the underlying molecular programs are which may specify antigen-specific $CD8^+$ T cell exhaustion development in a chronic infection compared their counterparts at early times after an acute-resolving infection. Moreover, it is well-appreciated that sex differences in immune responses, including T cell responses to infection and cancer can occur, however it remains uncharacterized how biological sex affects $CD8^+$ T cell responses and their underlying transcriptional profiles during a developing acute versus chronic infection. We use the LCMV mouse model to analyze early antigen-specific $CD8^+$ T cell transcriptional profiles during acute vs. chronic infection and investigate any sex-based differences. By examining both early $CD8^+$ T cell responses and sex-based differences, this work addresses a gap in our understanding of early transcriptional signatures of exhaustion that may be differentially regulated between males and females.

2.2 Overall goal and Hypothesis

The overall goal of this project is to define the early molecular profiles of how $CD8^+$ T cells may differentiate into an exhausted state compared to effector and memory cell fates and to characterize any sex differences.

Hypothesis: Determinants of exhaustion may occur during early phases of a developing chronic infection and there are sex-specific differences in $CD8^+$ T cell responses to acute and chronic infection.

2.3 Specific Objectives

There are four specific objectives:

1. Generate transcription profiles of mature $CD8^+$ T cells (effectors (day 7)), exhausted (day 28) and memory (day 40) responding to acute and chronic LCMV infection by single-cell RNA sequencing.
2. Generate transcription profiles of early differentiating $CD8^+$ T cells (first division, day 4-post infection) in acute and chronic infection by single-cell RNA sequencing.
3. Identify potential early regulators of $CD8^+$ T cell exhaustion using computational analysis.
4. Characterize sex-based $CD8^+$ T cell responses during a developing acute and chronic infection

3 Materials and Methods

3.1 Mice

All animal work was approved by the Animal Care Committee (ACC) of the University of Manitoba, Winnipeg. All mice were bred and housed in specific pathogen-free conditions. CD45.1 C57BL/6N mice were crossed with CD45.2 P14 (Jackson Laboratory) to generate CD45.1 P14 transgenic mice. Donor mice (CD45.1 P14 homozygous) were male or female, 6–8 weeks old. Recipient (CD45.2 C57BL/6) mice were male or female, 6–8 weeks old, males or females were housed in the same cage.

3.2 Adoptive cell transfer and viral infection

For analysis of cells undergoing early cellular divisions, P14 $CD8^+$ T cells were first labeled with carboxyfluorescein diacetate succinimidyl ester (CFSE). 1×10^6 cells per mouse were transferred intravenously (i.v) into recipient mice. 24 hours later, mice were infected intraperitoneally (i.p) with 2×10^5 plaque-forming units (pfu) of LCMV-Arm per mouse or intravenously with 1.14×10^6 pfu of LCMV-CL13 per mouse. At 18-, 24-, 36- and 48-hours post-infection (hpi), spleens were harvested and analysis of CFSE-labelled by flow cytometry. For analysis of cells at 4 days post-infection (dpi), 20 000 $CD45.1^+$ P14 $CD8^+$ T cells were transferred into $CD45.1^+$ recipient mice.

For analysis of cells at 7,14,21,28 and 42 dpi, 5×10^3 $CD45.1^+$ P14 $CD8^+$ T cells were transferred into $CD45.1^+$ recipient mice that were infected 24 hours later with LCMV-Arm or LCMV-CL13. Blood and splenocytes were analyzed at days 4, 7,14,21,28 and 42 dpi.

3.3 Flow cytometry and antibodies

Cells were stained with the following antibodies used at 1:200 dilution: CD8α (53-6.7), CD45.1 (A20), CD45.2, Vα2, CD25 (PC61), CD62L (MEL-14), CD44 (IM7), IFNγ (XMG1.2), TNFα (MP6-XT22), KLRG1 (2F1), -IL-7R (A7R34), CD27 (LG.7F9), T-bet (4B10), all from Biolegend. Intracellular antigens were stained using the Foxp3 Transcription Factor Staining Buffer Set (eBioscience) according to manufacturer's instructions. For intracellular staining of IFN-γ and TNF-α, isolated $CD8^+$ T cells were cultured ex vivo for 6 h at 37 °C with a cell Stimulation Cocktail (500X) of 0.5 µg/ml phorbol 12-myristate 13-acetate and 5 µg/ml ionomycin (PMA/ionomycin) (ThermoFisher Scientific) in the presence of 10 µg/ml brefeldin A ((Sigma-Aldrich)Sigma). After 6h incubation, cells were stained with surface antibodies, fixed in 4% paraformaldehyde (Electron Microscopy Services) and then permeabilized with PBS (Mediatech) containing 1% FBS (Life Technologies), 1% saponin (Sigma-Aldrich), and 0.1% sodium azide (Sigma-Aldrich). The cells were stained with antibodies against IFN-γ and TNF-α at 1:100 dilution factor. All samples were analyzed on an Accuri C6, FACSAria II (BD Biosciences) or CytoFLEX (Beckman Coulter). Analysis was performed with FlowJo software (TreeStar).

3.4 Cell Sorting

Splenocytes were isolated from recipient mice at 4-, 7-, 28- and 40-days post LCMV-Arm or LCMV-CL13. $CD8^+$ T cells were purified using the negative selection $CD8^+$ T cell Isolation Kit (Miltenyi Biotec). P14 $CD45.1^+$ $CD8^+$ T cells were sorted on the FACSAria II (BD Biosciences) for downstream cDNA library generation and scRNA-Seq.

3.5 Single-cell RNA-sequencing

6.0×10^3 to 1×10^4 P14 $CD8^+$ T cells sorted by flow cytometry were loaded onto the Chromium Next GEM Chip G (10x Genomics) according to the manufacturer's instructions. Cell lysis, single-cell barcoding, and gel-emulsion (GEM) generation were performed in the Chromium Controller (10x Genomics). GEM reverse transcription was performed on the ABI 7500 Thermal Cycler (ThermoFischer Scientific) according to the manufacturer's instructions. Full-length cDNA from the GEM-RT reaction was purified using silane magnetic beads (10x Genomics). Barcoded, full-length cDNA was amplified via PCR on the Veriti 96 Well Thermal Cycler. Illumina Single Cell 3' complementary DNA (cDNA) libraries were generated according to the manufacturer's instructions (10x Genomics). Quality control measures of the single-cell cDNA libraries were performed on the 2100 Bioanalyzer (Agilent Technologies) and Qubit 4.0 Fluorometer (Thermo Fisher Scientific). Single-cell cDNA libraries were sequenced (50000 paired-end reads, single-indexing) on the NovaSeq 6000 at Genome Quebec. Our collaborators (Dr. O. Wilkins and S. Robertson, Department of Biological Sciences, University of Manitoba) performed ScRNAseq analysis. ScRNA-seq data from 29000 murine $CD8^+$ T cells were processed in Cell Ranger and Seurat 4.0 for quality control (QC). Filtering criteria was as follows: for each sample, we retained cells in which at least 100 genes were detected in at least 10 cells. Cells had less than 5% mitochondrial reads and no more than 6000 genes.

3.6 In Vitro CD8$^+$ T cell Assays

In Vitro effector and Memory CD8$^+$ T cell differentiation Model

For *in vitro* effector and memory CD8$^+$ T cell differentiation, single CD8$^+$ T cell suspensions were prepared from spleens of female P14 mice by lysing with red blood cell lysis buffer and resuspending the lysed cells in 1 ml HBSS+5% FBS. TCR transgenic CD8$^+$T cells were isolated using the CD8$^+$T cell isolation kit II (Miltenyi Biotec). 300,000 CD8$^+$ T cells per well were cultured with immobilized anti-CD3 and anti-CD28 (Bio X Cell) for 1 hour. Cells were then washed and resuspended in media containing IL-2 and IL-15 ((10 U/ml) (PeproTech), along with T cell media for 72 hours.

In Vitro CD8$^+$ T cell Exhaustion Model

For *in vitro* exhausted CD8$^+$ T cell differentiation, inhibitory receptor induction was performed as described by (92,93), with slight modification of 5 days of culture. Naive P14 cells from the spleen of a female mouse were isolated using the negative selection CD8$^+$T cell isolation kit (Miltenyi Biotec). Dendritic cells were derived from the spleen of a separate female transgenic mouse and isolated by magnetic separation with CD11c MicroBeads (Miltenyi Biotec). DCs were pulsed with gp33 (0.1 µM) for 1h. After the 1h incubation time, P14 CD8$^+$ T cells and DCs were resuspended in a 1:1 ratio (300,000 DCs: 300,000 CD8$^+$ T cells) per well, in T cell media containing IL-2 or IL-15 (10 U/ml) and gp 33 of LCMV (0.1 µM). At Day 1, flow cytometry was performed to assess CD8$^+$ T cell activation status by staining for CD8, CD44 and CD62L.

At days 2 and 4 of co-culture, P14 cells were washed, resuspended and cultured in T cell media complemented with gp33 peptide (0.1 µM) in combination with IL-2 (R&D) or IL-15 (R&D) at 10 U/mL. At Day 5, cells were harvested for flow cytometry and qRT-PCR experiments.

3.7 qRT-PCR

RNA isolation: Total RNA was extracted from "effector-like", "memory-like" and "exhausted-like" $CD8^+$ T cells differentiated in vitro using TRIzol reagent, following the manufacturer's protocol. The quality and quantity of the extracted RNA were assessed using a NanoDrop spectrophotometer.

cDNA synthesis: Reverse transcription was performed using SuperScript VILO cDNA Synthesis Kit (ThermoFisher Scientific) that included a reaction master mix and an enzyme blend containing SuperScript III Reverse Transcriptase(RT). I used 0.25µg RNA of each sample as input for each reaction. The cDNA synthesis settings were 25°C for 10 min, 42°C for 60 min, followed by 85°C for 5min and final temperature of 4°C. The resulting cDNA was stored at -20°C until use.

qRT-PCR: Quantitative real-time PCR (qRT-PCR) was performed using the TaqMan Fast Advanced Master Mix and TaqMan Gene Expression Assays on Quant Studio 3 Real-Time PCR System. The TaqMan assays used were specific for the genes of interest that were identified by single-cell RNA sequencing analysis. The PCR cycling conditions were 50°C for 2 min, 95°C for 10 min, followed by 40 cycles of 95°C for 1 s and 60°C for 20 s.

Data analysis: The relative expression levels of the target genes were calculated using the comparative Ct method with β-actin as the reference gene. The data were analyzed using

Microsoft Excel software and presented as mean ± standard deviation. Two independent experiments were performed with three technical replicates of each sample.

3.8 Plaque assays

Vero E6 cells were seeded in 6-well plates and grown to 70-80% confluency in DMEM supplemented with 10% FBS, 2 mM L-glutamine, 100 U/ml penicillin, and 100 µg/ml streptomycin. The cells were then infected with 1:2 dilutions of sera isolated from infected mice at Day 5, 12 and 28 post LCMV-Arm and LCMV-CL13 infection. The virus was allowed to adsorb to the cells for 1 hour at 37°C with gentle rocking in the incubator every 15 minutes. The inoculum was then removed, and the cells were washed with PBS. The cells were overlaid with 2mL of 1% agarose dissolved in Milli-Q water + EMEM media containing 14% FBS, 2% L-Glutamine and 2% streptomycin at a 1:1 ratio of agarose:media. The plates were then incubated at 37°C, 5% CO2 for 6 days. At 6 dpi, the cells were fixed with 9.375% paraformaldehyde in PBS for 1h at room temperature. After the 1 h incubation, the overlay was removed, then the fixed cells were stained with 1% crystal violet solution for 10 minutes at room temperature. Crystal violet stock solution was prepared using 2mL ethanol, 8mL dH20 and 0.1g Crystal Violet.

The plates were then washed with water and allowed to air dry. The plaques were counted, and the viral titers were calculated using the following formula: viral titer = (number of plaques counted x dilution factor x 1/volume of inoculum). The viral titers for LCMV-Arm and LCMV-CL13 were determined at day 5, 12, and 28 post-infections.

4 Chapter 4 – Validation of the LCMV model system

4.1 Rationale

The LCMV model system has been extensively utilized to investigate various aspects of $CD8^+$ T cell biology, including effector functions, memory differentiation and exhaustion. This model has proven valuable in studying the antigen-specific T cell response to both acute and chronic viral infections (14,76,91,94). The Arsenio lab established the LCMV model system at the University of Manitoba. To generate a colony of donor CD45.1 P14 mice for this model system, we crossed CD45.2 P14 transgenic (Tg) homozygous mice (Jackson Laboratories) with CD45.1 C57BL/6 mice (Jackson Laboratories) to obtain CD45.1 homozygous P14 (Tg/Tg) homozygous progeny. Mouse genotypes are determined using established genotyping protocols in our lab involving genomic DNA isolation from mouse ear clippings and PCR amplification then HpyCH4 restriction enzyme digests to confirm the presence and homozygosity of the CD45.1 allele, and qRT-PCR analysis to confirm the P14 transgene homozygosity. Dr. David Safronetz at the National Microbiology Laboratory provided LCMV-Arm and LCMV-CL13 strains. LCMV-Arm and LCMV-CL13 strains were propagated in BHK21 cells to optimal high viral titres for *in vivo* studies.

As it was the first time to establish this mouse LCMV model of infection at the University of Manitoba, we first validated the LCMV model system for *in vivo* studies of $CD8^+$ T cell differentiation. To confirm the reliability and reproducibility of our model prior to generating cDNA libraries, we analyzed the $CD8^+$ T cell response after *in vivo* infection with LCMV-Arm and LCMV-CL13 strains. We compared the $CD8^+$ T cell kinetics and phenotypes generated in our study with those previously published by (14,15,29,91).

Additionally, I performed plaque assays to confirm replication of both strains at early time points, followed by LCMV-Arm clearance and LCMV-CL13 persistence in the infected mice at later time-points.

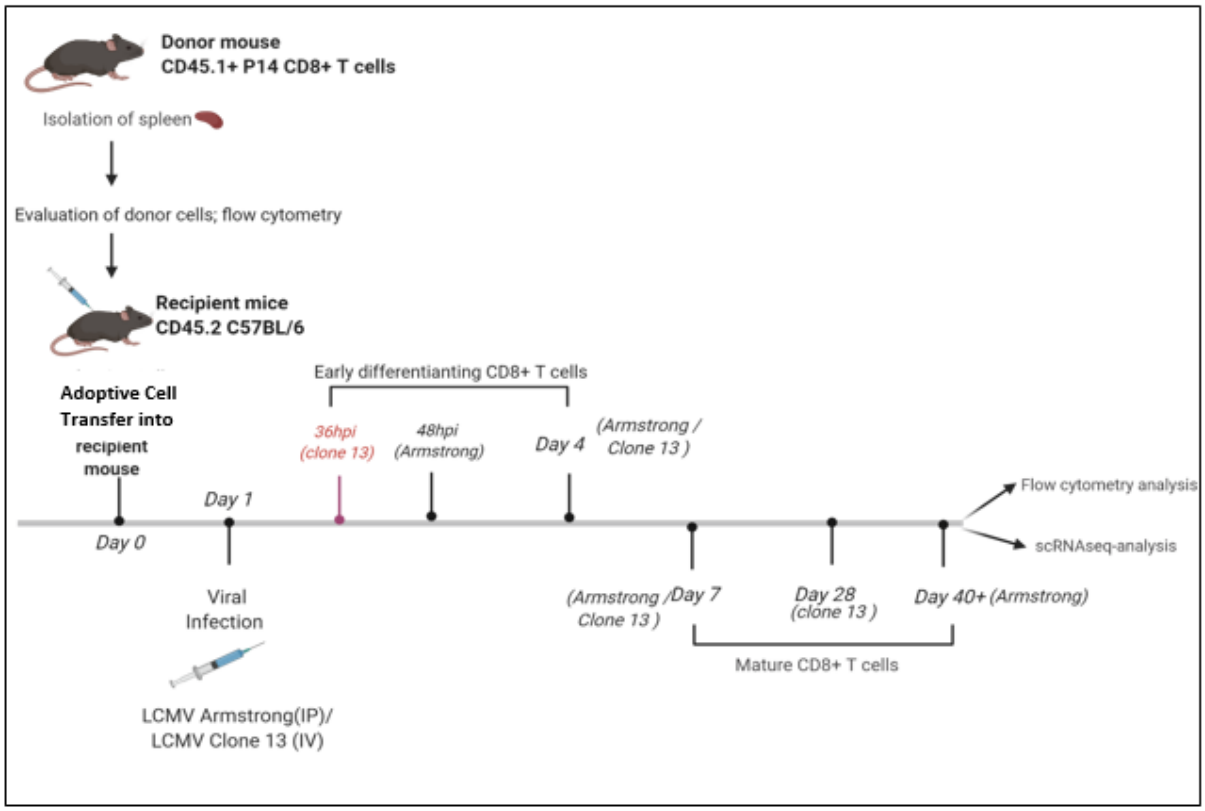

Figure 4: LCMV Experimental Model System. This figure depicts the experimental model system utilized for in vivo LCMV studies and includes the following key components: donor and recipient mice genotypes, LCMV viral strains and the different time-points of antigen-specific $CD8^+$ T cell analysis post-infection.

4.2 Validation of in vivo viral replication

Research has previously shown that during an acute LCMV infection in adult mice, the viral load reaches maximum levels at around day seven, after which there is a peak in CTL activity between days 7 and 9, facilitating optimal viral clearance. By 14 dpi, most of the virus has been cleared (95).

In this study, the infection of mice with LCMV was confirmed by measuring viral titers in sera at 5, 14 and 50 dpi. The 5-dpi time-point corresponds to the acute phase of the infection and represents the peak of LCMV replication. This time-point allows for the measurement of virus that has successfully infected and replicated in the host, providing insight into the magnitude of the immune response required to control the infection.

During the acute phase, the immune system is activated and initiates a response against the virus. $CD8^+$ T cell responses reach their peak at 7 dpi, shortly after the peak of viral replication(95). Viral titers in the sera were further measured at 14 dpi. Day 14 represents an intermediate time-point in the course of the infection, which corresponds to the contraction phase of the CTL response. At this stage, most of the virus has been cleared by responding $CD8^+$ T cells, but can persist in blood and some tissues, such as the spleen, at lower levels of replication. Day 50 represents a later stage when memory $CD8^+$ T cells and terminally exhausted $CD8^+$ T cells can be detected in circulation during LCMV-Arm and LCMV-CL13 infections, respectively. Measuring virus titres at day 14 and day 50 allows us to assess clearance of LCMV-Arm and persistence of LCMV-CL13 in the mice.

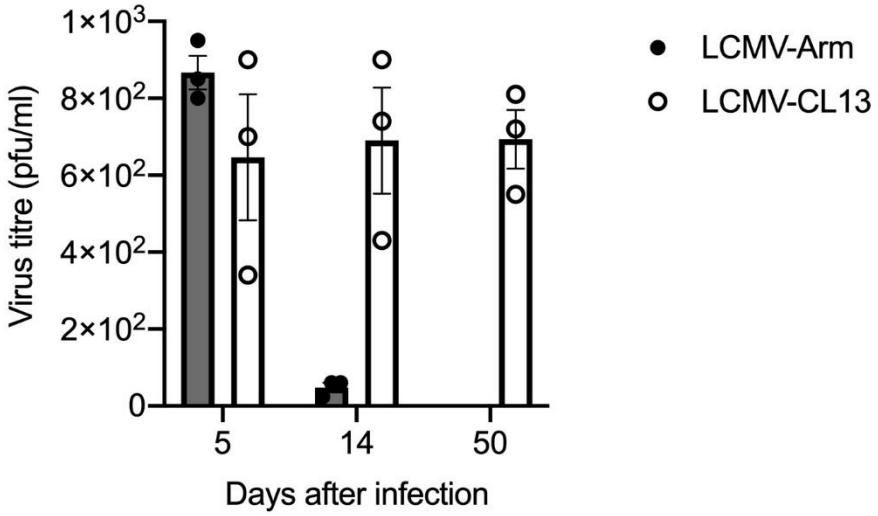

Figure 5. Levels of replicating virus at Day 5, Day 14 and Day 50 post-infection in sera of male P14 mice infected with either LCMV-Arm (shaded) or LCMV-CL13. Data is representative of at least 3 independent experiments.

As seen in Figure 5, the presence of plaques at day 5 post infection demonstrated successful viral replication of both LCMV-Arm and LCMV-CL13 in the recipient mice. Absence of plaques at Day 14 and Day 50 in LCMV-Arm infections, confirmed successful clearance of the acute strain, following the peak of the $CD8^+$ T cell response. Conversely, the presence of LCMV-CL13 in the sera at day 14 and 50 confirm persistence of the chronic infection in the mice.

4.3 $CD8^+$ T cell response Kinetics

To validate the kinetics of the $CD8^+$ T cell response *in vivo*, I conducted adoptive cell transfer experiments as previously described and implemented by Arsenio *et al.*,(91). P14 $CD45.1^+$ $CD8^+$ T cells were obtained from spleens of naïve female donor mice and transferred into male recipients. I confirmed the naïve status of the P14 cells by assessing $CD62L^{hi}CD44^{lo}$ expression and verified the CD45.1 TCR homozygosity by measuring CD45.1+Vα2+ (>96% positive). A total of 5000 P14 $CD8^+$ T cells were transferred into each mouse. One day following adoptive cell transfer, I infected recipient mice with LCMV-Arm at 2 ×

10^5 PFU/mouse IP or LCMV-Cl13 at 1.14×10^6 PFU/mouse IV. I performed flow cytometry and functional characterization assays at various times post-infection (7, 15, 21, 28, 42 dpi), to analyze the $CD8^+$ T cell response in the spleen and blood. My assessments included the absolute cell numbers of responding $CD8^+$ T cells as well as the expression of surface markers (CD44, CD62L, PD-1, TIM-3, LAG-3, CD127/IL-7Rα and KLRG1). Additionally, I analyzed the expression of transcription factors (TBET, EOMES), cytokines (IFN-γ and TNF-α) and the cytolytic molecule Granzyme B, to define the $CD8^+$ T cell phenotypes.

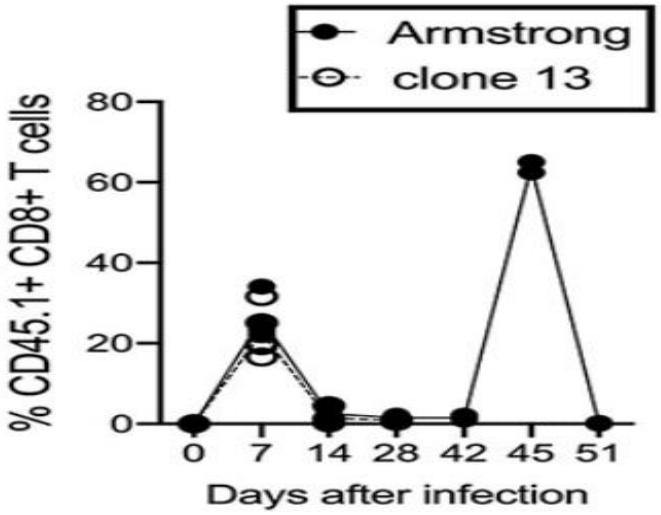

Figure 6. Kinetics of activated gp33+ specific P14 CD8+ T cells in the blood during in vivo LCMV-Arm and LCMV-CL13. Data is representative of at least 4 independent experiments (n=4 per infection type).

I observed activation and robust clonal expansion of naïve $CD8^+$ T cells upon infection with LCMV-Arm or LCMV CL13. The peak of $CD8^+$ T cell expansion was evident at day 7-8, as measured in the spleen (refer to Figure 3). These findings are consistent with previous studies utilizing this model, which have also demonstrated antigen-specific $CD8^+$ T cell expansion, with an evident peak at 7-9 dpi (14,19,47,51).

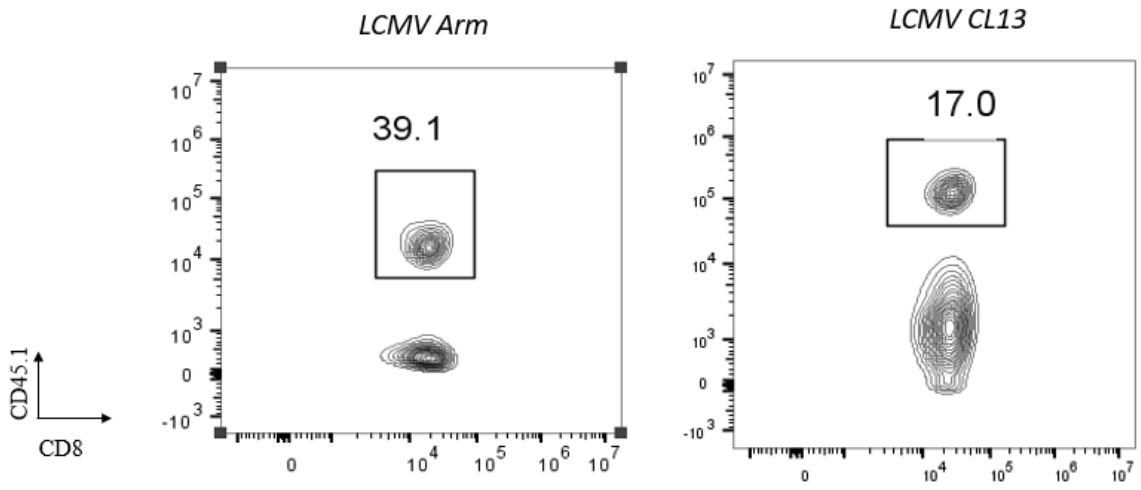

Figure 7. Frequency of antigen specific (gp33+) P14 CD8+ T cells expanding at 7 dpi in response to LCMV-Arm and LCMV-CL13 infection. Detection of antigen specific P14 $CD8^+$ T cell subsets in the spleen is determined by CD45.1+ expression. Antigen specific P14 $CD8^+$ T cells shown are gated on CD44hi CD45.1+ $CD8^+$ T cells. Data is representative of at least four independent experiments.

At 7 dpi, I observed higher frequencies of antigen-specific $CD8^+$ T cells in the spleen of mice infected with LCMV-Arm compared to those infected with LCMV-CL13 (refer to Figure 7). Following the peak of expansion, $CD8^+$ T cells underwent a contraction phase during which the majority of effector $CD8^+$ T cells were cleared from circulation. This contraction phase was observed in both acute and chronic viral infections between 8-14 dpi as expected (refer to Figure 3).

4.4 Memory Formation in LCMV-Arm

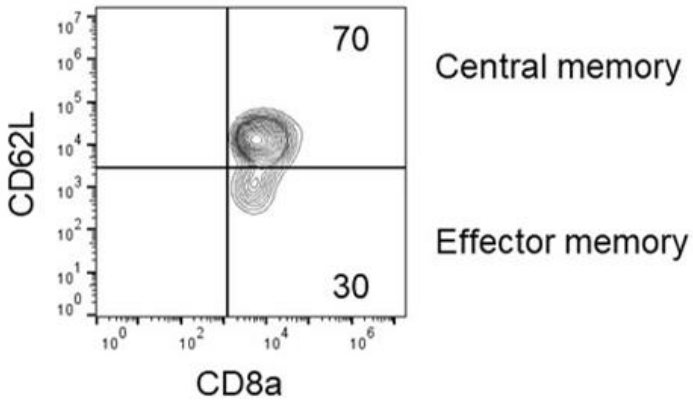

Figure 8. Frequency of antigen-specific (gp33+) memory CD8+T cells in the blood of LCMV-Arm infected recipient mice at 40 dpi. Shown are central memory CD62Lhi and effector memory CD62lo $CD8^+$ T cells, gated on $CD45.1^+$ CD44hi parental cells. Data is representative of at least two independent experiments.

In LCMV-Arm infection, memory $CD8^+$ T cells were formed and maintained as their presence could be detected in circulation at 40 dpi (refer to Figure 6 and **Error! Reference source not found.**). I confirmed the presence of circulating central memory $CD8^+$ T cells (T_{CM}) characterized by $CD62L^{hi}$ expression, as well as effector memory $CD8^+$ T cells (T_{EM}) with low CD62L expression at 40 dpi, in the blood (refer to **Error! Reference source not found.**)

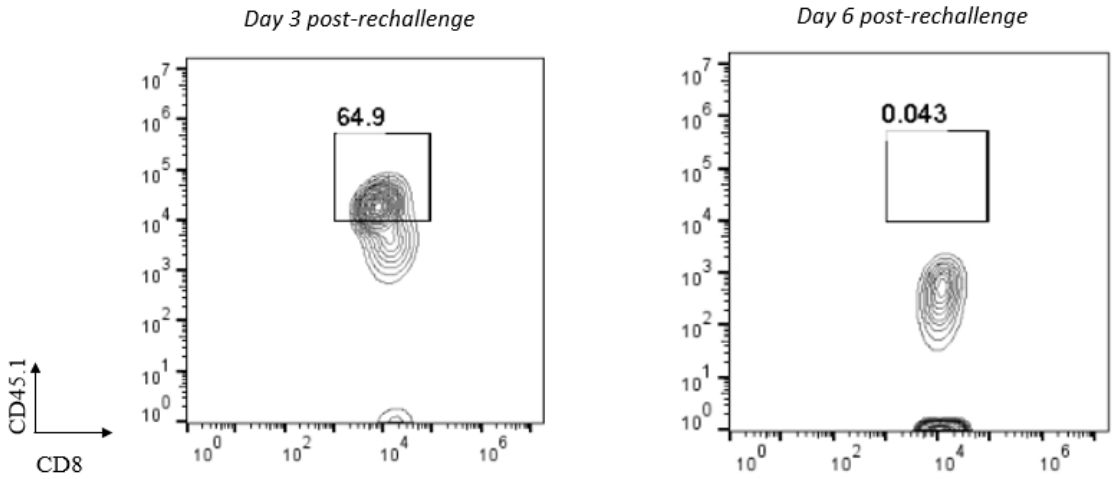

Figure 9. Frequency of antigen-specific (gp33+) memory CD8+T cells responding to a secondary LCMV infection, 3 and 6 days post re-challenge. Detection of antigen-specific memory P14 CD8+ T cell subsets in the spleen determined by CD45.1 expression. Antigen specific P14 memory CD8+ T cell sets shown are gated on CD44hi CD45.1+ CD8+ T cells. Data is representative of at least four independent experiments (n=4).

Upon re-exposure to the initial antigen, memory $CD8^+$ T cells exhibit a stronger immune response compared to the primary immune response. This phenomenon is known as the memory recall response. In this model, I observed a robust $CD8^+$ T cell recall response, reaching its peak at 3 days post-rechallenge (refer to Figure 6 and Figure 9). This finding indicates that the antigen-specific memory $CD8^+$ T cells generated in our model are functional and capable of mounting an effective immune response upon re-exposure to the same antigen.

4.5 $CD8^+$ T cell exhaustion in LCMV-CL13

4.5.1 PD-1 expression

To confirm the presence of exhausted $CD8^+$ T cells, I performed flow cytometry to compare the $CD8^+$ T cell phenotypes derived from LCMV-CL13 versus LCMV-Arm at 15 dpi.

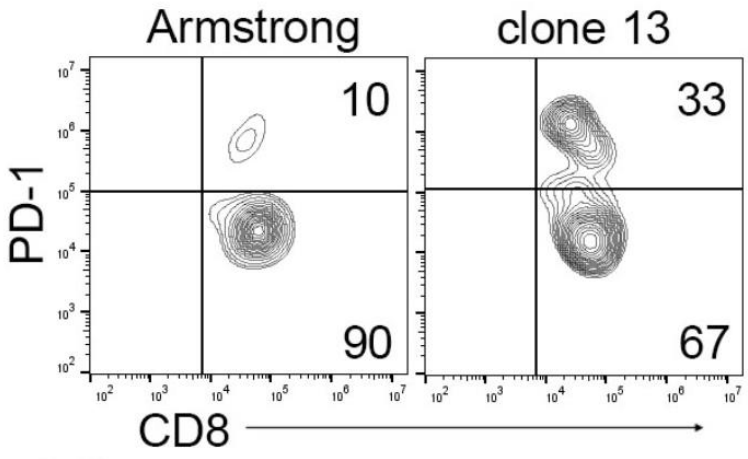

Figure 10. PD-1 expression of activated gp33+ specific P14 CD8+ T cells responding to in vivo LCMV-Arm and LCMV-CL13 infections at Day 15 post infection. Detection of exhausted antigen-specific P14 $CD8^+$ T cell subsets in the spleen determined PD-1 expression. Exhausted P14 $CD45.1^+$ $CD8^+$ T cell sets shown are gated on PD-1hiCD44hi$CD45.1^+$ $CD8^+$ T cells. Data is representative of at least two independent experiments.

At this time-point, I observed that $CD8^+$ T cells responding to chronic LCMV infection exhibited higher PD-1 expression than their counterparts in acute LCMV infection (refer to Figure 10). This finding aligns with my expectation, as PD-1 is a well-known maker a marker for monitoring T cell exhaustion in viral infections(29,38,96).Specifically, in LCMV-CL13 infection, approximately 30% of $CD8^+$ T cells demonstrated high levels of PD-1 expression, whereas only 10% of $CD8^+$ T cells exhibited high levels of PD-1 expression in LCMV-Arm infection. Since PD-1 is indicative of $CD8^+$ T cell exhaustion, these results suggest that $CD8^+$ T cells in the chronic LCMV infection are exhausted compared to those responding to acute LCMV infection.

4.5.1.1 Heterogenous exhausted CD8⁺ T cell subsets

PD-1, T-bet, and Eomes can be used to classify CD8+ T cells into distinct exhausted subsets (19,97).

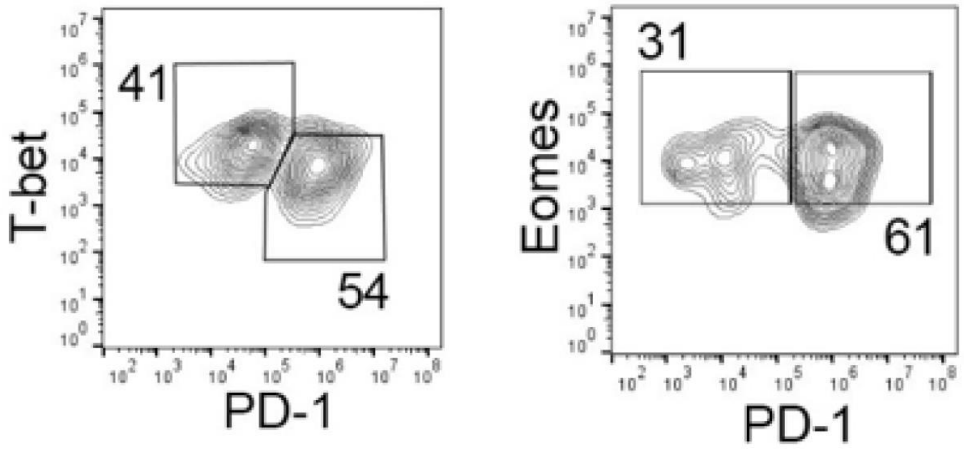

Figure 11. Frequency of exhausted P14 CD8+ T cell subsets determined by PD-1 expression with T-bet (left) and Eomes (right) in the spleen at 28 days post LCMV-CL13 infection. Detection of exhausted antigen-specific P14 CD8+ T cell subsets in the spleen determined by PD-1 expression. Exhausted P14 CD45.1+ CD8+ T cell sets shown are gated on PD-1hiCD44hiCD45.1+ CD8+T cells. Data is representative of at least two independent experiments.

In line with previous studies (29,51), I also observed heterogeneity within the PD-1⁺ CD8⁺ T cell population, evidenced by distinct subsets characterized by differential expression of T-bet and Eomes as shown in Figure 11.

4.5.2 Decreased production of pro-inflammatory cytokines

A characteristic feature of exhausted CD8⁺ T cells is their diminished ability to produce intracellular cytokines compared to functional effector CD8⁺ T cells (34,35).

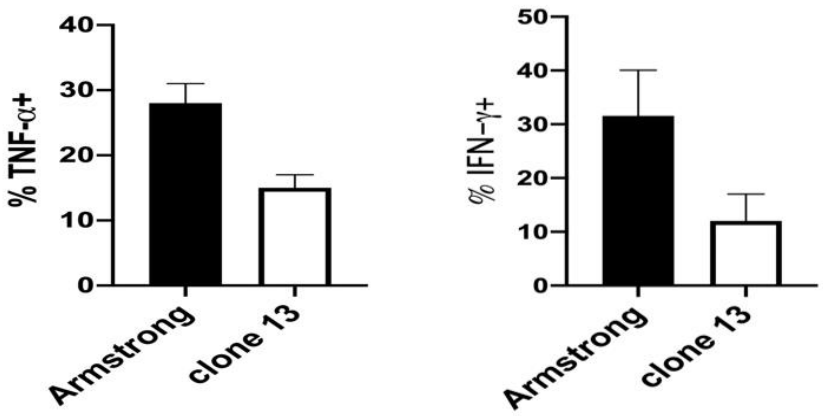

Figure 12. Frequency of antigen specific P14 CD8+T cells producing TNF-α(left) and IFN-γ(right) in response to in vivo LCMV-Arm and LCMV-CL13 infections at 15 dpi. Detection of antigen specific P14 CD8+ T cell subsets in the spleen are determined by CD8+ CD45.1+ expression. Cytokine producing T cells shown are gated on TNF-αhi and IFN-γhi CD45.1+ CD8+ T cells. Data is representative of at least two independent experiments.

As depicted in Figure 12 above, I observed notable differences in the frequency of $CD8^+$ T cells expressing pro-inflammatory cytokines, IFN-γ and TNF-α, between acute and chronic LCMV infections at 15 dpi. Specifically, the frequency of $CD8^+$ T cells producing TNF-α in response to LCMV-Arm was 28% compared to a lower frequency of 15% in response to LCMV-CL13. Similarly, the frequency of $CD8^+$ T cells producing IFN-γ in response to LCMV-Arm was 30% compared to 10% in response to LCMV-CL13. Decreased cytokine production in chronic LCMV at 15 dpi is an indication of functional exhaustion.

4.6 Validation of effector, memory and exhausted CD8⁺T cells

To ensure the reliability of my findings, I assessed the expression of a subset of genes with known roles in effector-, memory- and exhausted-CD8⁺ T cell differentiation during LCMV infection. I generated cDNA libraries of naïve and activated antigen-specific CD8⁺ T cells isolated later after infection as described in the Materials and Methods section. We examined the scRNA-seq dataset for the expression of effector, memory and exhausted associated genes at Day 7 (effector), Day 28 (exhausted) and Day 40(memory). This analysis confirmed that the gene expression patterns we observed in the CD8⁺ T cell subsets aligned with previous reports(19,29,47).

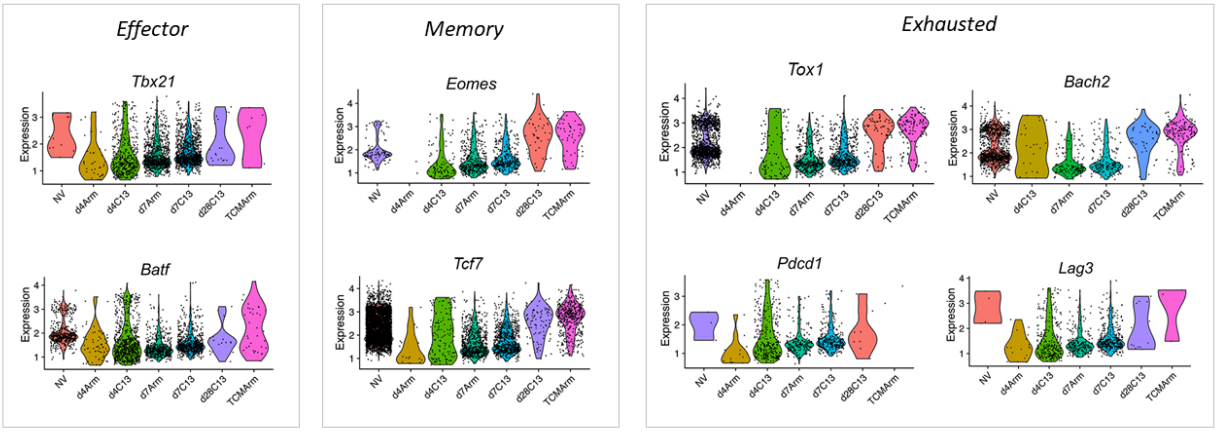

Figure 13. Violin plots illustrating the expression of selected CD8⁺ T cell effector, memory, and exhausted associated genes.

Figure 13 shows violin plots illustrating the expression patterns of selected genes associated with CD8⁺ T cell effector, memory, and exhausted phenotypes. The expression of specific terminal effector-associated genes, such as *Batf* and *Tbx21*, was absent in naïve cells and gradually increased as the cells approached the terminal effector phase, 7 dpi. Furthermore, the expression of exhausted-associated genes, including *Pdcd1, Tox1, Bach2* and *lag-3*, were highest in the exhausted T cell subpopulation (d28CL13)(refer to Figure 13). Conversely,

memory-associated genes including *Tcf7* and *Eomes* displayed high expression levels in naïve cells, but decreased during effector-phase and were robustly re-expressed in memory cells (refer to Figure 13). These findings demonstrate that the expression of well-known $CD8^+$ T cell effector-associated, exhausted-associated and memory-associated genes can be detected at the single-cell level using our methods and aligns with previous studies (19,29,47), providing further validation to our findings.

5 Early $CD8^+$ T cell responses

5.1 Rationale

Early $CD8^+$ T cell responses to LCMV-Arm and LCMV-CL13 including activation and interaction with APCS such as DCs and macrophages, are critical parameters in determining the outcome of infection. Early CTL responses may play a role in initiating robust adaptive immune responses that clear LCMV-Arm. On the contrary, these early CTL responses may be less effective in mounting strong and hinder the ability of the immune system to clear LCMV-CL13. Although much of the CTL responses to LCMV-Arm and LCMV- CL13 have been elucidated at later stages of infection, there is a gap in the understanding of early $CD8^+$ T cell responses. A thorough comprehension of the cellular interactions involved in early CTL responses can give insight into how some viral infections can become chronic while others are resolved. In line my hypothesis that $CD8^+$ T cell exhaustion may develop in the early phases of a developing infection, I analyzed $CD8^+$ T cell response characteristics at early time points (18h, 36h, 48h and 4 days) post LCMV-Arm and LCMV-CL13.

5.2 Early Cell Division Profiles

In this study, I performed CFSE proliferation assays to analyze $CD8^+$ T cells undergoing early cellular divisions in response to either LCMV-Arm or LCMV-CL13 infections. CFSE proliferation assays are a commonly used technique in immunology to measure the proliferation of lymphocytes in response to various stimuli such as pathogens, vaccines, and immunotherapies. The assay is based on the incorporation of CFSE into daughter cells, which fluoresces at a specific wavelength when excited by light. As the cells divide, the fluorescence intensity decreases due to the dilution of CFSE among the daughter cells. The decrease in fluorescence intensity serves as a measure of cell proliferation(98).

To identify cells undergoing cellular divisions at early time points, I first labelled $CD8^+$ P14 T cells with CFSE prior to transfer. I validated CFSE fluorescent intensities of naïve CD8+ T cells using flow cytometry prior to transfer. I transferred a total of 1×10^6 cells CFSE-labeled antigen-specific $CD8^+$ T cells per mouse into recipient mice. One day following cell transfer, I infected with LCMV-Arm at 2×10^5 PFU/mouse IP or LCMV-Cl13 at 1.14×10^6 PFU/mouse as previously described in (91). For controls, naïve ($CD44^{lo}CD62L^{hi}$) CFSE-labelled $CD8^+$ P14 T cells were adoptively transferred into uninfected mice and isolated at 36 and 48h post-cell transfers. The fluorescence intensity of the cells was measured at 18, 36, and 48 hours after LCMV-CL13 infection and 48 h after LCMV-Arm infection, in line with previous studies by (14,91).

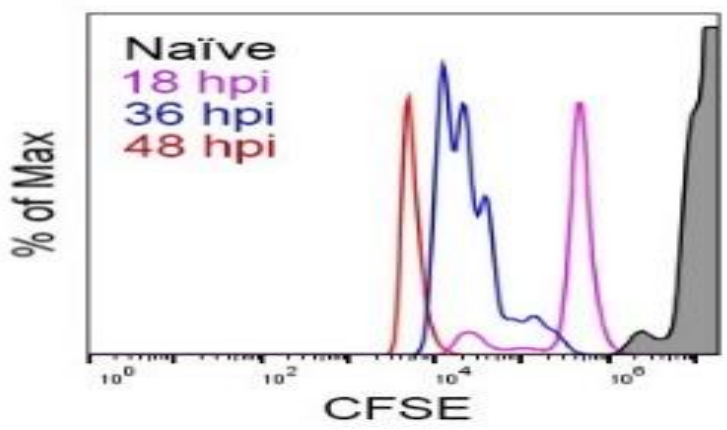

Figure 14. CFSE proliferation profile of activated antigen specific (gp33+) P14 CD8+ T cells responding to in vivo LCMV-CL13 at early time-points. Antigen-specific cells were isolated at 18 hpi (pink), 36 hpi (blue), and 48 hpi (red). Shown in gray are inactivated, CFSE-labeled naïve P14 $CD8^+$ T cells prior to cell transfer. Data is representative of at least three independent experiments.

Results were presented in a histogram showing the distribution of fluorescence intensities of the cells, indicating the extent of cell divisions (refer to Figure 14). Majority of the naïve CFSE-labelled $CD8^+$ T cells (shaded grey) exhibited high fluorescence intensities, indicating they had not undergone cell divisions. This confirms that the naïve $CD8^+$ T cells were not activated before the infection. In contrast, activated $CD8^+$ T cells showed lower fluorescence intensities, indicating that they underwent cell divisions following LCMV-Arm and LCMV-CL13 infections.

The CFSE proliferation assays revealed interesting differences in the proliferation profiles of $CD8^+$ T cells responding early to LCMV-Arm versus LCMV-CL13. Notably, $CD8^+$ T cells responding to LCMV-CL13 were dividing earlier (36 hpi) than those in the LCMV-Arm infection (48 hpi) Figure 14. I don't see LCMV-Arm in Figure 11?The early cellular divisions observed at 48h post-LCMV-Arm infection are consistent with observations made in previous scRNAseq analyses studies (14,91).

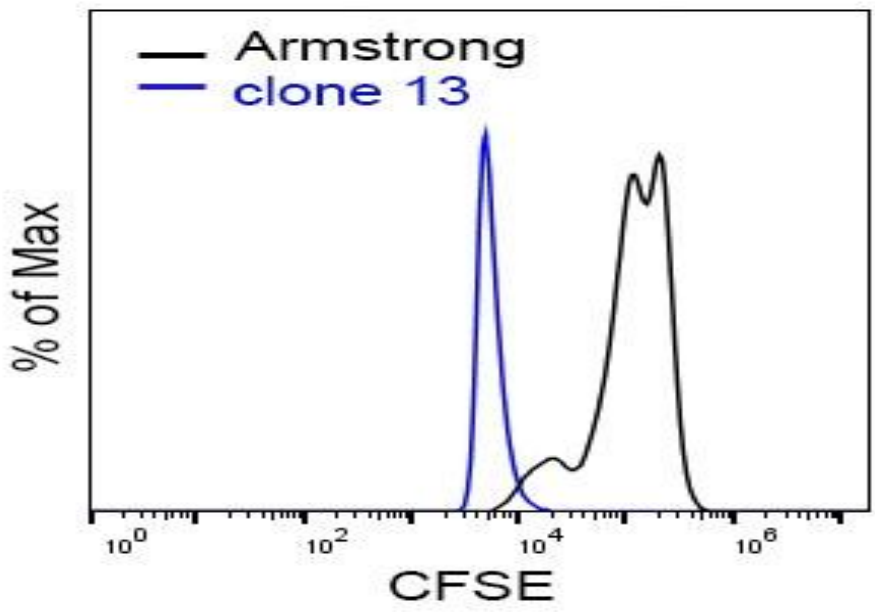

Figure 15. CFSE proliferation profile of activated gp33+ specific P14 $CD8^+$T cells responding to *in vivo* LCMV-Arm and LCMV-CL13 infections at 48 hpi.

Interestingly, $CD8^+$ T cells responding to LCMV-CL13 were not undergoing cellular divisions at 48hpi (refer to Figure 15), as evidenced by lack of multiple-peaks on the histogram, at that time-point. This finding suggests a distinct kinetic pattern of $CD8^+$ T cell response to LCMV-CL13 compared to LCMV-Arm, in that division events occur earlier in the chronic infection.

Collectively, these findings provide preliminary insight into the early dynamics of responding $CD8^+$ T cells and their proliferation patterns in response to LCMV-Arm versus LCMV-CL13.

5.2.1 Viral load at early time-points

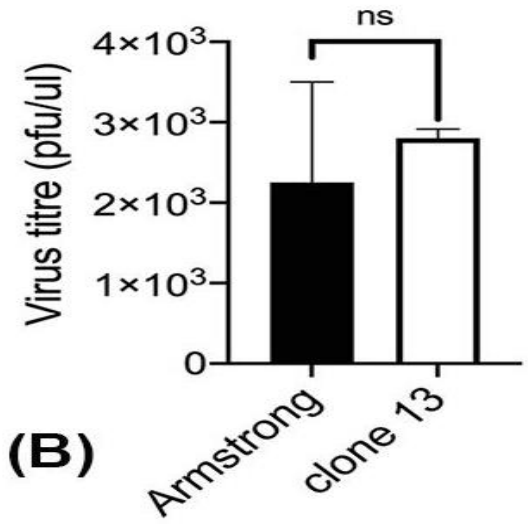

Figure 16. Levels of replicating virus 36 hpi in sera of male P14 mice infected with either LCMV-Arm (shaded) or LCMV-CL13.

To assess whether the variations in infection doses and routes influenced the viral antigen load and subsequently $CD8^+$ T cell proliferation, I performed plaque assays at designated early time-points. I evaluated the presence of replicating virus at 36 hours following LCMV-CL13 infection and 48 hours after LCMV-Arm infection, as described in the methods section. Results showed no statistically significant differences in levels of replicating virus in the sera, between the two time points (refer to Figure 16).

5.3 Early Transcriptional Profiles

To further explore the hypothesis that $CD8^+$ T cell exhaustion may be specified during early stages of a developing infection, we conducted a comprehensive analysis of the transcriptional profiles of antigen-specific $CD8^+$ T cells responding at specific time-points post-infection. These included: during the early phase (Day 4), at the peak of infection (Day 7) and at later time points (Day 28-LCMV-CL13 and Day 40-LCMV-Arm) after LCMV-Arm or LCMV-CL13 infection. At day 28 post LCMV-CL13, I was able to isolate and detect functionally exhausted $CD8^+$ T cells from total splenocytes and blood. At Day-40 post LCMV-Arm infection, I was able to isolate and identify central memory $CD8^+$ T cells from total splenocytes and

blood. My main objective was to determine whether there were differences in the transcriptional signatures of $CD8^+$ T cells generated in acute versus chronic LCMV infection using our model, specifically during the early phases of infection. I hypothesized that distinct $CD8^+$ transcriptional profiles in the early stages of LCMV-CL13 could be predictive of $CD8^+$ T cell exhaustion. This projection is in line with a recent observation that precursors of exhausted $CD8^+$ T cells can be identified as early as after the first cell division (1).

To do this, I adoptively transferred 20,000 (for day 4 harvest) and 5000 $CD8^+CD45.1^+$ P14 T cells for later time-points (Day 7, Day 28 and Day 40), from female P14 donor mice into separate age-matched $CD45.1^+$ male recipients. 24 hours later, I infected recipient mice with LCMV-Arm or LCMV-CL13, as outlined in the Materials and Methods section. I harvested splenocytes at the designated time points after infection. Donor P14 $CD8^+$ T cells were FACS-isolated followed by generation of single-cell cDNA libraries using the 10x Genomics Chromium platform. Of note, I was unable to sort sufficient cell numbers of $CD8^+$ T cells undergoing early cellular divisions following infection. Thus, I focused on day 4 as the earliest time-point for scRNA-seq analysis. The target cell recovery for sc-cDNA library generation ranged 6000 – 10000 single $CD8^+$ T cells. Quality control measures of the single-cell cDNA libraries were performed on the 2100 Bioanalyzer (Agilent Technologies) and Qubit 4.0 Fluorometer (Thermo Fisher Scientific). Single-cell cDNA libraries were sequenced (50000 paired-end reads, single-indexing) on the NovaSeq 6000 at Genome Quebec. The resulting RNA-seq data was pre-processed to remove low-quality cells and to filter out lowly expressed genes. The data set consisted of approximately 29000 cells. We performed t-SNE (t-Distributed Stochastic Neighbor Embedding) analysis using R Seurat v4.3.0, enabling the visualization of gene expression profiles of all the individual cells collected at the different time points on a two-dimensional plot.

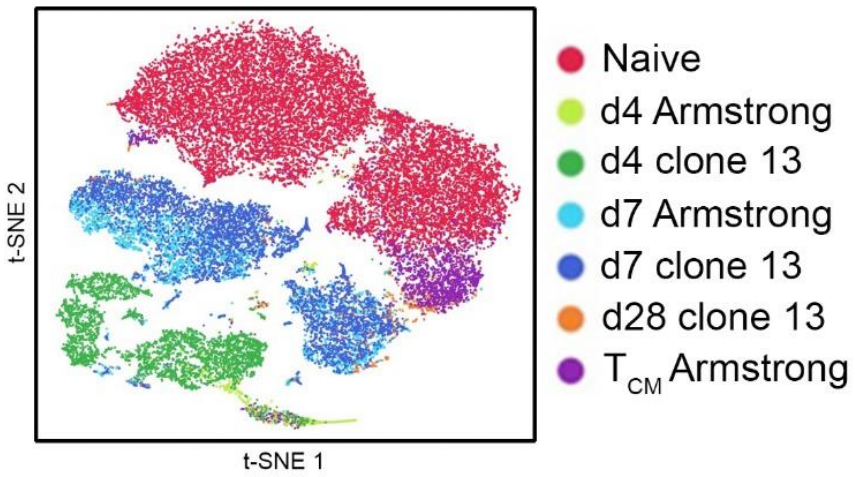

Figure 17. tSNE showing transcription profiles of CD8⁺T cells responding at day 4, day 7, day 28 and day 40 post infection.

Figure 17 displays the t-SNE plot, where each dot represents a single cell, and the color of the doe corresponds to its assigned cluster. Distinct clustering of cells into the following groups is observed: naïve (red), d4-LCMV-Arm (light green), d4-Cl13 (dark green), d7-LCMV-Arm (light blue), d7-CL13 (dark blue), d28-CL13 (orange) and d40-LCMV-Arm (Purple). This t-SNE plot provides a global visualization of the transcriptional profiles of $CD8^+$ T cells responding to acute versus chronic infection, facilitating the identification of distinct cell populations at different time points. The t-SNE analysis of the scRNA-seq data highlights interesting findings regarding the gene expression profiles of $CD8^+$ T cells. Notably, cells from different time points cluster separately, indicating that their gene expression profiles undergo changes over time. For instance, cells collected at Day 0 (naïve) cluster together in one area of the plot, while cells collected at Day 28-CL13 and Day 40-LCMV-Arm cluster in a separate area. This data suggests that genes expressed in the naïve cells differs from those expressed in cells responding at Day 28(CL13) and Day 40(LCMV-Arm). Interestingly, we observed similar gene expression profiles of responding $CD8^+$ T cells from d7 LCMV-Arm (lighter blue) and d7 clone 13 (darker blue), as reflected in their overlapping clusters. This suggests that there may

be shared molecular mechanisms underlying the response of the antigen-specific $CD8^+$ T cells to both chronic and acute LCMV infections at the peak of infection.

Importantly, our analysis also revealed distinct transcriptional profiles of $CD8^+$ T cells responding to LCMV-Arm versus LCMV-CL13 at Day 4. As seen on the t-SNE plot, d4 Armstrong (lighter green) clusters separately from d4 Clone 13(darker green). This suggests that the transcriptional divergence of $CD8^+$ T cells responding to acute versus chronic LCMV occurs early in the infection process. $CD8^+$ T cells responding to LCMV-Arm versus LCMV-CL13 may be progressing along different differentiation paths at 4 dpi, which could contribute to the distinct outcomes observed in the acute versus chronic LCMV infections. The distinct clustering of $CD8^+$ T cells responding to LCMV-Arm versus LCMV-Cl13 at 4 dpi, as observed in the t-SNE analysis, aligns with previous findings reported in recent studies (15,45,94). This consistency in clustering patterns reinforces the notion that $CD8^+$ T cells responding to LCMV-CL13 and LCMV-Arm infections exhibit unique transcriptional profiles during early phases of the infection.

5.3.1 Distinct biological pathways at 4 dpi

To further investigate early $CD8^+$ T cell responses between the two infection types, we analyzed the differentially expressed genes (DEGs) between the two Day 4 clusters of $CD8^+$ T cells responding to LCMV-Arm versus LCMV-CL13.

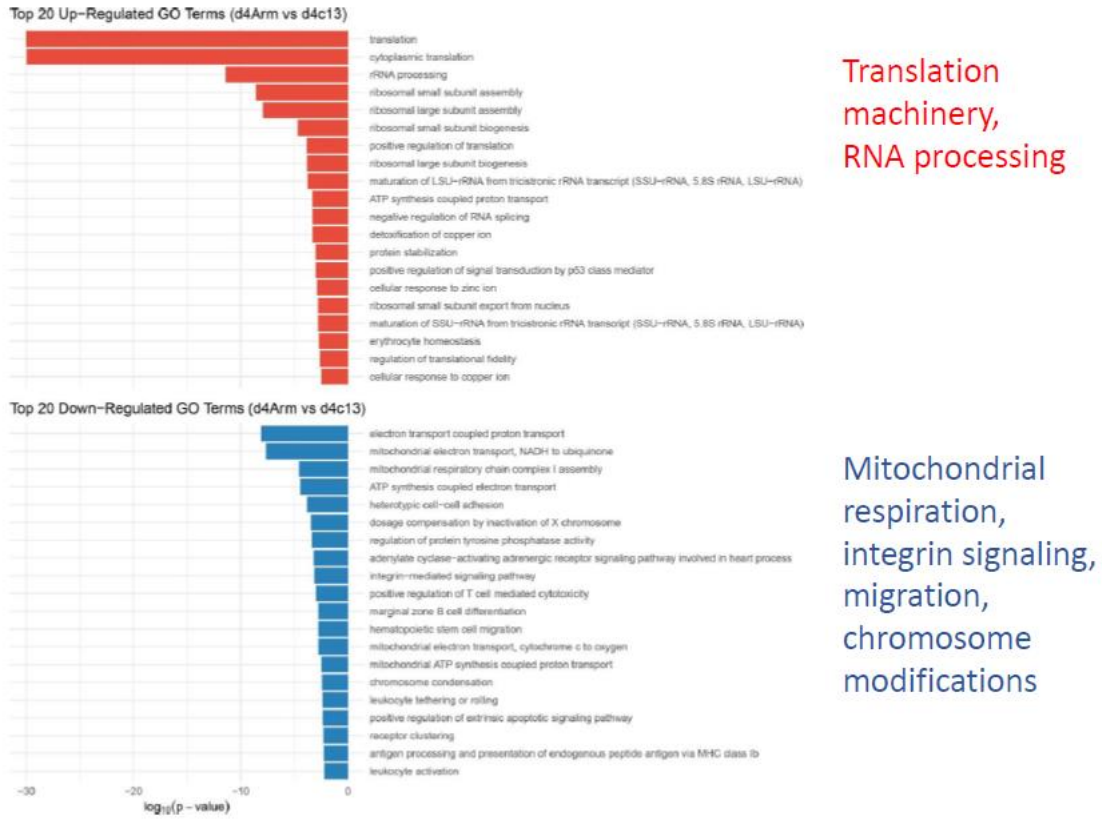

Figure 18. Gene Ontology analysis showing biological pathways in acute vs. chronic LCMV infection at Day 4 post-infection

Gene ontology analysis identified the enriched biological pathways associated with each infection type (refer to Figure 18). In LCMV-Arm infection, there is an upregulation of genes involved in translation machinery and RNA processing. This finding suggests that at this early time point (Day 4), $CD8^+$ T cells in LCMV-Arm infection may be engaged in robust protein synthesis and RNA processing, likely to support effector functions such as production of cytolytic enzymes and pro-inflammatory cytokines. On the other hand, at Day 4 post LCMV-CL13 infection, $CD8^+$ T cells shows a shift towards mitochondrial respiration, integrin signaling, migration and chromosome modifications. This suggests that $CD8^+$ T cells responding to LCMV-CL13 at Day 4 exhibit a different metabolic profile, potentially reflecting early signs of altered migratory capacity and cellular exhaustion.

Taken together, the different biological pathways enriched in each infection type at Day 4 provide valuable insights into the early molecular events that shape the subsequent CTL responses and potentially contribute to the establishment of distinct $CD8^+$ T cell fates and functional outcomes in acute versus chronic LCMV.

5.3.1.1 Integrin signalling upregulated in Day 4 LCMV-CL13

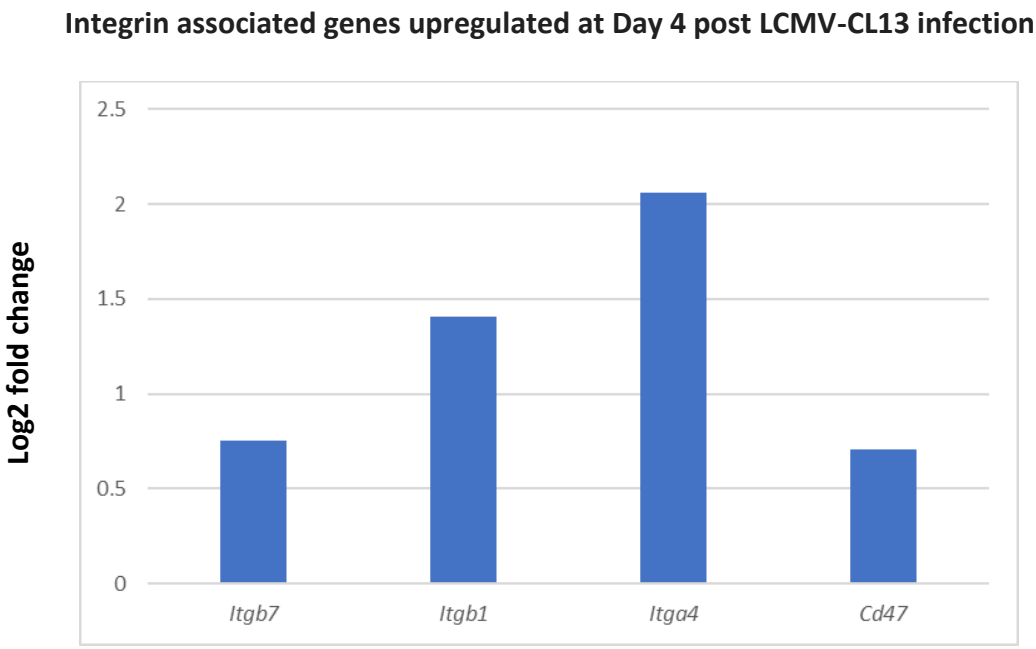

Figure 19. Genes associated with integrin signalling upregulated at day 4 post LCMV-CL13

Further analysis of DEGs between $CD8^+$ T cells responding to LCMV-CL13 versus LCMV-Arm at 4 dpi revealed that genes encoding integrins, such as, *itgb1, itgb7, itga4* and *Cd47*, were highly expressed in $CD8^+$ T cells in the LCMV-CL13 infection (refer to Figure 19). Integrins are cell surface receptors that mediate the adhesion of activated T cells to vasculature and their extravasation into tissues (51). Additionally, *Cd47*, also known as Integrin-Associated Protein (IAP), was significantly upregulated in Day 4 LCMV CL13 (refer to Figure 19). Research has shown that CD47 can regulate integrin activity by associating in cis with β1, β2 and β3 integrin conformations. CD47–integrin interactions modulate adhesive functions of T cell, thereby playing a critical role in T cell recruitment and trans-endothelial migration(99).

The upregulation of integrin-associated genes in $CD8^+$ T cells responding to LCMV-CL13 infection at 4 dpi suggests they may have enhanced adhesion properties and migratory capabilities compared to $CD8^+$ T cells in LCMV-Arm infection at the same time-point. The increased expression of integrin genes in $CD8^+$ T cells during LCMV-CL13 infection may contribute to their recruitment and localization at specific sites of infection in the spleen and enhance their interactions with APCs such as DCs. Altogether, these findings highlight the potential importance of integrin signaling in the early responses of $CD8^+$ T cells to LCMV-CL13 infection.

6 Sex-based differences in $CD8^+$T cell responses to viral infection

6.1 Rationale

Sex-based differences in immune responses have been widely reported in various infectious diseases and autoimmune disorders. In the context of viral infections like HIV and HCV, the role of sex in influencing disease susceptibility and outcomes has received increasing attention. $CD8^+$ T cells play a crucial role in controlling viral infections by recognizing and eliminating virus-infected cells. Investigating sex-based differences in $CD8^+$ T cell responses to viral infection can provide valuable insights into the mechanisms that underlie sex disparities in susceptibility and disease outcomes of viral infections.

The second key objective of this study was to characterize sex-based differences of $CD8^+$T cell responses to LCMV infection. To achieve this, a sex-based approach was incorporated into the established LCMV model system. This involved adoptive cell transfer experiments of female donor cells-to-female recipients (F-F) and male donor cells-to male recipients (M-M).

Adoptively transferring female or male or a combination donor transgenic CD8^{+}T cells into male recipients(F-M) has been the standard approach for this model system in the field (14,15,47,91), precluding the ability to perform sex-disaggregated analysis, thus the investigation of how biological sex influences CD8^{+} T cell responses in acute versus chronic infection remains unknown.

Sex-based LCMV Experimental Model

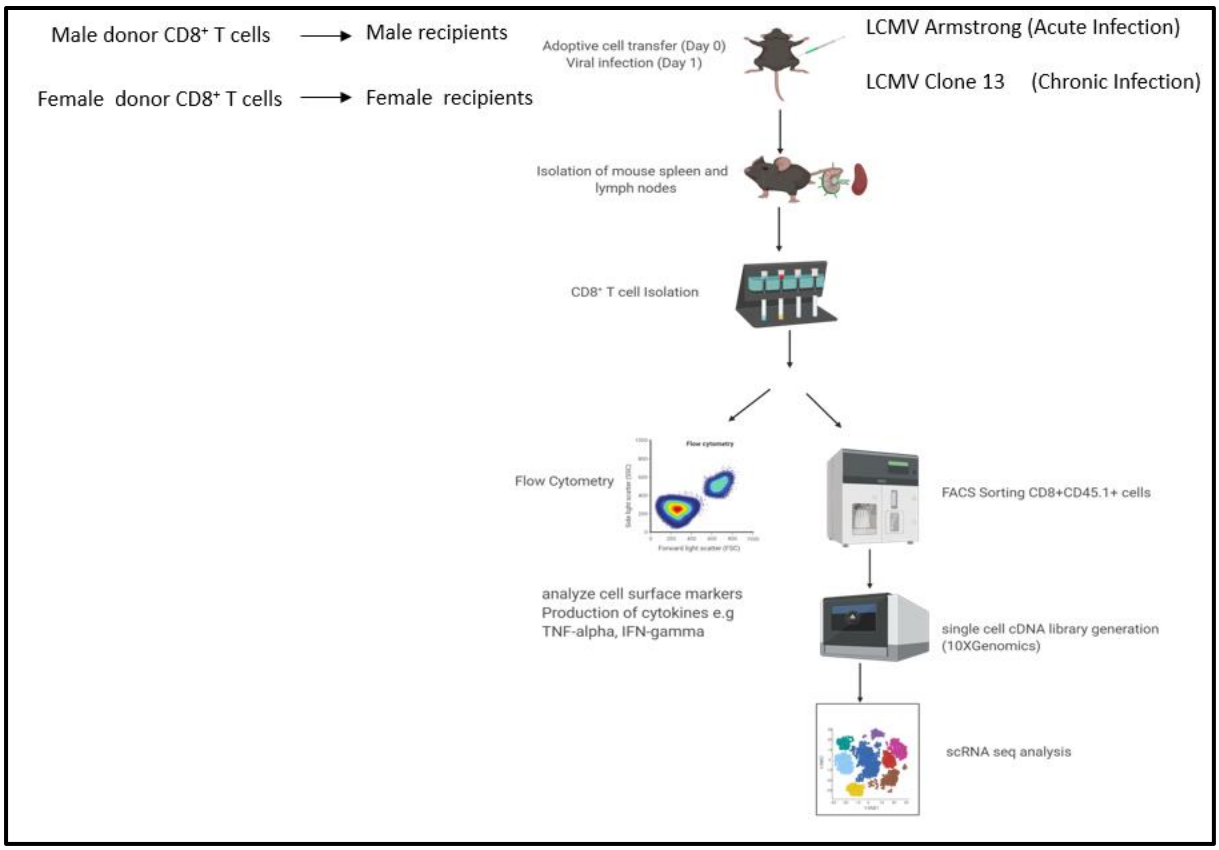

Figure 20. Sex-based LCMV Experimental Model. This figure depicts the experimental model system utilized for *in vivo* sex-based LCMV studies. The diagram includes the following key components: donor and recipient mice genotypes, LCMV viral strains and significant time-points post-infection.

6.2 Sex-based differences in CD8⁺ T cell expansion during acute and chronic viral infection

In this analysis, I first looked at the production of pro-inflammatory cytokines and the CD8⁺ T cell expansion at the peak of infection (Day 7) after acute and chronic LCMV infection.

Figure 21. Frequency of female and male CD8+CD45.1+ T cell expansion at Day 7 post LCMV-Arm and LCMV CL13 infection. Detection of antigen-specific P14 CD8⁺ T cell subsets in the spleen determined by CD45.1 expression. Antigen specific P14 CD45.1⁺ CD8⁺ T cell sets shown are gated on CD44hi CD45.1⁺ CD8⁺ T cells. Data is representative of at least two independent experiments (n=4-5). Student's unpaired t-test, $p<0.05$* is significant, $p<0.01$ ** is very significant, $p>0.05$ is ns, not significant.

In the LCMV-CL13 infection, male CD8⁺ T cells exhibited greater expansion than their female counterparts at 7 dpi. A similar trend of greater expansion in male CD8⁺ T cells was observed in the LCMV-Arm infection at the same time-point (refer to Figure 21). These results highlight sex-based differences in the CD8⁺ T cell expansion following chronic LCMV infection, with males exhibiting a more robust response. The observed trend in the LCMV-Arm infection further supports this notion, although further investigation may be required to determine the statistical significance.

6.3 Sex-based differences in intracellular cytokine profiles of responding CD8⁺ T cells during acute and chronic viral infection

Figure 22. Frequency of female and male P14 CD45.1+ CD8+ T cells producing TNF-α in response to in vivo LCMV-Arm and LCMV-CL13 at Day 7. Detection of antigen-specific P14 CD8⁺T cell subsets in the spleen is determined by CD8 CD45.1 expression. Cytokine producing T cells shown are gated on TNF-αhi CD45.1⁺ CD8⁺ T cells. Data is representative of at least two independent experiments (n=4-5).

As seen in Figure 22, I observed a notable difference in the frequencies of TNF-α expressing CD8⁺ T cells between males and females. Specifically, we observed a higher frequency of female CD8⁺ T cells expressing TNF-α compared to males, at the peak of LCMV-Arm infection (Day 7). However, the sex-based difference in TNF-α expression was not observed in the LCMV-CL13 infection. TNF-α is an important pro-inflammatory cytokine that plays a role in the inflammatory response and cell-mediated cytotoxicity. CD8⁺ T cells and other immune cells, express known TNF-α receptors, TNFR1 and TNFR2. TNF signalling can influence differentiation and functional properties of CD8⁺ T cells, mediating downstream CTL responses (100). The increased frequencies of TNF-α expressing CD8⁺ T cells in females during LCMV-Arm suggest that female CD8⁺ T cells may have a greater capacity to produce TNF-α upon activation than their male counterparts, thereby eliciting a more robust pro-

inflammatory. However, the downstream effects of TNF-α signalling in CD8⁺ T cells are complex and involve interactions with other immune cells, cytokines and signalling pathways. Further research is needed to fully understand the implications of the observed sex-based differences in TNF-α expression by CD8⁺ T cells during acute LCMV-infection, including the downstream effects on CTL responses and viral control.

6.4 Sex-based differences in single CD8⁺ T cell gene expression profiles during acute and chronic LCMV infection

As we found early differences in the transcriptional profiles of responding CD8⁺ T cells in acute versus chronic infection Figure 17, we next sought to investigate whether biological sex influences this disparity. To accomplish this, I performed sex-based LCMV experiments as depicted in Figure 20. I generated single-cell- cDNA libraries of female and male CD8⁺ T cells at 4 and 7 dpi with both LCMV-Arm and LCMV-CL13.

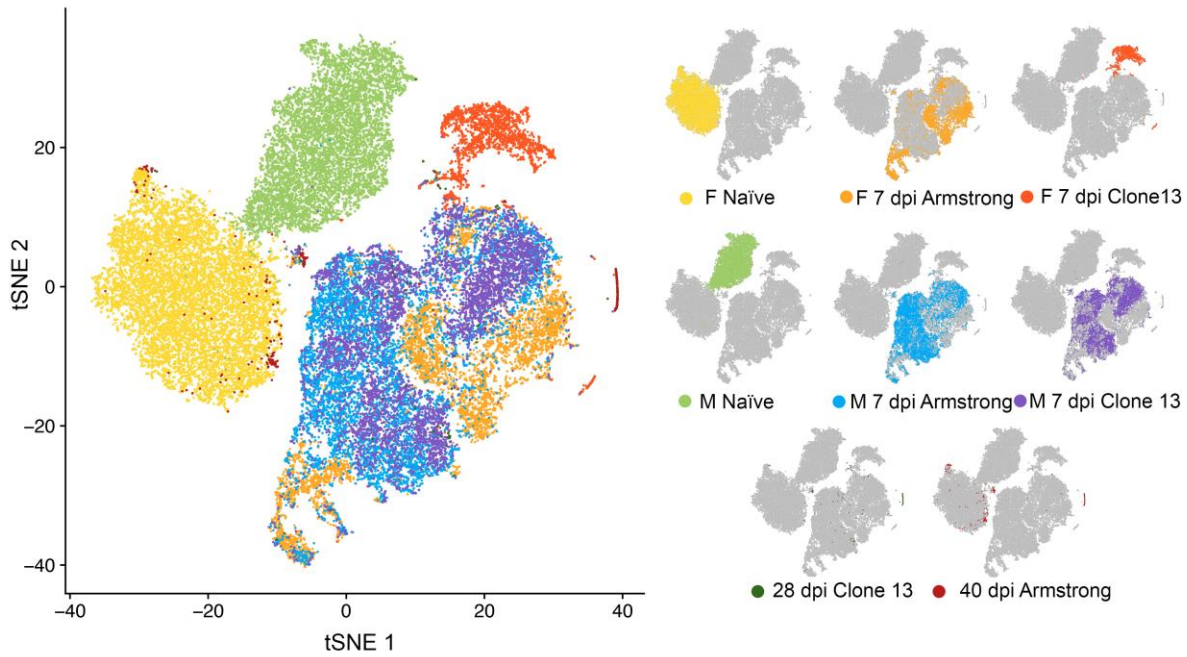

Figure 23. tSNE projection of single-cell RNA-seq profiles from female and male P14 CD8⁺ T cells responding to LCMV-ARM and LCMV-CL13 at 4 and 7 dpi, colored by cluster.

The t-SNE analysis of scRNA-seq data revealed distinct clustering of female and male $CD8^+$ T cells at naïve time-point, day 4 and day 7. Female and male cells collected at Day 0 (Female Naïve in yellow and male naïve in green) were in proximity to one another, yet clustered separately. This finding suggests that the transcription profiles of naïve female and male $CD8^+$ T cells are similar in gene expression when compared activated cells, but differ between sexes. At 7 dpi, which corresponds to peak of infection, male and female $CD8^+$ T cells responding to LCMV-Arm versus LCMV-CL13 clustered separately. In the acute infection, female d7-LCMV-Arm (orange) cluster separately from male d7-LCMV-Arm (light blue). During chronic LCMV, female d7-LCMV-CL13 (red) are distinct from male-d7-CL13 (purple) (refer to Figure 23).

Interestingly, the transcription profiles of male $CD8^+$ T cells responding to LCMV-Arm and LCMV-CL13 at 7dpi overlap. As seen on the t-SNE projection, the male-d7-CL13 (purple) cluster overlaps with the male d7-LCMV-Arm (light blue) cluster. On the other hand, there is a distinct separation between transcription profiles of female $CD8^+$ T cells responding to LCMV-Arm (female d7-LCMV-Arm in orange) and LCMV-CL13 (female d7-LCMV-CL13 in red) at 7dpi. The overlap between male $CD8^+$ T cell profiles in acute and chronic LCMV infections indicates that the male $CD8^+$ T cell responses may be similar in both infection types. On the contrary, the clear separation of female $CD8^+$ T cell profiles between acute and chronic LCMV infections indicate a unique response pattern to each infection type in the female mice.

To further interrogate the distinct clustering of female and male $CD8^+$ T cells responding at peak of infection, we analyzed the DEGs between male and female $CD8^+$ T cells at 7 days post both LCMV-Arm and LCMV-CL13 infections. Gene ontology analysis of the DEGs

identified different biological pathways enriched in female and male CD8^{+} T cells based on the infection type.

Figure 24. Gene Ontology analysis showing biological pathways in male and female CD8+ T cells responding to LCMV-Arm at Day 7 post-infection. In red are the biological pathways upregulated in female vs male, while blue represents the biological pathways upregulated in male vs female CD8+ T cells.

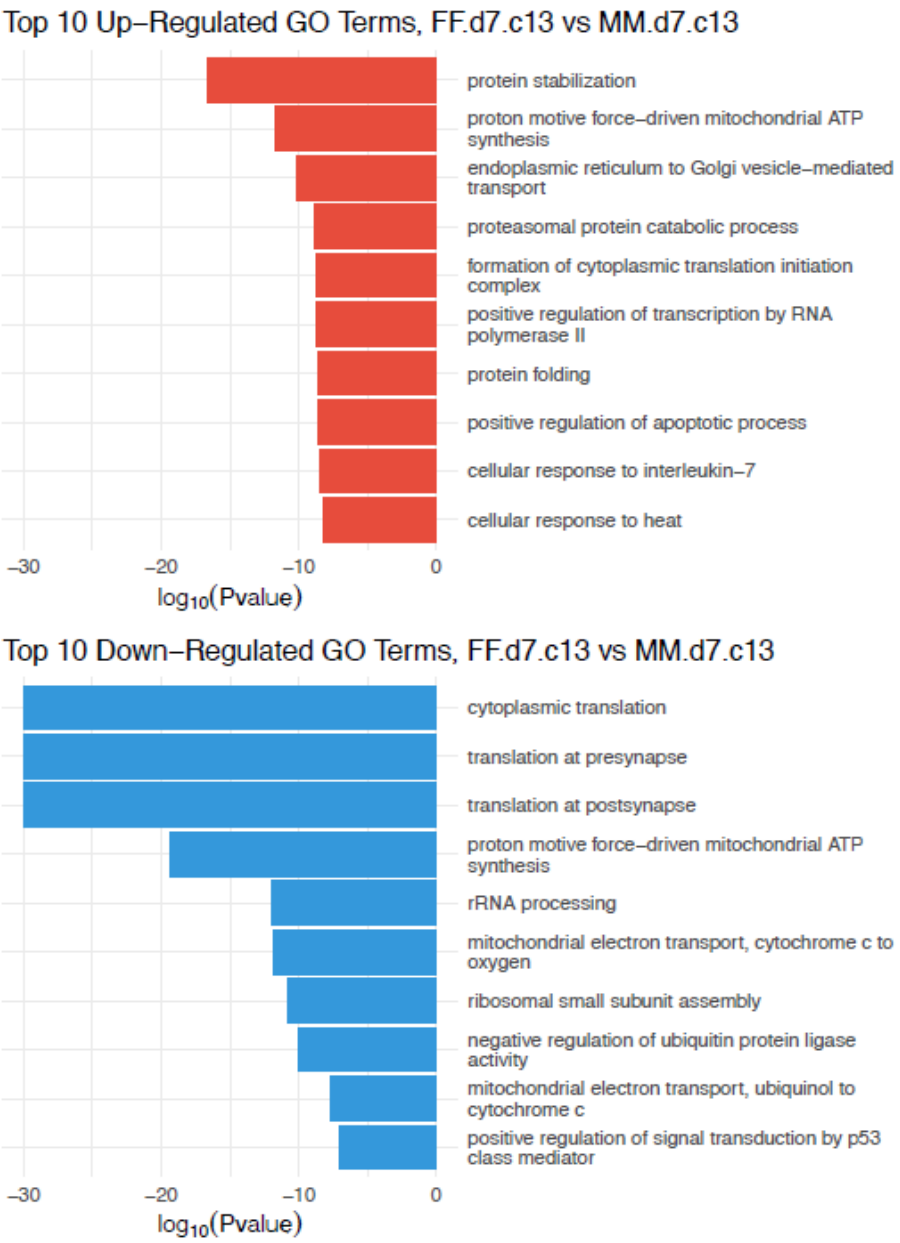

Figure 25. Gene Ontology analysis showing biological pathways in male and female CD8⁺ T cells responding to LCMV-CL13 at Day 7 post-infection. In red are the biological pathways upregulated in female vs male, while blue represents the biological pathways upregulated in male vs female CD8⁺ T cells.

At Day 7, there is an upregulation of genes involved in different biological pathways in female versus male CD8⁺ T cells and these vary based on the infection type (refer to Figure 24 and Figure 25). In response to LCMV-Arm, female CD8⁺ T cells shows a shift towards proton motive force-driven mitochondrial ATP synthesis, negative regulation of chromosome organization and regulation of plasma membrane repair. In contrast, male CD8⁺ T cells

responding to LCMV-Arm at day 7 show upregulation of genes involved in cytoplasmic translation, translation at pre-synapse and translation at post-synapse. In response to LCMV-CL13, female CD8$^+$ T cells shows a shift towards protein stabilization, proton motive force-driven mitochondrial ATP synthesis, and endoplasmic reticulum to Golgi vesicle-mediated transport. In contrast, male CD8$^+$ T cells responding to LCMV-Arm at day 7 show upregulation of genes involved in cytoplasmic translation, translation at pre-synapse and translation at post-synapse.

These results highlight that the mechanisms modulating CD8$^+$T cell responses to chronic and acute LCMV infections, including gene expression, signalling pathways and interactions with other immune cells are differentially regulated between males and females.

6.4.1 Early sex-based differences in CD8$^+$T cell responses

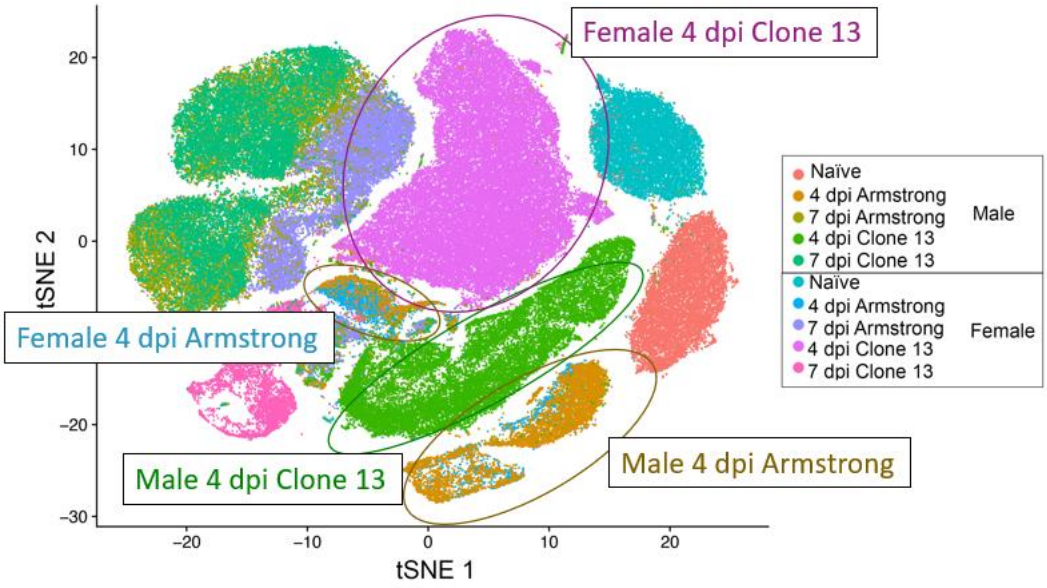

Figure 26. tSNE projection of single-cell RNA-seq profiles from female and male P14 CD8$^+$T cells responding to LCMV-ARM and LCMV-CL13 at Day 4 , colored by cluster.

To capture CD8$^+$ T cell responses during the initial stages of infection, we examined the transcriptional profiles of female and male P14 CD8$^+$ T cells responding at Day 4 to both

LCMV-Arm and LCMV-CL13. As seen on the t-SNE projection(refer to Figure 26), female and male P14 $CD8^+$ T cells at 4 dpi revealed distinct clustering patterns, based on the infection type as follows: Female d4 LCMV-Arm (light blue), Male d4 LCMV-ARM (light brown) Female d4-LCM-CL13(pink) and male d4-LCMV-CL13(green). We found that female cells responding to LCMV-C13 at Day 4 (pink) cluster separately from male $CD8^+$ T cells responding to LCMV-C13 at Day 4 (green). This finding suggests that there are differences in the molecular mechanisms underlying $CD8^+$ T cell response to LCMV-CL13 between the males and females.

Interestingly, the gene expression profiles of female P14 $CD8^+$ T cells responding to LCMV-Arm (light blue) showed some overlap with male responding to LCMV-Arm (light brown) at Day 4. This finding indicates that there may be shared molecular mechanisms underlying $CD8^+$T cell responses to LCMV-ARM in male and female P14 $CD8^+$ T cells.

To further interrogate the distinct clustering of female and male $CD8^+$ T cells responding at 4 dpi in both infection types, we analyzed DEGs between male and female $CD8^+$ T cells at 4 dpi. Gene ontology analysis identified different biological pathways enriched in female and male $CD8^+$ T cells based on the infection type.

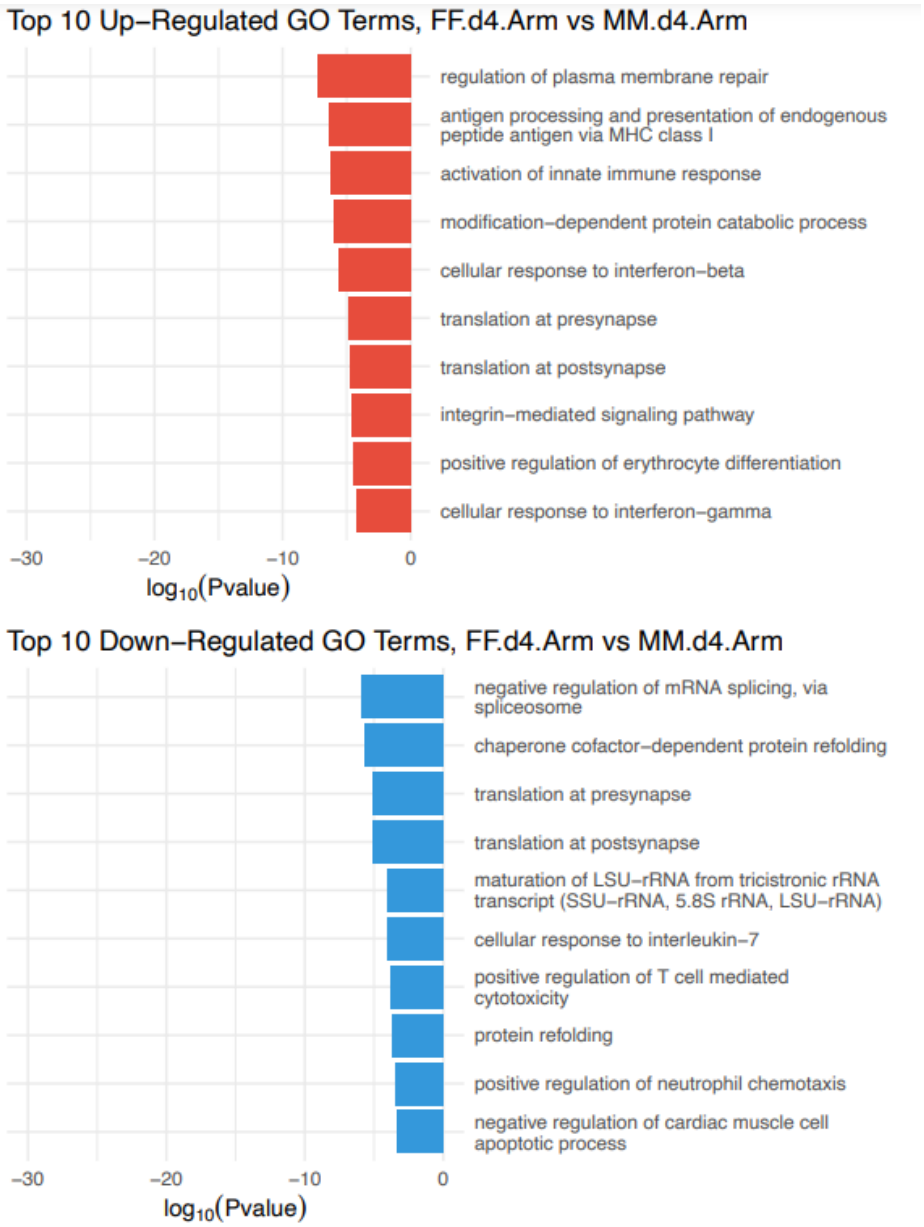

Figure 27. Gene Ontology analysis showing biological pathways in male and female CD8+ T cells responding to LCMV-Arm at Day 4 post-infection. In red are the biological pathways upregulated in female vs male, while blue represents the biological pathways upregulated in male vs female $CD8^+$ T cells.

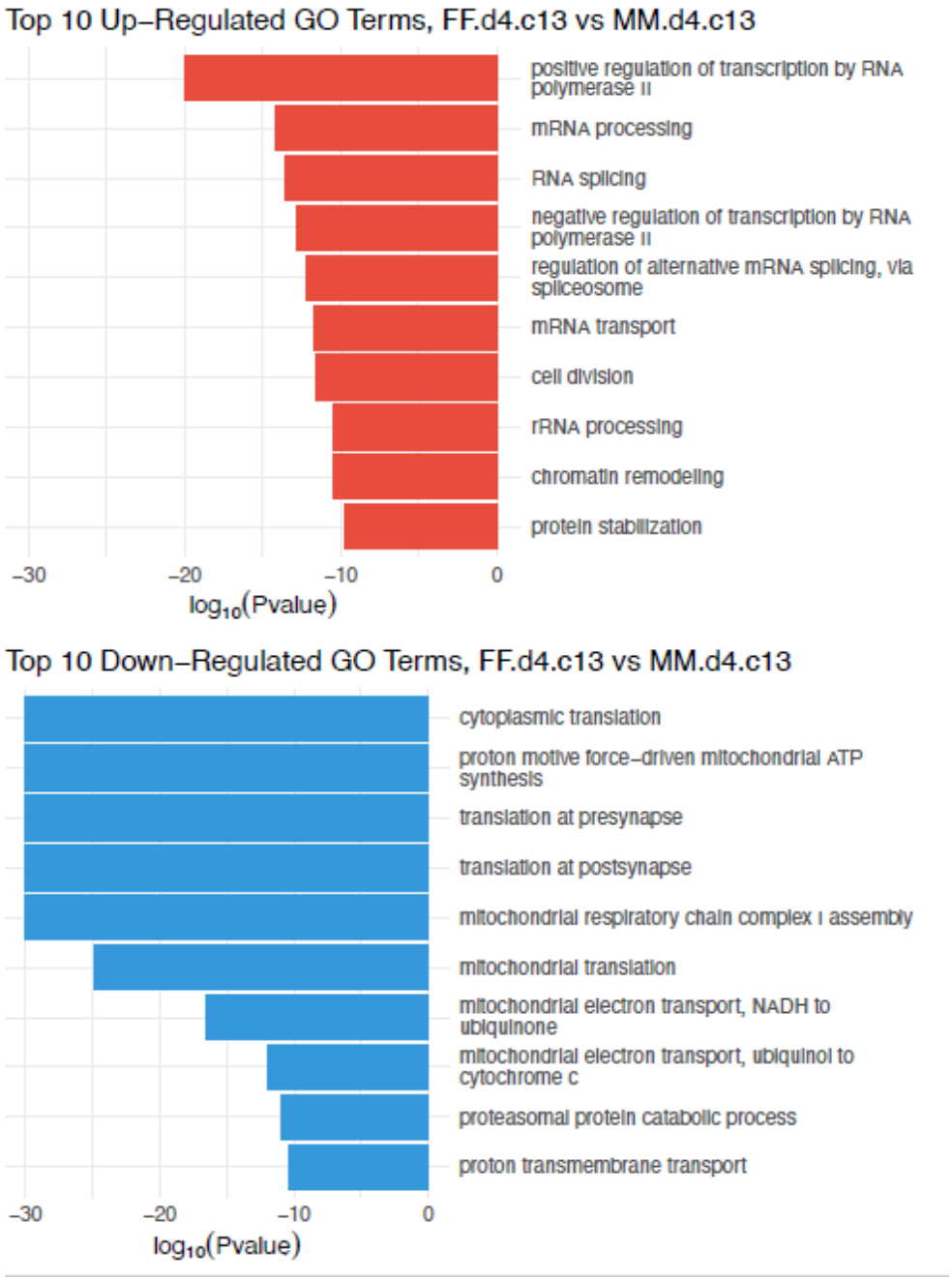

Figure 28. Gene Ontology analysis showing biological pathways in male and female CD8+ T cells responding to LCMV-CL13 at Day 4 post-infection. In red are the biological pathways upregulated in female vs male, while blue represents the biological pathways upregulated in male vs female $CD8^+$ T cells.

In response to LCMV-Arm (refer to Figure 27), female $CD8^+$ T cells shows a shift towards regulation of plasma membrane repair, antigen processing and presentation of endogenous peptide antigen via MHC class I and activation of innate immune responses, cellular responses to interferons and integrin mediated signalling pathways. On the contrary,

male CD8⁺ T cells responding to LCMV-Arm at day 7 show upregulation of genes involved in negative regulation of mRNA splicing via spliceosome, chaperone cofactor-dependent protein refolding, translation at pre-synapse, translation at post-synapse and cellular response to IL-7. In response to LCMV-CL13 at 4 dpi, female CD8⁺ T cells shows a shift towards positive regulation of transcription by RNA polymerase II, negative regulation of transcription by RNA polymerase II, mRNA processing, mRNA transport and RNA splicing. In contrast, male CD8⁺ T cells responding to LCMV-Arm at 4 dpi, show upregulation of genes involved in cytoplasmic translation, proton motive force-driven mitochondrial ATP synthesis, translation at pre-synapse and translation at post-synapse (refer to Figure 28).

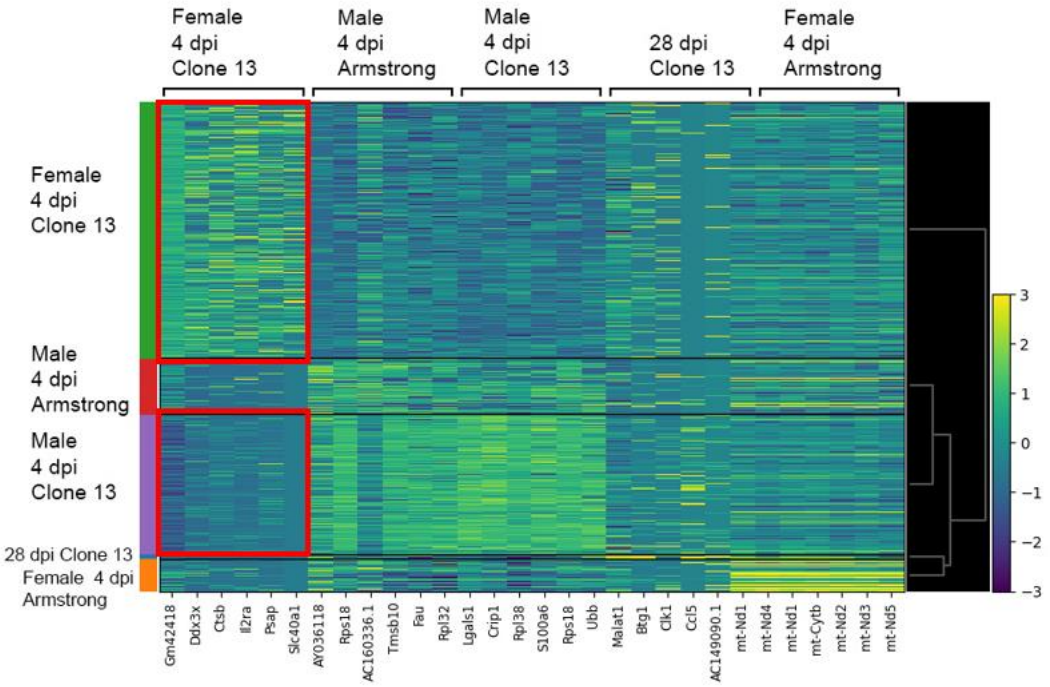

Figure 29. Heat map illustrating expression of candidate genes between male and female CD8⁺ T cells responding at day 4 post LCMV-Arm and LCMV-CL13 infection.

Illustrated in Figure 29 are some examples of DEGs between male and female P14 CD8⁺ T cells responding at Day 4 post LCMV-Arm and LCMV-CL13. These include *Gm42418, Ddx3x, Ctsb, IL2rα, Psap* and *slc40a1* among others.

Altogether, these results demonstrate the important role that sex plays in shaping early $CD8^+$ T cell responses to acute and chronic viral infection and highlights the need for further research to better understand the molecular mechanisms underlying sex-based differences in T cell responses to viral infection.

6.5 Sex Differences in Viral load

I further investigated if viral antigen load between male and females at early time-points (Day 4) or at peak of infection (Day 7) was driving the disparity in the $CD8^+$ T cell response. The level of replicating virus may be substantially different female versus males, potentially leading to differences in TCR signaling that ultimately influence $CD8^+$ T cell responses. In this study, we administered LCMV-Arm at 2×10^5 PFU/mouse IP and LCMV-Cl13 at 1.14×10^6 PFU/mouse IV as these infection doses and routes have been routinely used to model acute and chronic infections(101,102).

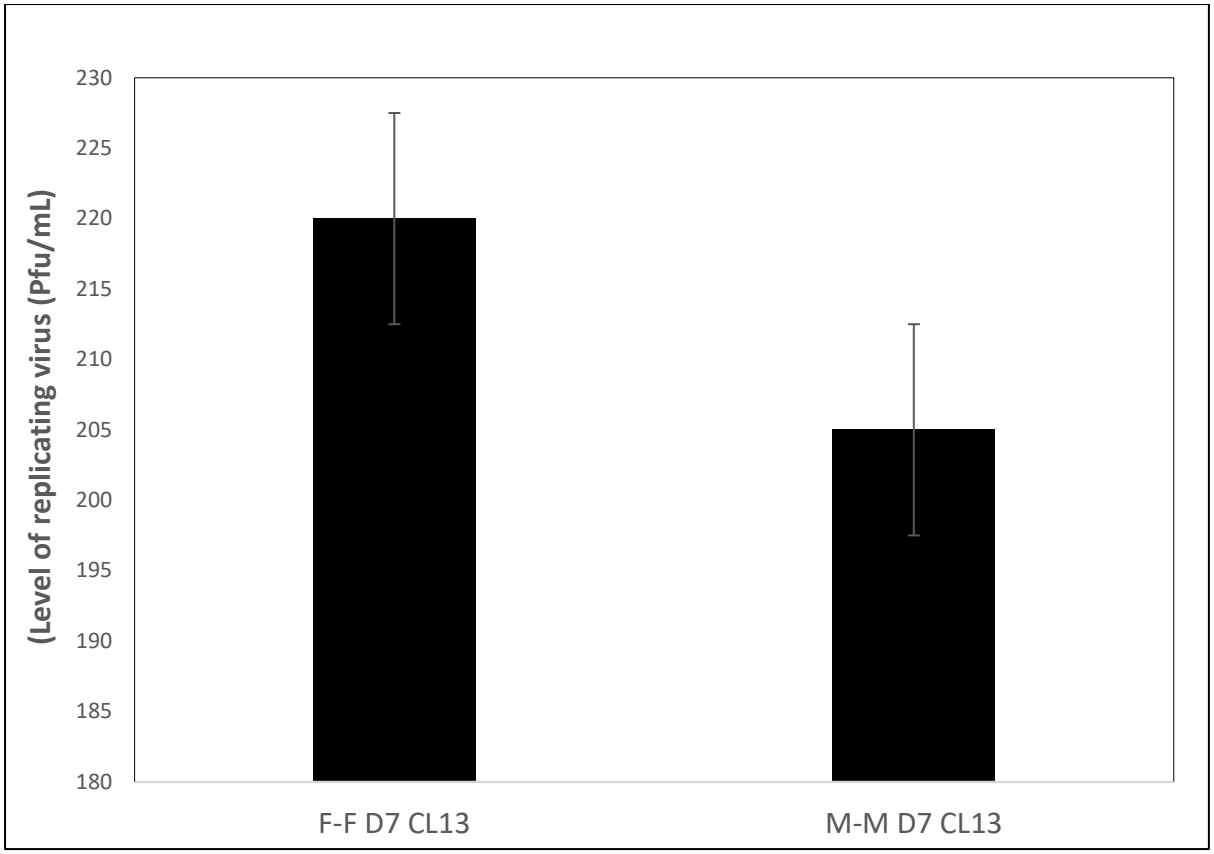

Figure 30. Levels of replicating virus at Day 7 in sera of female and male P14 mice infected with either LCMV-CL13. Data is representative of one experiment.

At Day 7 post LCMV-CL13, the viral titres detected from the sera of both male and female mice were comparable (refer to

Figure 30).

6.6 Sex-Based Differences in Expression of exhaustion-associated genes.

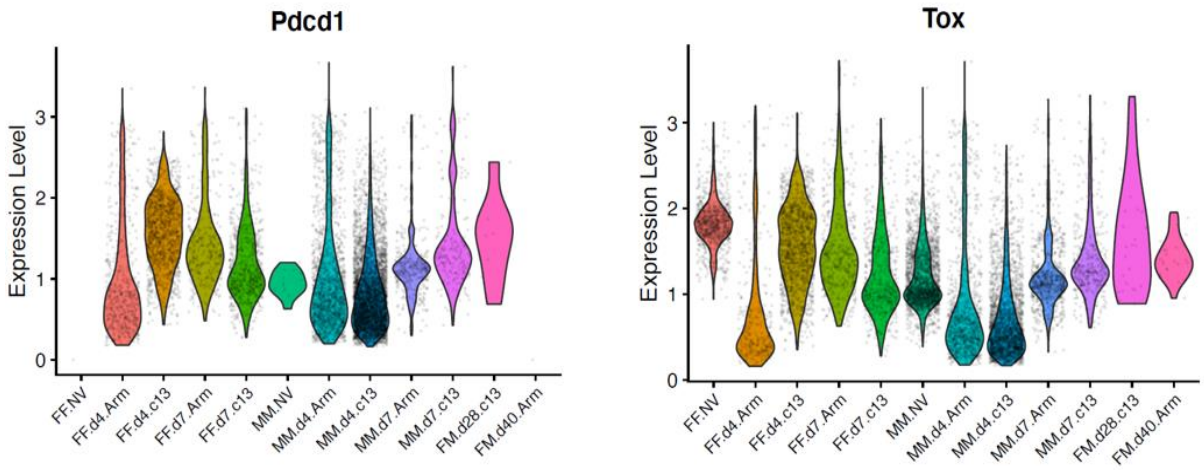

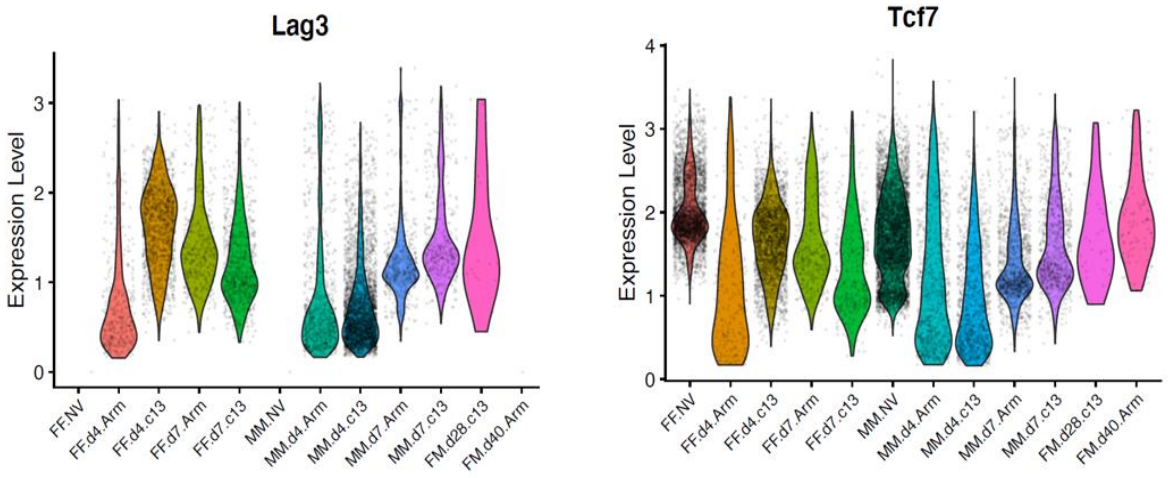

Figure 31. Violin plots representing the expression of exhaustion associated genes in male and female $CD8^+$ T cells responding at day 4 and day 7 post LCMV-Arm and LCMV-CL13.

As depicted in Figure 31, the expression of exhausted associated genes *Pdcd1, Lag3 , Tox, Tcf7* was greater in female compared to male $CD8^+$ T cells responding to LCMV-CL13 infection at day 4, suggesting that female $CD8^+$ T cells may be progressing earlier towards an exhausted state or may have an early molecular program which may predispose them towards exhaustion.

7 Validation of candidate gene regulators of early CD8$^+$T cell responses

7.1 Rationale

Candidate gene regulators identified via scRNA-seq analysis were next validated using *in vitro* assays of CD8$^+$ T cell differentiation followed by flow cytometry and quantitative real-time polymerase chain reaction (qRT-PCR) analysis. I chose to validate the following genes: CD8*α, IFN-γ, TNF-γ, Itgβ7* and *CXCR3* for the following reasons. Itgβ7 and CXCR3 have been reported to mediate CD8$^+$ T lymphocyte activation, differentiation, and function. *CXCR3* is an X-linked gene that encodes a chemokine receptor associated with CD8$^+$ T cell migration tissue homing (63). *Itgβ7* encodes an integrin associated with cell adhesion during CD8$^+$ T cell activation and trans-endothelial migration(51). *IFN-γ* and *TNF-α* genes encode their respective cytokines and were included to confirm the effector functions of the *in vitro* differentiated CD8$^+$ T cells.

7.2 In-vitro effector and memory CD8⁺ T cell differentiation model

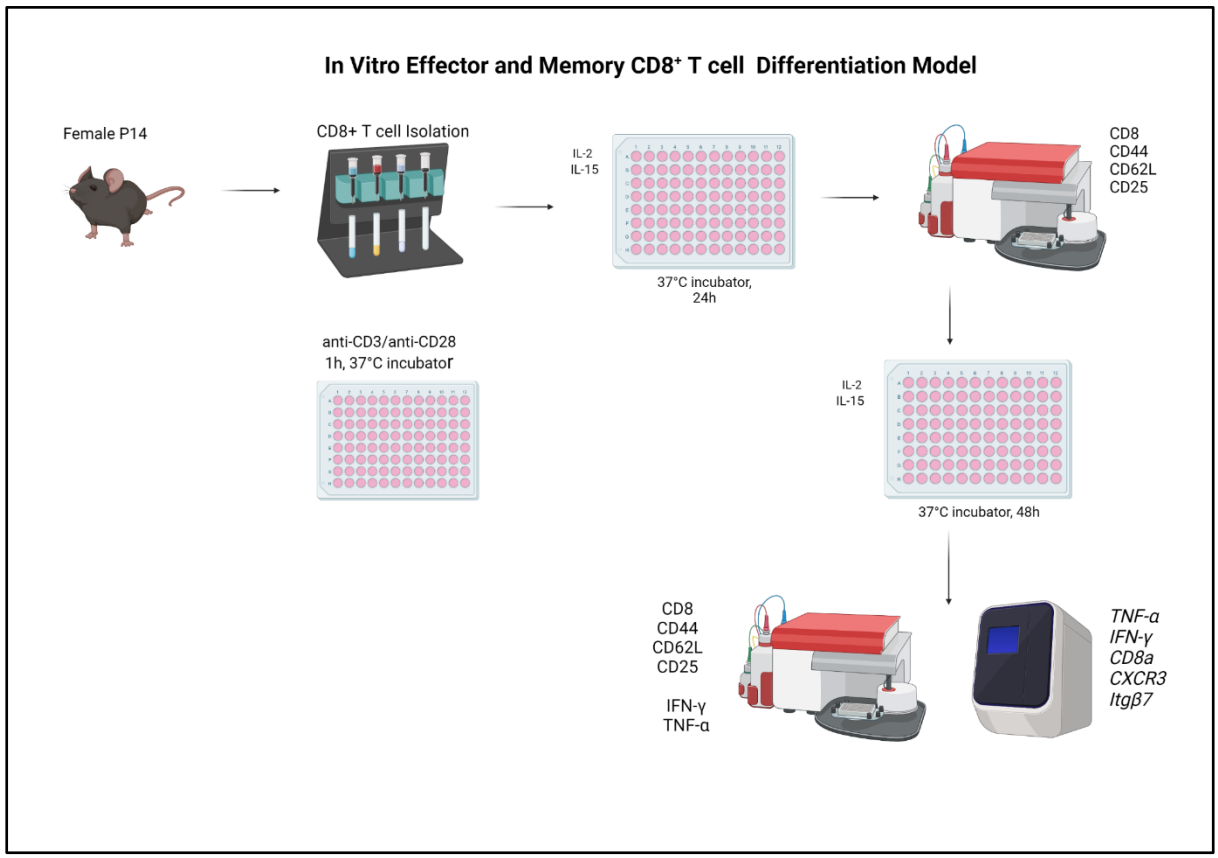

Figure 32. In Vitro CD8+ T cell Differentiation Model. This figure depicts the experimental model system utilized to generate "effector-like and "memory-like" CD8⁺ T cells.

To validate the findings from the *in vivo* LCMV studies, primary CD8⁺ T cells were isolated from the spleen of a female donor P14 mice by negative selection, following the methods described in Methods section. Subsequently, these cells were differentiated *in vitro* into effector-like, memory-like and exhausted-like CD8⁺ T cells in vitro, following established protocols (91–93). Following CD8⁺ T cell isolation, 2×10^5 CD8⁺ T cells per well were cultured in the presence of either IL-2 or IL-15 (10 U/ml) and plate-bound anti-CD3/anti-CD28 antibodies for 72 hours as previously outlined by (91). IL-2 drives the expansion and differentiation of effector T cells , while Il-15 is critical for the generation and maintenance of CD8⁺ memory T cells (91,103). During this time, the cells undergo activation, proliferation,

and differentiation into either effector-like or memory-like CD8+ T cells. To monitor the differentiation process, flow cytometry analysis is performed at 24 and 72 hours after activation. Specific markers are used to detect the different stages of CD8+ T cell differentiation including, CD62L for homing status, CD44 for activation, and pro-inflammatory cytokine markers such as TNF-α and IFN-γ for functional characterization. CD25hiCD62Llo indicate 'effector-like' whereas $CD25^{lo}CD52L^{hi}$ denote 'memory-like' CD8+ T cells as previously described in (91).

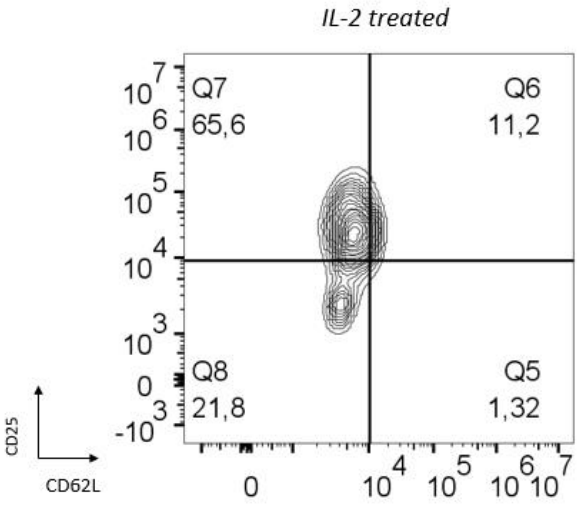

Figure 33. Frequency of "effector-like" CD8+ T cells 72h post in vitro stimulation and co-culture with IL-2. "Effector-like" P14 CD8+ T cells are gated on the upper-left quadrant. Detection of "effector-like" CD8+ T cells is determined by CD25hi CD62Llo expression. Data is representative of at least two independent experiments.

As seen in Figure 33, generation of 'effector-like' CD8+ T cells differentiated in the presence of IL-2 was confirmed by CD25hiCD62Llo expression as described previously by (91).

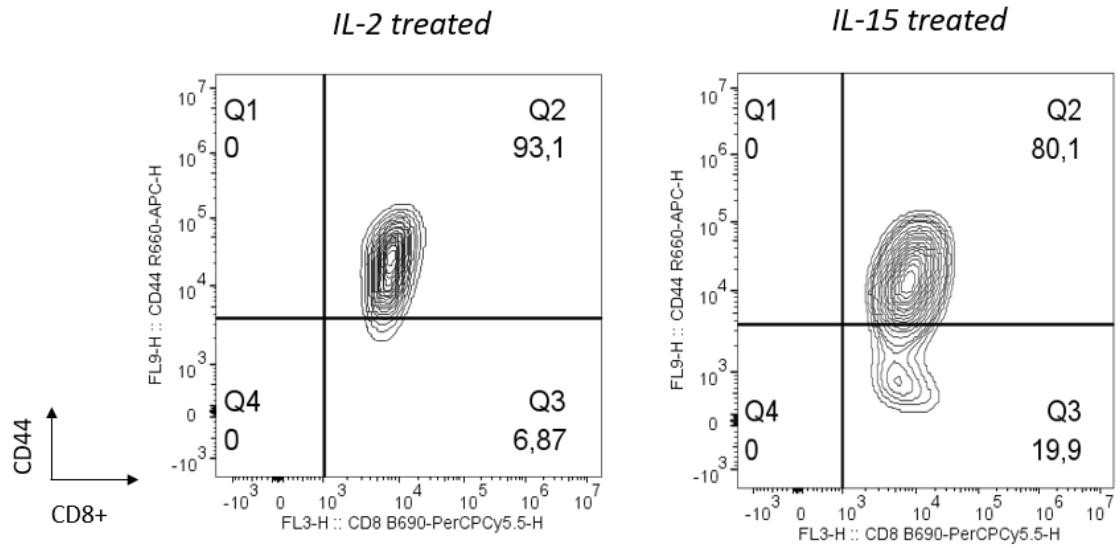

Figure 34. Frequencies of activated CD8+ T cells 72h post in vitro stimulation and co-culture with IL-2 (right) or IL-15(left). Activated P14 $CD8^+$ T cells shown are gated on CD44hi $CD45.1^+$ $CD8^+$ T cells. Data is representative of at least two independent experiments.

'Effector-like' $CD8^+$ T cells expressed higher CD44 levels than 'memory-like' $CD8^+$ T cells differentiated in the presence of IL-15 (refer to Figure 34). Given that CD44 is marker for activation, this finding indicates that the 'effector-like' $CD8^+$ T cells may be more activated than their 'memory-like' counterparts.

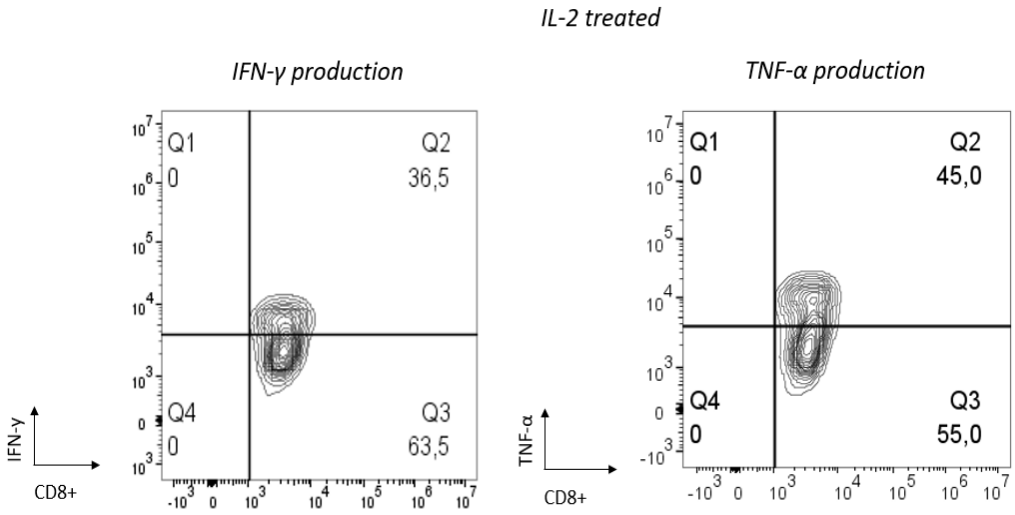

Figure 35. Frequencies of "effector-like" P14 CD8+ T cells producing IFN-γ (left) and TNF-α (right) 72h post in vitro stimulation and co-culture with IL-2. Cytokine producing T cells

shown are gated on TNF-αhi and IFN-γhi CD8+ T cells. Data is representative of at least two independent experiments.

Effector functions were confirmed by detection of CD8⁺ T cells producing either IFN-γ or

TNF-α (refer to Figure 35).Figure 35

7.3 In-vitro CD8⁺T cell exhaustion model

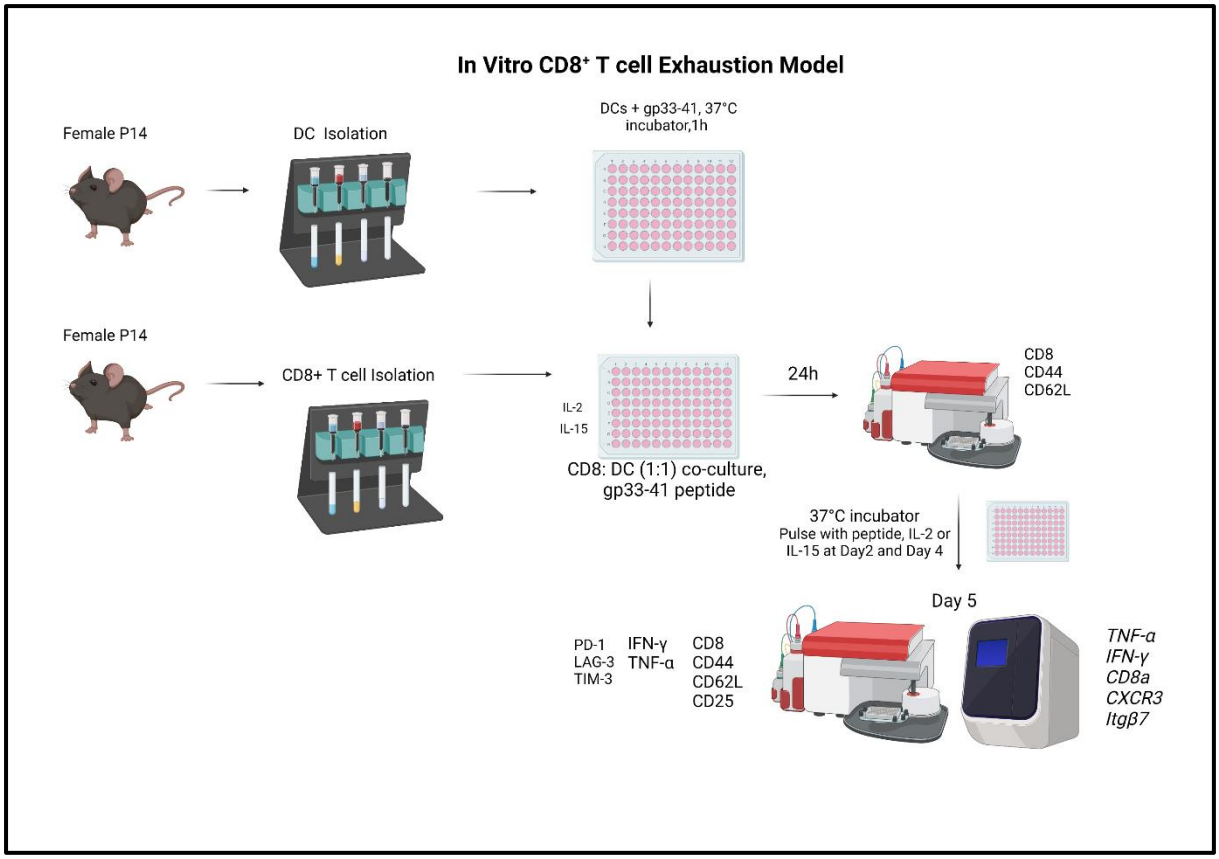

Figure 36. In Vitro CD8+ T cell Exhaustion Model. This figure depicts the experimental model system utilized to generate "exhausted-like" CD8⁺ T cells.

In this study, I utilized an established *in vitro* model of chronic antigen stimulation of P14 CD8⁺ T cells, based on previously established (92,93). This model allowed us to investigate key phenotypic, functional and transcriptional features of exhausted CD8⁺ T in comparison to *in vivo* exhausted CD8⁺ T cells. I modified the protocol by culturing the cells for five instead of usual 8 days to minimize cell death.

To mimic the development of exhausted CD8⁺T cells that occurs in the chronic model of LCMV infection, I co-cultured primary CD8⁺ T cells isolated from the spleen of a female P14 transgenic mouse with dendritic cells derived from the spleen of a different female transgenic mouse. Antigen specific CD8⁺ T cells and DCs were co-cultured with IL-2 or IL-15 and antigen (LCMV-gp33 peptide) for 120 hours. Differentiated CD8⁺ T cells were characterized using flow cytometry as described in section 3.6, to confirm their phenotype and functional properties before gene expression validation using qRT-PCR.

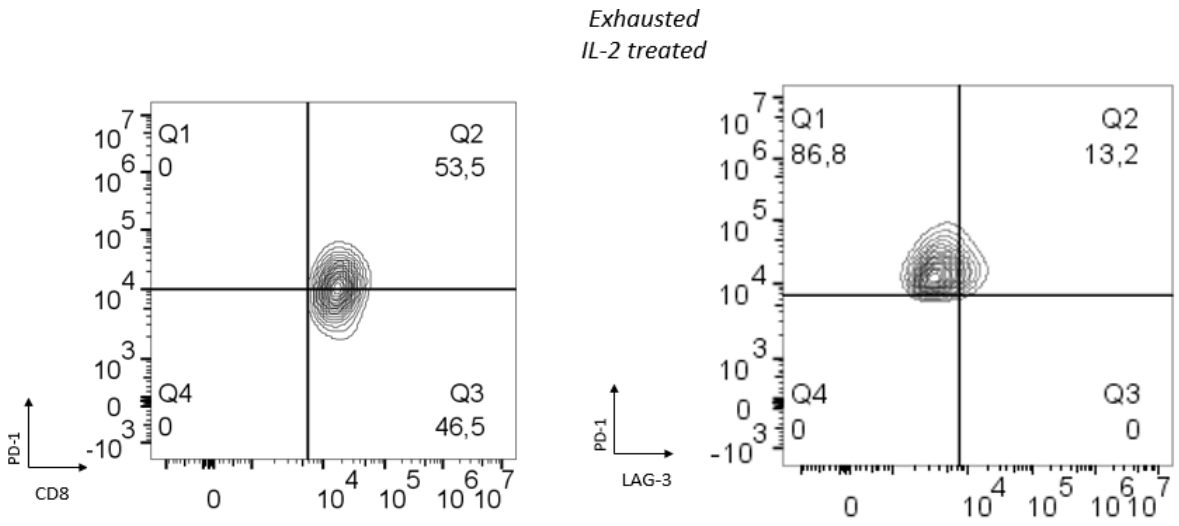

Figure 37. Frequencies of exhausted CD8+ T cells 120h post in vitro stimulation with glycopeptide 33 of LCMV virus and IL-2. Exhausted P14 CD8⁺ T cells shown are gated on PD-1hi CD8⁺ T cells (left) and PD-1hiLAG-3hi CD8⁺ T cells (right). Data is representative of one experiment.

Generation of "Exhausted-like" CD8⁺ T cells in our *in vitro* culture system was confirmed by PD-1 expression (refer to Figure 37). Heterogeneous "exhausted-like" CD8⁺ T cells were confirmed by expression of additional inhibitory receptors LAG-3 and TIM-3 as previously determined by (92).

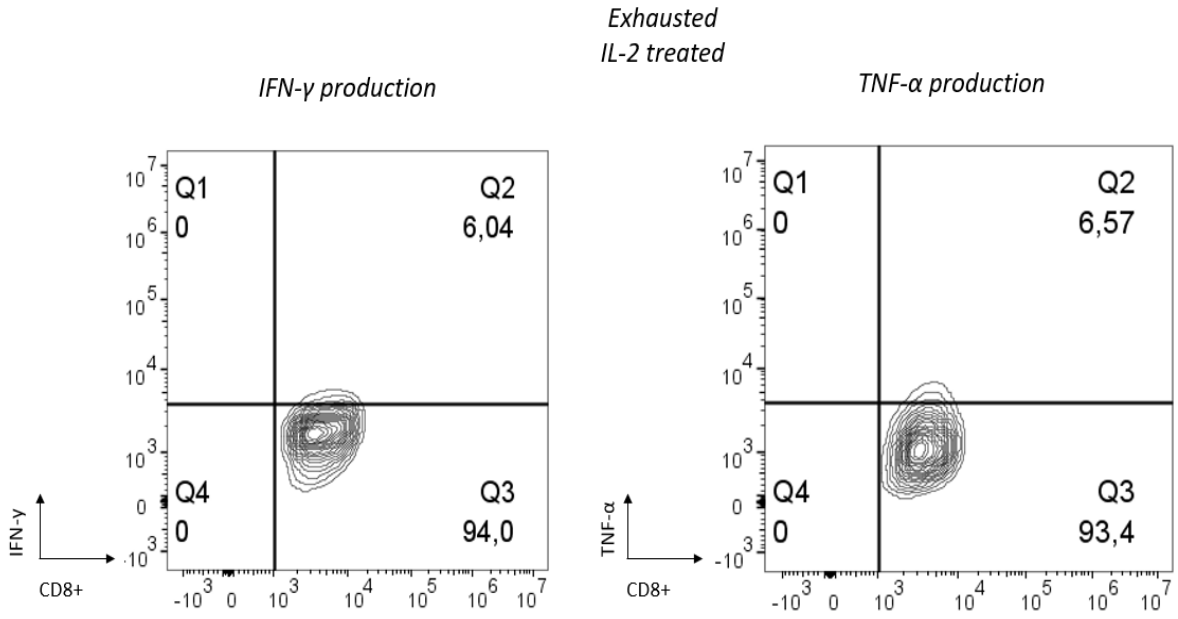

Figure 38. Frequencies of "exhausted-like" P14 CD8+ T cells producing IFN-γ (left) and TNF-α (right) 120h post in vitro stimulation with glycopeptide 33 of LCMV virus and co-culture with IL-2. Cytokine producing T cells shown are gated on TNF-αhi and IFN-γhi CD8+ T cells. Data is representative one experiment.

Effector functions of "exhausted-like" $CD8^+$ T cells were assessed by looking at the frequencies of $CD8^+$ T cells producing either IFN-γ or TNF-α. In this *in vitro* system of exhausted $CD8^+$ T cell differentiation. As expected, I observed the diminished ability to produce pro-inflammatory cytokines in the 'exhausted-like' $CD8^+$ T cells (refer to Figure 38).

As seen in Figure 38 and Figure 35, the 'exhausted-like, $CD8^+$ T cells produce considerably lower TNF-α and IFN-γ compared to the 'effector-like' $CD8^+$ T cells. Taken together, these results demonstrate a successful generation of 'exhausted-like' $CD8^+$ T cells *in vitro* as evidenced by PD-1 expression and poor effector functions demonstrated by decreased production of TNF-α ad IFN-γ.

7.4 Validation of candidate gene regulators by qRT-PCR

To validate the expression of selected DEGs in the *in vitro* differentiated CD8⁺ T cell populations (i.e. effector vs. memory vs. exhausted), qRT-PCR was performed. cDNA was generated as described in the Materials and Methods section from "effector-like", "memory-like" and ""exhausted-like"" female P14 CD8⁺ T cells differentiated *in vitro* as described in Section 3.6. I first analyzed CD8a expression to confirm that the cells were CD8⁺ T cells. *TNF-α* and *IFN-γ* gene expression were subsequently analyzed to confirm the effector functions of the CD8⁺ T cells, specifically their cytokine production.

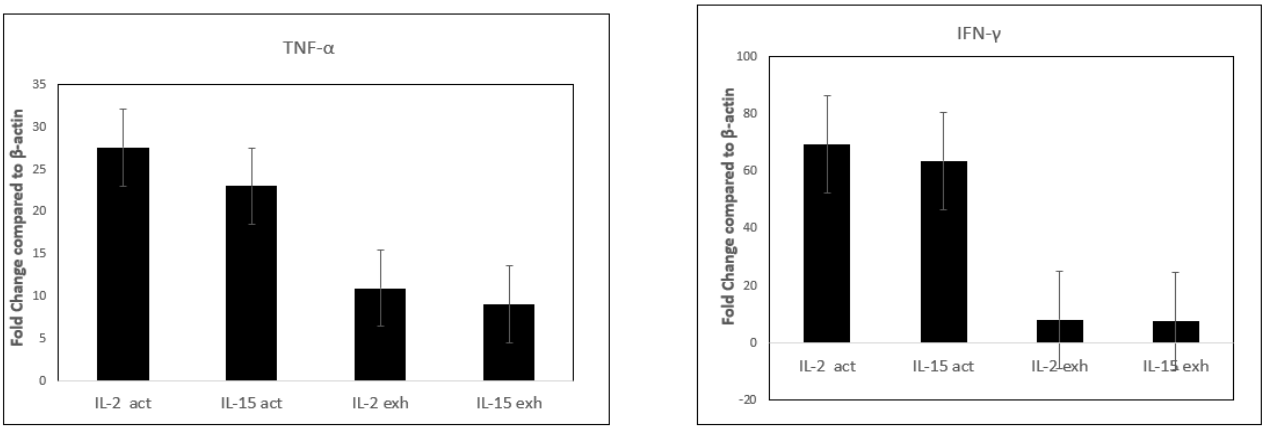

Figure 39. Gene expression of TNF-α (left) and IFN-γ (right) in "effector-like" and "exhausted-like" CD8+ T cells generated in vitro. Data is representative of one experiment.

The relative fold change in expression of both *TNF-α* and *IFN-γ* was highest in the "effector-like" (IL-2 activated), followed by the "memory-like" (IL-15 activated) CD8⁺ T cells and lowest in the "exhausted-like" (exh IL-2) and "terminally-exhausted" (exh-IL15) cells (refer to. Decreased gene expression of *TNF-α* and *IFN-γ* in "exhausted-like" compared to "effector-like" and "memory-like" CD8⁺ T cells indicates a potential loss of effector functions in the exhausted CD8⁺ T cell populations and confirms the successful generation of *in vitro* derived exhausted CD8⁺ T cells(refer to Figure 39).

Next, I investigated two candidate gene regulators of early CD8⁺T cell responses following LCMV-CL13, *CXCR3* and *Itgβ7*.

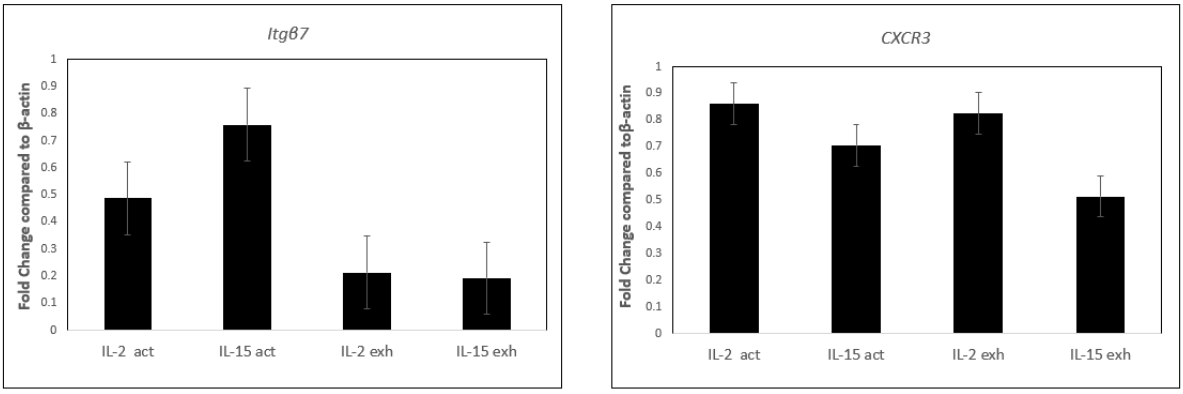

Figure 40. Gene expression of *Itgβ7* and *CXCR3* in "effector-like" and "exhausted-like" CD8⁺ T cells generated *in vitro*. Data is representative of one experiment.

CXCR3 is expressed by effector-like (act IL-2), memory-like (act-IL15) and exhausted-like (exh-IL2 and exh-IL15) CD8⁺ T cells. On the other hand, *Itgβ7* expression is highest in "memory-like" CD8⁺ T cells (IL-15act) and lowest in "exhausted-like" cells (refer to Figure 40).

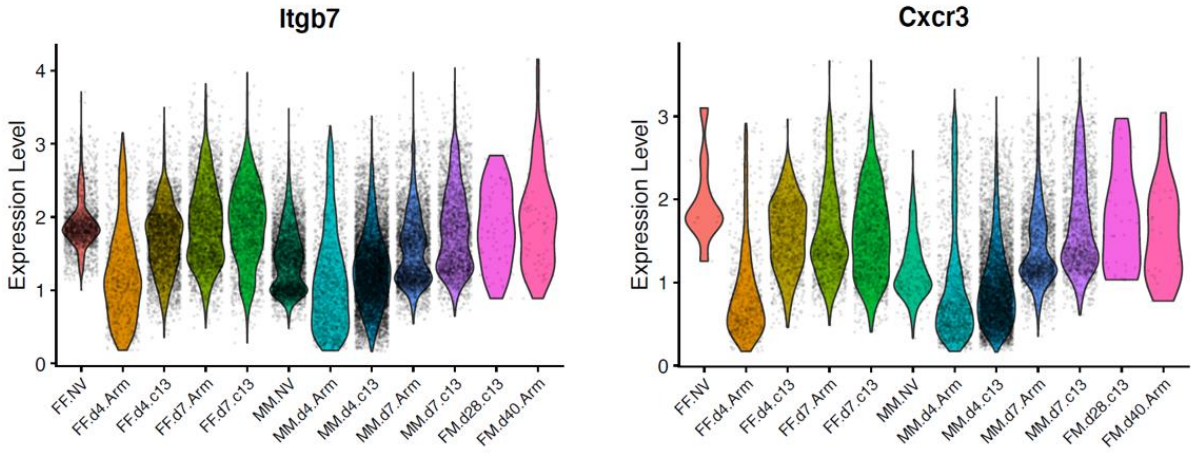

Figure 41. Violin plots illustrating the expression of *Itgβ7* and *CXCR3* in female and male CD8⁺ T cells responding to LCMV-Arm or LCMV-CL13 *in vivo* at 4,7,28 and 40 dpi.

Confirmation of the expression of these genes in our *in vitro* differentiated T cells aligned with the scRNA-seq results as shown in Figure 41.

8 Discussion

Chronic infections or tumors can cause $CD8^+$ T cells to undergo a process called T cell exhaustion, where they become dysfunctional and lose their ability to fight off the infection or tumor. This phenomenon has been extensively studied in mice infected with chronic LCMV, as well as in humans with chronic viral infections such as HIV, hepatitis B, and hepatitis C(45,97,104). This study investigated the transcriptional programs underlying how $CD8^+$ T cells may differentiate into an exhausted state compared to effector and memory cell fates. We specifically investigated early $CD8^+$ T cell responses to acute and chronic LCMV strains. To accomplish this, we sequenced cDNA libraries of antigen specific $CD8^+$ T cells responding at different times post-infection. The LCMV model of $CD8^+$ T cell differentiation in combination with single-cell transcriptional analysis revealed key insights in early $CD8^+$ T cell responses that may underlie development towards the exhausted $CD8^+$ T phenotype compared to effector and memory $CD8^+$ T cell fates.

This study provides a comprehensive view of the transcriptional programs underlying early $CD8^+$ T cell responses during acute and chronic LCMV infections with the integration of biological sex comparison, which can be extrapolated to identify molecular mechanisms regulating $CD8^+$ T cell differentiation and potentially be applied to other viral diseases.

8.1 Early $CD8^+$T cell responses to LCMV

8.1.1 Early cellular divisions in LCMV-CL13 vs LCMV-Arm

Proliferation rates of antigen-specific $CD8^+$ T cells were assessed by CFSE dilution assays at 18, 36, and 48 h following LCMV-Arm or LCMV-CL13 infection. Intriguingly, our findings revealed a difference in the kinetics of $CD8^+$ T cell proliferation between the two infection models. Specifically, LCMV-CL13 triggered earlier proliferation and cell division events (36 hours post-infection), whereas LCMV-Arm infection exhibited a delayed response, (48 hours post-infection) (see Figure 14). The rapid lymphocyte proliferation of $CD8^+$ T cells observed during the early stages of LCMV-CL13 infection piques considerable interest and suggests the presence of distinct signaling mechanisms in comparison to LCMV-Arm. One possibility is that viral antigen load may be substantially higher at early time points in LCMV-Cl13 compared to LCMV-Arm infection, potentially leading to increased TCR signaling. In this study, I administered LCMV-Arm at 2×10^5 PFU/mouse IP and LCMV-Cl13 at 1.14×10^6 PFU/mouse IV as these infection doses and routes have been routinely used to model acute and chronic infections (101,102).

Results showed no statistically significant differences in levels of replicating virus in the sera, between the two time points (refer to Figure 17**Error! Reference source not found.**). T his finding suggests that earlier $CD8^+$ T cell proliferation events observed in LCMV-CL13 infection cannot be solely attributed to increased TCR signaling, that may result from enhanced antigen presentation due to higher viral loads. Other factors within the spleen microenvironment such as preferential infection of FRCs and stromal cells by LCMV-CL13 can cause enhanced local viral titres impacting T cell activation. Additionally, distinct signaling pathways between chronic and acute LCMV infections may contribute to the observed disparities in $CD8^+$ T cell proliferation kinetics.

Previous studies have explored the divergent immune responses elicited by LCMV-CL13 and LCMV-Arm infections during early stages of infection. Studies have demonstrated

LCMV-CL13 infections result in a higher percentage of infected pDCs and significantly elevated levels of serum IFNα and IFNβ at 24 hours post-infection compared to LCMV-Arm infections(105,106). Building upon these observations, I hypothesize that differential rates APC infection, particularly involving pDCs, could explain the distinct kinetics observed in the early response to LCMV-Arm versus LCMV-CL13. Higher levels of IFNα and IFNβ, and other cytokines produced by pDCs such as IL-12 could be playing a crucial role in driving the earlier divisions of antigen-specific $CD8^+$ T cells observed in response to LCMV-CL13 as compared to LCMV-Arm.

Alternatively, studies have reported LCMV-Arm and LCMV-CL13 may preferentially localize to different regions of the spleen. LCMV binds to the αDG receptor expressed on splenic DCs (85,87). LCMV-CL13 exhibits high affinity binding to αDG and shows a preference for replication in splenic DCs, ultimately leading to viral replication in the white pulp. Conversely, LCMV-Arm demonstrates low affinity binding to αDG and displays minimal replication in splenic DCs (87,107). Similarly, in this study, I presume that the differential localization patterns and preferential interactions with distinct subsets of splenic DCs observed between LCMV-CL13 and LCMV-Arm infections could potentially affect the activation and subsequent proliferation of $CD8^+$ T cells. For example, increased replication of LCMV-CL13 in splenic DCs may explain rapid the $CD8^+$ T cell proliferation we observed in the CTL response to LCMV-CL13 compared to LCMV-Arm.

Taken together, cell tropism, cytokine milieu, and anatomic localization of LCMV-Arm versus LCMV-Cl13 in the spleen could influence $CD8^+$ T cell differentiation in the different infections at early time points. In fact, a recent scRNA-seq study identified a transcriptional and epigenetic divergence between $CD8^+$ T cells that have undergone their first division in

response to LCMV-Cl13 or LCMV-Arm. Interestingly, Quezada *et al*, showed that $Div1_{LCMV-ARM}$ cells exhibited transcriptional but not epigenetic heterogeneity, whereas $Div1_{CL13}$ cells exhibited epigenetic but not transcriptional heterogeneity (15). Although the functional importance of these transcriptional and epigenetic disparities remains to be fully understood, it is intriguing to observe the early differences between $CD8^+$ T cells responding to LCMV-Arm versus LCMV-CL13, which are in support of my findings.

A limitation of our study was that I was unable to sort enough $CD8^+$ T cells undergoing early divisions cDNA library generation and scRNA-seq analysis, despite multiple attempts. Further optimization of the cell sorting protocol will be necessary for future studies at early time points. One improvement to the protocol could involve transferring higher cell numbers (3×10^6 CFSE-labeled cells as previously described in (101,102), to potentially improve cell recovery for downstream analysis.

8.1.2 Early transcriptional differences in $CD8^+$T cells responding to LCMV-Arm Vs LCMV-CL13

To investigate the transcriptional differences between $CD8^+$ T cells responding to acute versus chronic infection, we analyzed data from multiple time points together (days 4, 7, 28, and 40). T-SNE analysis revealed distinct transcriptional profiles of early-responders (d4), effector (d7), memory (d40-LCMV-Arm) and exhausted (d28-cl13) $CD8^+$T cells. Notably, during the initial stages of infection (day 4), a clear separation emerged between $CD8^+$ T cells responding to the LCMV-CL13 versus LCMV-Arm infection. This intriguing transcriptional divergence observed as early as day 4 aligns closely with my hypothesis that $CD8^+$ T cell fates may be predetermined during the early stages of developing infections, as corroborated by relevant literature (14,15,91).

$CD8^+$ T cells responding to acute-resolving vs chronic LCMV infection were distinguished by the upregulation of different genes and pathways (Figure 18), further supporting the notion of early specification of cell fates. Similarly, a prior scRNA-seq study identified a transcriptional divergence between $CD8^+$ T cells responding to LCMV-Arm versus LCMV-Cl13 occurring after day 4.5 but before day 7 post-infection(49). A more recent scRNAseq study identified a transcriptional divergence between $CD8^+$ T cells responding to LCMV-Arm versus LCMV-Cl13 in $CD8^+$ T cells that have undergone their first division and early time points (day 5 and Day 6 pi)(15), suggesting that an exhausted state may be specified early after infection which is consistent with my hypothesis.

To investigate the distinct clustering of $CD8^+$ T cells at Day 4, we analyzed the gene expression patterns of the two Day 4 clusters. GO analyses of genes differentially expressed by the two Day 4 clusters revealed an enrichment of genes related to mitochondrial respiration, integrin signaling, migration and chromosome modifications in Day 4 LCMV-CL13. In Day 4 LCMV-Arm, there is an upregulation of genes involved in translation machinery and RNA processing (refer to Figure 18). Focusing next on specific genes, I observed that transcription factors associated with integrin signalling were only highly expressed by Day 4 LCMV-CL13 cells. These included *itgb1, itgb7 and itga4*. Integrin signaling plays a critical role in cell adhesion, migration, and immune cell interactions, suggesting that variations in these processes may contribute to the distinctive $CD8^+$ T cell response observed in LCMV-CL13 infection.

Alternatively, as discussed in previous sections, studies have reported LCMV-Arm and LCMV-Cl13 may preferentially localize to different regions of the spleen by binding to different splenocytes that express αDG (85,87). Similarly, I hypothesize that the differential tropism of LCMV-Arm and LCMV-CL13 within the spleen, particularly the of preferential

replication of LCMV-CL13 in the white pulp, may be orchestrating unique patterns of $CD8^+$ T cell activation, yielding the observed variations in transcriptional profiles of $CD8^+$ T cells responding to LCMV-Arm versus LCMV-CL13 at early time-points (day 4). Additionally, innate immune responses may be driving early CTL responses in LCMV-Arm vs LCMV-CL13. The infection, activation and function of DCs, macrophages and other APCs during LCMV ARM and LCMV-CL13 infection are critical parameters in determining the outcome of infection. Differences in LCMV-Arm and LCMV-CL13 interaction with the innate immune system are likely to have a significant impact in initiating the adaptive immune responses, including the CTL responses that clear LCMV-Arm and the mechanisms hinder the ability of the immune system to clear LCMV-CL13.

Innate responses to LCMV have been detected within the first day of infection. For example, plasmacytoid DC are preferentially infected by LCMV-CL13 and activated to produce of IFN-α and IL-12, stimulating CTL responses(105). LCMV-CL13 may elicit distinct patterns of activation and cytokine production in innate cells such as pDCs, which may contribute to the impaired CTL responses observed during chronic LCMV infection.

Another possibility to explain differences in early $CD8^+$ T cell responses to acute versus chronic LCMV is that viral antigen load may be substantially higher at Day 4 in LCMV-CL13 compared to LCMV-Arm infection, potentially leading to increased TCR signaling. In this study, we administered LCMV-Arm at 2×10^5 PFU/mouse IP and LCMV-Cl13 at 1.14×10^6 PFU/mouse IV as these infection doses and routes have been routinely used to model acute and chronic infections. I have not yet performed plaque assays at Day 4 pi to assess the numbers of replicating virus, due to unresolvable experimental challenges. While these experiments are ongoing, I must acknowledge that the level of replicating virus in LCMV-Arm vs LCMV-CL13 may have influenced the observed differences in $CD8^+$ T cell responses. Future studies could

aim to include plaque assays at various early time points to investigate the potential confounding effects of TCR signalling more comprehensively on $CD8^+$ T cell responses during the early phases of a developing infection.

8.2 Sex-based differences in $CD8^+$ T cell responses to viral infection

To address my fourth objective, I investigated sex-based differences in $CD8^+$ T cell responses to LCMV-CL13 versus LCMV-Arm. First, I observed higher TNF-α expression in female $CD8^+$ T cells compared to males in LCMV-Arm compared to LCMV-CL13 at the peak of infection (Day 7). I also observed a trend of higher frequencies of antigen-specific P14 $CD8^+$ T cells in males compared to females, in response to both acute and chronic LCMV.

To further investigate the sex-specific differences between male and female $CD8^+$ T cells responding to acute versus chronic LCMV infection, we analyzed the transcriptional profiles of naïve and responding $CD8^+$ T cells. At the peak of infection (Day 7), scRNA-seq revealed that female and male $CD8^+$ T cells separated into distinct clusters based on infection type (LCMV-Arm versus LCMV-CL13) and sex (male versus female). First, male $CD8^+$ T cells cluster distinctly from their female counterparts both at naïve and Day 7 time-points. Strikingly, female $CD8^+$T cells responding to LCMV-CL13 clustered separately from those responding to LCMV-Arm suggesting that they may already be proceeding along distinct differentiation paths. Surprisingly, this distinction was absent in the male $CD8^+$ T cell response, as there was significant overlap between clusters of male $CD8^+$ T cells responding to LCMV-CL13 and LCMV-Arm.

This study uncovered novel findings of early sex-based differences in $CD8^+$ T cell responses acute versus chronic LCMV infection in mice at 4 dpi. Our analysis revealed distinct clustering patterns, based on the infection type and sex. Female cells responding to LCMV-

C13 at Day 4 cluster separately from male CD8$^+$ T cells responding to LCMV-C13 at the same time-point. Interestingly, the gene expression profiles of female P14 CD8$^+$ T cells responding to LCMV-Arm showed some overlap with male responding to LCMV-Arm at Day 4. Further analysis of DEGs between the clustered revealed additional sex-based differences. For example, *itgb7*, associated with integrin signalling was more highly expressed by female Day 7 LCMV-CL13 cells compared to female Day 7 LCMV-Arm. By examining the list of inflammation-related DEGs between females CD8$^+$ T cells responding to LCMV-Arm vs LCMV-CL13, we identified X-linked genes that were more highly expressed in Female d7 LCMV-CL13 vs Female d7-LCMV-Arm. From this list, I chose to further investigate *CXCR3.*

Sex-specific CD8$^+$ T cell responses during early phases and at peak of infection suggest that there are differences in the molecular mechanisms underlying the female and male CD8$^+$ T cell response to LCMV. Sex-based differences in disease susceptibility and outcomes can be attributed to differences in the expression of steroid hormones, differences in anatomy, differences in X and Y chromosome–linked factors, such as X chromosome inactivation or genes encoded on the Y chromosome.

Potential biological reasons for sex-based differences in CD8$^+$T cell responses

8.2.1 Immune-associated genes mapped to the X chromosome:

Sex-based differences in CD8$^+$ T cell responses to infection may be due immune associated genes mapped to the X-chromosome. As discussed in the introduction section, genetic and epigenetic factors that contribute to sexual dimorphism are largely centered on the X chromosome. Females posses two X chromosomes (XX) while males have one X chromosome (XY). XCI occurs in females to equalize gene expression between sexes (108). However, several X-linked genes escape XCI and display biallelic gene expression (109).

Notably, genes that escape XCI vary, depending on the cell type, tissue, individual, age, and even the methods used(110–112).

Immune-associated genes that are mapped to the X chromosome are of particular interest because they could affect the nature and intensity of immune responses that exist between sexes, depending on whether they escape XCI. In this study, several Immune-associated genes that map to the X chromosome were identified. I identified CXCR3 as one such gene that was more highly expressed in Female d7-LCMV-CL13 vs Female d7 LCMV-Arm. CXCR3 is an important X-linked immune-associated gene, an inducible chemokine receptor and a significant regulator of T cell immune responses (63,113). Unlike all other chemokine receptors, CXCR3 uniquely maps to the X chromosome(113) and is expressed by activated CD4+ T cells, $CD8^+$ T cells, macrophages and DCs (114). Previous research has shown that CXCR3 mRNA has been shown to be overexpressed in female T cells relative to males, lupus patients (115). Moreover, studies utilizing a CXCR3 bicistronic dual-reporter mouse model demonstrated that CXCR3 escapes XCI in T cells when activated *in vitro* as well as during *in vivo* infection with *L. mexicana*(64). Biallelic CXCR3- expressing T cells from spleens and lymph nodes of infected mice displayed higher CXCR3 protein on their cells compared with monoallelic CXCR3- expressing cells. Similarly, in our study, given that CXCR3 is involved in immune cell migration, differentiation, and activation, the increased protein expression observed in biallelic CXCR3-expressing cells in female $CD8^+$ T cells may contribute to different immune responses compared to the males. Additionally, biallelic expression of other X-linked genes that potentially escape XCI could potentially result in sex-based differences in $CD8^+$ T cell responses between males and females.

In addition to protein-coding genes, other RNA species such long non-coding RNA (lncRNAs) and micro-RNAs that are highly enriched on the X chromosome could potentially

play a role in the molecular mechanisms underlying sex-based differences in $CD8^+$ T cell responses. Further investigation into these RNA species and their interactions with immune-related pathways may provide additional insights into observed disparities between male and female $CD8^+$ T cell responses.

8.2.2 Sex-specific differences in innate immune responses

In our investigation of early $CD8^+$ T cell responses, we explored sex-based differences and their potential influences on transcriptional programs of responding $CD8^+$ T cells. Early differences in $CD8^+$ T cell responses may be partly attributed to innate immune responses that mount the first line of immune defense before the adaptive immune system is activated. Within the realm of innate immunity, literature provides valuable insights into the involvement of pDCs in sex-specific differences observed in specific disease outcomes such as HIV-1 disease progression. pDCs are capable of sensing single-stranded RNA via TLR7/8 (116,117). Activation of pDCS triggers the production of type I IFNs, including IFN-α, which serves as a potent antiviral mediator. In HIV-1 disease, pDCs derived from women produced significantly higher amounts of interferon α (IFN-α) in response to TLR7/8 ligands compared to pDCs from men(118,119). As a result, the secondary activation of $CD8^+$ T cells is stronger in female than in males, and this mechanism could explain why women are more susceptible to rapid HIV-disease progression than men. Drawing from this knowledge, I suspect that the sex-based differences observed in the transcriptional programs of $CD8^+$ T cells responding to early to LCMV-Arm and LCMV-CL13, could be influenced by innate immune responses, including pDCs activation and effector functions. In particular, enhanced TLR7 signalling followed by higher IFN-α and IL-12 production by female pDCs could be contributing to the divergent $CD8^+$ T cell responses between males and females observed at 4 dpi. In line with

these findings, a recent study demonstrated that male and female $CD8^+$ T cells could respond differently to intracellular pathogens due to their varying sensitivity to inflammatory cues. In murine infections with vaccinia(virus) and *Listeria monocytogenes* (bacteria) female $CD8^+$ T cells displayed a higher tendency to become short-lived effector while male $CD8^+$T cells were more likely to become memory precursor effector cells, in response to IL-12 produced by pDCs (61). The established link between pDC-derived IL-12 and the differential fate of male and female $CD8^+$ T cells during infection provide valuable context for considering that similar mechanisms underlie the observed differences in early $CD8^+$ T cell responses between males and females, in our study. Overall, the interplay between the innate and adaptive immune responses contribute to the complex mechanisms underlying sex-related disparities in immune responses.

8.2.3 Sex differences in viral load

At Day 7 post LCMV-CL13, the viral titres detected from the sera of both male and female mice were comparable (refer to

Figure 30).Thereby, we can speculate that the observed differences in $CD8^+$ T cell responses between male and female mice during peak of LCMV-CL13 infection may not be attributed to variations in viral replication and antigen load. Instead, other factors, such as sex-specific immune responses, hormonal influences and distinct transcriptional $CD8^+$ T cell profiles are likely contributing to the sex-based differences observed at day 7. However, I must acknowledge that I was unable to get conclusive results from sex-based plaque assays performed at Day 7 LCMV-Arm due to unresolvable experimental challenges. Future studies will investigate the viral titres of LCMV-Arm in sera of male and female infected mice, aiming to uncover potential differences in their susceptibility to LCMV-Arm infection.

Alternatively, in accordance with previous studies, (85,87), it is plausible that LCMV-Arm and LCMV-CL13 may localize to different regions of the spleen. Additionally, female and male antigen specific $CD8^+$ T cells may home differently in the female versus male spleen, respectively. Of note, naïve male and female $CD8^+$ T cell transcriptional profiles cells are distinct without activation (refer to Figure 23), suggesting the possibility of pre-existing differential programming related to migratory patterns, proliferation, and transcriptional machinery. Additionally, virus replication and $CD8^+$ T cell migration patterns could be affected by hormones potentially leading to different homing patterns, in female versus male environment.

In summary, potential disparity in viral load, differential patterns of virus homing and distinct intrinsic programming between female and male $CD8^+$ T cells in the spleen may contribute to the observed sex-based differences in $CD8^+$ T cell responses during LCMV infection.

8.2.4 Sex Hormones

A possible explanation for sex-based differences between female and male $CD8^+$ T cells could be differential signalling of sex hormones between males and females. Estrogens and androgens contribute to sex-specific differences in viral infections. Numerous studies in animal models have demonstrated the direct influence of sex hormones on viral infections. For example, rhesus macaques were found to be more susceptible to intravaginal simian immunodeficiency virus (SIV) infection during the luteal phase (high progesterone levels) compared to follicular phase (high estrogen levels)(120). Additionally, systemic administration of estrogens protected female rhesus macaques against intravaginal challenge

with highly pathogenic SIV (121). Similar associations between sex hormones and HIV-1 acquisition have been observed in humans during the menstrual cycle and in pregnancy(70).

In the context of our LCMV study, I suspect that progesterone and estrogen could contribute to the sex-specific differences in $CD8^+$ T cell responses. These hormones may affect the spleen microenvironment thereby influencing $CD8^+$ T cell activation, differentiation and response during early and later stages of infection. Notably, in female mice, the menstrual cycle could influence their susceptibility to infection based on the phase of the cycle. The role of androgen in regulating T cell exhaustion has garnered much attention recently, with contradictory findings on molecular mechanisms at play (67,72). Studies have shown that blocking androgen receptor signaling can restore $CD8^+$ T cell function and enhance $CD8^+$ T cell responsiveness to anti-PD1/PD-L1 treatment in males. This finding aligns with previous reports on castration-resistant prostate cancer, suggesting a potential role of androgen in driving sex-based differences observed in chronic conditions such as persistent viral infections or cancer(122).

In the context of our LCMV study, I suspect that androgen could contribute to the sex-specific differences we observed in response to LCMV infection. Androgens may exert their effects during early stages of infection, affecting initial $CD8^+$ T cell activation and differentiation events that can be maintained through epigenetic memory and influence $CD8^+$ T cell responses during later stages of infection. Further research is necessary to unravel the precise molecular mechanisms through which sex hormones, including estrogens and androgens, modulate $CD8^+$ T cell responses during viral infections and their implications for sex-based differences in disease outcomes.

8.3 Conclusion and significance

The LCMV model of acute and chronic infection of mice has been instrumental in studying the adaptive immune responses to viral infection. LCMV studies have provided valuable insights into functional exhaustion during chronic infections and the identification of markers associated with protective $CD8^+$ T cell responses. The focus of this study was to investigate early and sex-based differences in $CD8^+$ T cell responses to acute and chronic LCMV infection, with the aim of better understanding the molecular mechanisms underlying the development of $CD8^+$ T cells exhibiting protective versus exhausted phenotypes. Our findings revealed previously unrecognized sex-based differences in early $CD8^+$ T cell responses to acute versus chronic viral infection, within the classical LCMV infection model. These findings underscore the need for further exploration of the often-underappreciated role of biological sex in cellular mediated immune responses. The observed early and sex-based differences in $CD8^+$ T cells responding to LCMV-CL13 infection in particular, warrant further interrogation to delineate early and sex-based differences in the formation of exhausted $CD8^+$ T cell subsets. Subsequently, mechanistic studies of candidate gene regulators of $CD8^+$ T cell exhaustion can be pursued to understand our understanding of this complex phenomenon.

The implications of these findings extend beyond LCMV infection and have significant relevance to our comprehension of immune responses to viral infections in general, as well as the development of $CD8^+$ T cell exhaustion. The identification of early and sex-based differences in $CD8^+$ T cell responses to acute and chronic viral infections opens new avenues for research in immunology. The potential identification of candidate gene regulators of $CD8^+$ T cell exhaustion holds promise for the design of new strategies aimed at modulating T cell

activity to elicit appropriate context-specific T cell response, including effector, memory and exhausted responses.

8.4 Future Directions

This study acknowledges certain limitations that should be addressed in future research. One such limitation is that we did not directly measure sex hormone steroid levels to determine their role in mediating the observed sex-based $CD8^+$ T cell responses and transcriptional patterns. Additionally, the effect of sex hormones on tissue microenvironments such as the spleen adds another layer of complexity for understanding the effects of biological sex in $CD8^+$ T cell responses to viral infection. Immune cells, including $CD8^+$ T cells express sex steroid receptors (123,124) and are responsive to estrogen and testosterone treatment. Future studies can examine: 1) hormone receptor expression changes in antigen-specific $CD8^+$ T cells following activation by viral antigen; 2) circulating sex steroids levels in plasma; and 3) the effect of the estrous cycle stage on modulating $CD8^+$ T cell responses to viral infection.

Ongoing experiments are currently addressing some of the questions. Our preliminary data analysis suggests that expression of sex steroid receptors, such as ERα and AR, change in response to infection indicating a potential role of sex steroids in mediating sex-related differences in $CD8^+$ T cell responses.

Related studies in mice investigating chronic inflammatory responses in the lung following air pollution exposure have revealed the estrous cycle stages can influence the inflammatory response to a pathogen. For example, female mice exposed to ozone in the follicular in mice it's termed estrous phase had significantly higher expression of inflammatory genes, including *Ccl2, Cxcl2, Ccl20,* and *IL-6*, compared to females exposed in the luteal in mice it's termed

diestrous phase (125). Therefore, it would be valuable to investigate the role of sex steroids on $CD8^+$ T cell responses and differentiation after infection with LCMV-Arm or LCMV-CL13 in future studies.

These studies can include investigating $CD8^+$ T cell differentiation *in vitro* using the *T cell* differentiated assays described earlier in this study, in the presence or absence of sex hormones. To further explore the effect of hormone signalling in the context of our study, responding male or female $CD8^+$ T cells can be isolated early (day 4) or at peak of infection (day 7) and cultured *ex-vivo* in the presence or absence of sex hormones to explore the difference in $CD8^+$T cell effector functions and proliferation.

An examination of a sex steroid panel (cortisol, testosterone, 17β-estradiol and progesterone) in serum of recipient male and female mice can be performed using mass spectrometry/LC-MS-MS at the Manitoba Centre for Proteomics and Systems Biology. Mass spectrometry is the optimal approach to assess steroid hormones as immunoassays have several limitations including standardisation and antibody sensitivity problems between labs.

Monitoring the mouse estrous cycle during chronic and acute LCMV infections through vaginal cytology will be useful to identify whether the stage of the estrous cycle influences the $CD8^+$ T cell responses observed in mice. The estrous cycle in mice is segregated into four main stages (proestrus, estrus, metestrus, and diestrus) which cycles every 4-5 days (126). Thus, vaginal cytology at the start of the experiment and at the designated humane end points, will allow monitoring the changes in the estrous cycle in the female mice. Importantly, correlating sex steroid levels with the differences observed in $CD8^+$ T cell responses in both sexes in mice may shed light on impact of sex steroids on $CD8^+$ T cell responses.

For early studies investigating early proliferation of responding $CD8^+$ T cells, there are plans to increase the number of adoptively transferred CFSE-labelled cells numbers from 1 ×

10^6 to 3×10^6 as described in (15). Increased transfer numbers will enable higher cell recovery during sorts for generation of single-cell cDNA libraries. So far, we have been unsuccessful in sorting enough cells for generation of cDNA libraries.

Early cellular interactions in the spleen during the activation phase can be further investigated using spatial transcriptomics. This approach requires *in situ* sequencing, which can map the spatial distribution of activated $CD8^+$ T cells in the spleen and their gene expression patterns. Immunohistochemistry can be applied to further explore APC-CD8 interactions during early phases, localization of female vs male $CD8^+$ T cells in the spleen and preferred sites of infection in female vs male spleen.

Overall, this study provides the foundation for several future mechanistic studies of how sex and early regulation of $CD8^+$ T cell responses influence the formation of diverse $CD8^+$ T cell fates and functions that are critical for protective immune responses to infection. Addressing the mentioned limitations will enhance our understanding of the underlying mechanisms driving sex-based differences in $CD8^+$ T cell responses and their implications for immunology and therapeutic interventions.

Appendix

9 References

1. Utzschneider DT, Gabriel SS. Early precursor T cells establish and propagate T cell exhaustion in chronic infection. [cited 2023 Feb 23]; Available from: https://doi.org/10.1038/s41590-020-0760-z

2. Abbas AK, Lichtman AH, Pillai S. BASIC IMMUNOLOGY Functions and Disorders of the Immune System FIFTH EDITION. ELSEVIER. 2014. 55–78 p.

3. Palmer E. Negative selection -- clearing out the bad apples from the T-cell repertoire. Nat Rev Immunol [Internet]. 2003 May 1 [cited 2023 Apr 13];3(5):383–92. Available from: https://go-gale-com.uml.idm.oclc.org/ps/i.do?p=HRCA&sw=w&issn=14741733&v=2.1&it=r&id=GALE%7CA188903120&sid=googleScholar&linkaccess=fulltext

4. Starr TK, Jameson SC, Hogquist KA. Positive and negative T cell selection. Annu Rev Immunol. 2003;21:139–76.

5. Capitani N, Baldari CT. The Immunological Synapse: An Emerging Target for Immune Evasion by Bacterial Pathogens. Front Immunol. 2022;13(July):1–11.

6. Raskov H, Orhan A, Christensen JP, Gögenur I. Cytotoxic CD8 + T cells in cancer and cancer immunotherapy. [cited 2023 Apr 13]; Available from: https://doi.org/10.1038/s41416-020-01048-4

7. D'Souza WN, Lefrançois L. IL-2 Is Not Required for the Initiation of CD8 T Cell Cycling but Sustains Expansion. J Immunol [Internet]. 2003 Dec 1 [cited 2023 Jun 5];171(11):5727–35. Available from: https://journals.aai.org/jimmunol/article/171/11/5727/35967/IL-2-Is-Not-Required-for-the-Initiation-of-CD8-T

8. Stemberger C, Huster KM, Koffler M, Anderl F, Schiemann M, Wagner H, et al. A Single Naive CD8+ T Cell Precursor Can Develop into Diverse Effector and Memory Subsets. Immunity [Internet]. 2007 Dec 21 [cited 2023 Mar 15];27(6):985–97. Available from: http://www.cell.com/article/S1074761307005407/fulltext

9. Gerlach C, Van Heijst JWJ, Swart E, Sie D, Armstrong N, Kerkhoven RM, et al. One naive T cell, multiple fates in CD8+ T cell differentiation. J Exp Med [Internet]. 2010 Jun 6 [cited 2023 Mar 15];207(6):1235. Available from: /pmc/articles/PMC2882844/

10. Kaech SM, Cui W. Transcriptional control of effector and memory CD8 + T cell differentiation. Nat Rev | Immunol [Internet]. 2012 [cited 2023 Jun 5];12:749. Available from: www.nature.com/reviews/immunol

11. Ahmed R, Gray D. Immunological Memory and Protective Immunity: Understanding Their Relation. New Ser. 1996;272(5258):54–60.

12. Buchholz VR, Flossdorf M, Hensel I, Kretschmer L, Weissbrich B, Gräf P, et al. Disparate Individual Fates Compose Robust $CD8^+$ T Cell Immunity. New Ser. 2013;340(6132):630–5.

13. Chang JT, Palanivel VR, Kinjyo I, Schambach F, Intlekofer AM, Banerjee A, et al. Asymmetric T Lymphocyte Division in the Initiation of Adaptive Immune Responses. New Ser. 2007;315(5819):1687–91.

14. Arsenio J, Kakaradov B, Metz PJ, Kim SH, Yeo GW, Chang JT. Early specification of CD8 + T lymphocyte fates during adaptive immunity revealed by single-cell gene expression analyses HHS Public Access. Nat Immunol [Internet]. 2014 [cited 2023 Feb 22];15(4):365–72. Available from: http://www.nature.com/authors/editorial_policies/license.html#terms

15. Quezada LK, Jin W, Liu YC, Kim ES, He Z, Indralingam CS, et al. Early transcriptional and epigenetic divergence of CD8+ T cells responding to acute versus chronic infection. PLOS Biol [Internet]. 2023 Jan [cited 2023 Mar 28];21(1):e3001983. Available from: https://journals.plos.org/plosbiology/article?id=10.1371/journal.pbio.3001983

16. Metz PJ, Lopez J, Kim SH, Akimoto K, Ohno S, Chang JT. Regulation of Asymmetric Division by Atypical Protein Kinase C Influences Early Specification of CD8 + T Lymphocyte Fates. Nat Publ Gr [Internet]. 2015 [cited 2023 Jun 6]; Available from: www.nature.com/scientificreports

17. Wherry EJ, Teichgräber V, Becker TC, Masopust D, Kaech SM, Antia R, et al. Lineage relationship and protective immunity of memory CD8 T cell subsets. Nat Immunol 2003 43 [Internet]. 2003 Feb 3 [cited 2022 Oct 19];4(3):225–34. Available from: https://www.nature.com/articles/ni889

18. Arsenio J. Single-cell analysis of CD8 T lymphocyte diversity during adaptive immunity. 2019; Available from: https://doi.org/10.1002/wsbm.1475

19. Chang JT, Wherry EJ, Goldrath AW. Molecular regulation of effector and memory T cell differentiation HHS Public Access. Nat Immunol [Internet]. 2014 [cited 2022 Oct 10];15(12):1104–15. Available from: http://www.nature.com/reprints/index.htmlhttp://www.nature.com/reprints/index.html

20. Ye LL, Wei XS, Zhang M, Niu YR, Zhou Q. The significance of tumor necrosis factor receptor type II in CD8+ regulatory T cells and CD8+ effector T cells. Front Immunol. 2018 Mar 22;8(MAR):583.

21. Bhat P, Leggatt G, Waterhouse N, Frazer IH. Interferon-γ derived from cytotoxic lymphocytes directly enhances their motility and cytotoxicity. Nat Publ Gr [Internet]. 2017 [cited 2023 Jun 6];8. Available from: www.nature.com/cddis

22. Böttcher J, Knolle PA. Global transcriptional characterization of CD8+ T cell memory. Semin Immunol. 2015 Feb 1;27(1):4–9.

23. Frebel H, Richter K, Oxenius A. How chronic viral infections impact on antigen-specific T-cell responses. Eur J Immunol [Internet]. 2010 Mar 1 [cited 2023 Mar 15];40(3):654–63. Available from: https://onlinelibrary.wiley.com/doi/full/10.1002/eji.200940102

24. Chen Y, Zander R, Khatun A, Schauder DM, Cui W. Transcriptional and Epigenetic Regulation of Effector and Memory CD8 T Cell Differentiation. Front Immunol. 2018 Dec 7;9:2826.

25. Trautmann L, Janbazian L, Chomont N, Said EA, Gimmig S, Bessette B, et al. Upregulation of PD-1 expression on HIV-specific CD8+ T cells leads to reversible immune dysfunction. Nat Med 2006 1210 [Internet]. 2006 Aug 20 [cited 2023 Mar 15];12(10):1198–202. Available from: https://www-nature-com.uml.idm.oclc.org/articles/nm1482

26. Moskophidis D, Lechner F, Pircher H, Zinkernagel RM. Virus persistence in acutely infected immunocompetent mice by exhaustion of antiviral cytotoxic effector T cells. Nat 1993 3626422 [Internet]. 1993 [cited 2023 Mar 15];362(6422):758–61. Available from: https://www-nature-com.uml.idm.oclc.org/articles/362758a0

27. Gallimore A, Glithero A, Godkin A, Tissot AC, Plückthun A, Elliott T, et al. Induction and Exhaustion of Lymphocytic Choriomeningitis Virus–specific Cytotoxic T Lymphocytes

Visualized Using Soluble Tetrameric Major Histocompatibility Complex Class I–Peptide Complexes. J Exp Med [Internet]. 1998 May 5 [cited 2023 Mar 15];187(9):1383. Available from: /pmc/articles/PMC2212278/

28. Zajac AJ, Blattman JN, Murali-Krishna K, Sourdive DJD, Suresh M, Altman JD, et al. Viral Immune Evasion Due to Persistence of Activated T Cells Without Effector Function. J Exp Med [Internet]. 1998 Dec 12 [cited 2023 Mar 15];188(12):2205. Available from: /pmc/articles/PMC2212420/

29. Wherry EJ, Ha SJ, Kaech SM, Haining WN, Sarkar S, Kalia V, et al. Molecular Signature of CD8+ T Cell Exhaustion during Chronic Viral Infection. Immunity. 2007 Oct 26;27(4):670–84.

30. Kahan SM, Zajac AJ. Immune Exhaustion: Past Lessons and New Insights from Lymphocytic Choriomeningitis Virus. Viruses 2019, Vol 11, Page 156 [Internet]. 2019 Feb 13 [cited 2023 Mar 15];11(2):156. Available from: https://www.mdpi.com/1999-4915/11/2/156/htm

31. Agnellini P, Wolint P, Rehr M, Cahenzli J, Karrer U, Oxenius A. Impaired NFAT nuclear translocation results in split exhaustion of virus-specific CD8+ T cell functions during chronic viral infection. Proc Natl Acad Sci U S A [Internet]. 2007 Mar 3 [cited 2023 Mar 15];104(11):4565. Available from: /pmc/articles/PMC1815473/

32. Mclane LM, Abdel-Hakeem MS, Wherry EJ. CD8 T Cell Exhaustion During Chronic Viral Infection and Cancer. 2019; Available from: https://doi.org/10.1146/annurev-immunol-041015-

33. Wherry EJ. T cell exhaustion. Nat Publ Gr. 2011;

34. Shin H, Wherry EJ. CD8 T cell dysfunction during chronic viral infection. Curr Opin Immunol. 2007 Aug 1;19(4):408–15.

35. Collier JL, Weiss SA, Pauken KE, Sen DR, Sharpe AH. Not-so-opposite ends of the spectrum: CD8+ T cell dysfunction across chronic infection, cancer and autoimmunity. Nat Immunol 2021 227 [Internet]. 2021 Jun 17 [cited 2023 Jun 6];22(7):809–19. Available from: https://www-nature-com.uml.idm.oclc.org/articles/s41590-021-00949-7

36. Barber DL, Wherry EJ, Masopust D, Zhu B, Allison JP, Sharpe AH, et al. Restoring function in exhausted CD8 T cells during chronic viral infection. Nat 2005 4397077 [Internet]. 2005 Dec 28 [cited 2023 Mar 15];439(7077):682–7. Available from: https://www-nature-com.uml.idm.oclc.org/articles/nature04444

37. Ye B, Liu X, Li X, Kong H, Tian L, Chen Y. T-cell exhaustion in chronic hepatitis B infection: current knowledge and clinical significance. Cell Death Dis [Internet]. 2015 [cited 2023 Jun 6];6(3):e1694. Available from: /pmc/articles/PMC4385920/

38. Fenwick C, Joo V, Jacquier P, Noto A, Banga R, Perreau M, et al. T-cell exhaustion in HIV infection. Immunol Rev [Internet]. 2019 Nov 1 [cited 2023 Jun 6];292(1):149. Available from: /pmc/articles/PMC7003858/

39. Day CL, Kaufmann DE, Kiepiela P, Brown JA, Moodley ES, Reddy S, et al. PD-1 expression on HIV-specific T cells is associated with T-cell exhaustion and disease progression. Nat 2006 4437109 [Internet]. 2006 Aug 20 [cited 2023 Mar 15];443(7109):350–4. Available from: https://www-nature-com.uml.idm.oclc.org/articles/nature05115

40. Petrovas C, Casazza JP, Brenchley JM, Price DA, Gostick E, Adams WC, et al. PD-1 is a regulator of virus-specific CD8+ T cell survival in HIV infection. J Exp Med [Internet]. 2006 Oct 10 [cited 2023 Mar 15];203(10):2281. Available from: /pmc/articles/PMC2118095/

41. Urbani S, Amadei B, Tola D, Massari M, Schivazappa S, Missale G, et al. PD-1 expression in acute hepatitis C virus (HCV) infection is associated with HCV-specific CD8 exhaustion. J Virol [Internet]. 2006 Nov [cited 2023 Mar 15];80(22):11398–403. Available from: https://pubmed.ncbi.nlm.nih.gov/16956940/

42. Radziewicz H, Ibegbu CC, Fernandez ML, Workowski KA, Obideen K, Wehbi M, et al. Liver-infiltrating lymphocytes in chronic human hepatitis C virus infection display an exhausted phenotype with high levels of PD-1 and low levels of CD127 expression. J Virol [Internet]. 2007 Mar 15 [cited 2023 Mar 15];81(6):2545–53. Available from: https://pubmed.ncbi.nlm.nih.gov/17182670/

43. Blackburn SD, Shin H, Freeman GJ, Wherry EJ. Selective expansion of a subset of exhausted CD8 T cells by αPD-L1 blockade. Proc Natl Acad Sci U S A [Internet]. 2008 Sep 30 [cited 2023 Mar 2];105(39):15016–21. Available from: www.pnas.org/cgi/content/full/

44. Zeyu Chen A, Ji Z, Foong Ngiow S, Vahedi G, Ji H, John Wherry Correspondence E. TCF-1-Centered Transcriptional Network Drives an Effector versus Exhausted CD8 T Cell-Fate Decision. Immunity [Internet]. 2019 [cited 2023 Mar 15];51:840–55. Available from: https://doi.org/10.1016/j.immuni.2019.09.013

45. Hudson WH, Gensheimer J, Hashimoto M, Wieland A, Valanparambil RM, Li P, et al. Proliferating Transitory T Cells with an Effector-like Transcriptional Signature Emerge from PD-1+ Stem-like CD8+ T Cells during Chronic Infection. Immunity [Internet]. 2019 Dec 17 [cited 2023 Mar 15];51(6):1043-1058.e4. Available from: http://www.cell.com/article/S1074761319304601/fulltext

46. Zander R, Schauder D, Xin G, Nguyen C, Wu X, Zajac A, et al. CD4+ T Cell Help Is Required for the Formation of a Cytolytic CD8+ T Cell Subset that Protects against Chronic Infection and Cancer. Immunity [Internet]. 2019 Dec 17 [cited 2023 Mar 15];51(6):1028-1042.e4. Available from: http://www.cell.com/article/S1074761319304534/fulltext

47. Giles JR, Ngiow SF, Manne S, Baxter AE, Khan O, Wang P, et al. Shared and distinct biological circuits in effector, memory and exhausted CD8+ T cells revealed by temporal single-cell transcriptomics and epigenetics. Nat Immunol 2022 2311 [Internet]. 2022 Oct 21 [cited 2023 Mar 15];23(11):1600–13. Available from: https://www-nature-com.uml.idm.oclc.org/articles/s41590-022-01338-4

48. Utzschneider DT, Charmoy M, Chennupati V, Pousse L, Ferreira DP, Calderon-Copete S, et al. T Cell Factor 1-Expressing Memory-like CD8+ T Cells Sustain the Immune Response to Chronic Viral Infections. Immunity. 2016;45(2):415–27.

49. Yao C, Sun HW, Lacey NE, Ji Y, Moseman EA, Shih HY, et al. Single-cell RNA-seq reveals TOX as a key regulator of CD8+ T cell persistence in chronic infection. Nat Immunol 2019 207 [Internet]. 2019 Jun 17 [cited 2023 Mar 29];20(7):890–901. Available from: https://www-nature-com.uml.idm.oclc.org/articles/s41590-019-0403-4

50. Alfei F, Kanev K, Hofmann M, Wu M, Ghoneim HE, Roelli P, et al. TOX reinforces the phenotype and longevity of exhausted T cells in chronic viral infection. Nat 2019 5717764 [Internet]. 2019 Jun 17 [cited 2023 Mar 15];571(7764):265–9. Available from: https://www-nature-com.uml.idm.oclc.org/articles/s41586-019-1326-9

51. Sandu I, Cerletti D, Oetiker N, Borsa M, Wagen F, Spadafora I, et al. Landscape of Exhausted Virus-Specific CD8 T Cells in Chronic LCMV Infection. Cell Rep [Internet]. 2020 Aug 25 [cited 2023 Mar 15];32(8). Available from: http://www.cell.com/article/S2211124720310639/fulltext

52. Klein SL, Flanagan KL. Sex differences in immune responses. 2016 [cited 2023 Mar 2]; Available from: www.nature.com/nri

53. Mauvais-Jarvis F, Merz NB, Barnes PJ, Brinton RD, Carrero J-J, Demeo DL, et al. Sex and gender: modifiers of health, disease, and medicine. www.thelancet.com [Internet]. 2020 [cited 2022 Oct 11];396:565. Available from: www.thelancet.com

54. Guerra-Silveira F, Abad-Franch F. Sex Bias in Infectious Disease Epidemiology: Patterns and Processes. PLoS One [Internet]. 2013 Apr 24 [cited 2023 Mar 15];8(4). Available from: /pmc/articles/PMC3634762/

55. Collazos J, Asensi V, Cartón JA. Sex differences in the clinical, immunological and virological parameters of HIV-infected patients treated with HAART. AIDS. 2007 Apr;21(7):835–43.

56. Grebely J, Page K, Sacks-Davis R, van der Loeff MS, Rice TM, Bruneau J, et al. The effects of female sex, viral genotype, and IL28B genotype on spontaneous clearance of acute hepatitis C virus infection. Hepatology [Internet]. 2014 Jan 1 [cited 2023 Mar 15];59(1):109–20. Available from: https://onlinelibrary-wiley-com.uml.idm.oclc.org/doi/full/10.1002/hep.26639

57. Klein SL, Hodgson A, Robinson DP. Mechanisms of sex disparities in influenza pathogenesis. J Leukoc Biol [Internet]. 2012 Jul 1 [cited 2023 Mar 15];92(1):67–73. Available from: https://onlinelibrary-wiley-com.uml.idm.oclc.org/doi/full/10.1189/jlb.0811427

58. vom Steeg LG, Klein SL. SeXX Matters in Infectious Disease Pathogenesis. PLoS Pathog. 2016;12(2):1–6.

59. Fischer J, Jung N, Robinson N, Lehmann C. Sex differences in immune responses to infectious diseases. Infection [Internet]. 2015 Aug 1 [cited 2023 Mar 15];43(4):399–403. Available from: https://link-springer-com.uml.idm.oclc.org/article/10.1007/s15010-015-0791-9

60. Ngo ST, Steyn FJ, McCombe PA. Gender differences in autoimmune disease. Front Neuroendocrinol. 2014;35(3):347–69.

61. Rudd BD, Joy K, Mon Y, Goldsmith E, Watson NB, Wang J, et al. T Cell Response to Infection + Differences in the CD8 Differential Sensitivity to IL-12 Drives Sex-Specific Downloaded from Differential Sensitivity to IL-12 Drives Sex-Specific Differences in the CD8 + T Cell Response to Infection. 2019 [cited 2022 Nov 25];3(4):121–32. Available from: http://www.immunohorizons.org/content/3/4/121https://doi.org/10.4049/

62. Fish EN. The X-files in immunity: sex-based differences predispose immune responses. Nat Rev Immunol 2008 89 [Internet]. 2008 Sep [cited 2023 Mar 16];8(9):737–44. Available from: https://www-nature-com.uml.idm.oclc.org/articles/nri2394

63. Hickman HD, Reynoso G V., Ngudiankama BF, Cush SS, Gibbs J, Bennink JR, et al. CXCR3 Chemokine Receptor Enables Local CD8+ T Cell Migration for the Destruction of Virus-Infected Cells. Immunity [Internet]. 2015 Mar 3 [cited 2023 Mar 16];42(3):524. Available from: /pmc/articles/PMC4365427/

64. Oghumu S, Varikuti S, Stock JC, Volpedo G, Saljoughian N, Terrazas CA, et al. Cutting Edge: CXCR3 Escapes X Chromosome Inactivation in T Cells during Infection: Potential Implications for Sex Differences in Immune Responses. J Immunol [Internet]. 2019 Aug 15 [cited 2023 Mar 16];203(4):789–94. Available from: https://journals.aai.org/jimmunol/article/203/4/789/109966/Cutting-Edge-CXCR3-Escapes-X-Chromosome

65. Pisitkun P, Deane JA, Difilippantonio MJ, Tarasenko T, Satterthwaite AB, Bolland S. Autoreactive B cell responses to RNA-related antigens due to TLR7 gene duplication. Science

(80-) [Internet]. 2006 Jun 16 [cited 2023 Mar 16];312(5780):1669–72. Available from: https://www-science-org.uml.idm.oclc.org/doi/10.1126/science.1124978

66. Hussain T, Kallies A, Vasanthakumar A. Sex-bias in CD8+ T-cell stemness and exhaustion in cancer. Clin Transl Immunol [Internet]. 2022 [cited 2022 Nov 25];11(8). Available from: /pmc/articles/PMC9418121/

67. Schafer JM, Xiao T, Kwon H, Collier K, Chang Y, Abdel-Hafiz H, et al. Sex-biased adaptive immune regulation in cancer development and therapy. iScience. 2022 Aug 19;25(8).

68. Related Content Estradiol Is Required for a Proper Immune Response to Bacterial and Viral Pathogens in the Female Brain The Role of Estrogen Receptors and Androgen Receptors in Sex Steroid Regulation of B Lymphopoiesis Estradiol Inhibits Th17 Cell Differentiation through Inhibition of RORγT Transcription by Recruiting the ERα/REA Complex to Estrogen Response Elements of the RORγT Promoter. 1999;

69. Navarro FC, Watkins SK. Estrogen Stimulation Differentially Impacts Human Male and Female Antigen-Specific T Cell Anti-Tumor Function and Polyfunctionality. https://www.liebertpub.com/loi/gg [Internet]. 2017 Dec 1 [cited 2023 Mar 27];1(4):1–13. Available from: https://www.liebertpub.com/doi/10.1089/gg.2017.0014

70. Shen Z, Rodriguez-Garcia M, Patel M V, Wira CR. Direct and Indirect endocrine-mediated suppression of human endometrial CD8+T cell cytotoxicity. Sci Reports | [Internet]. 123AD [cited 2023 Jun 8];11:1773. Available from: https://doi.org/10.1038/s41598-021-81380-8

71. Gunderson AJ, Yamazaki T, Mccarty K, Fox N, Phillips M, Alice A, et al. TGFβ suppresses CD8 + T cell expression of CXCR3 and tumor trafficking. [cited 2023 Jun 8]; Available from: https://doi.org/10.1038/s41467-020-15404-8

72. Kwon H, Schafer JM, Song NJ, Kaneko S, Li A, Xiao T, et al. Androgen conspires with the CD8+ T cell exhaustion program and contributes to sex bias in cancer. Sci Immunol [Internet]. 2022 Jul 1 [cited 2023 Mar 27];7(73):2630. Available from: https://www.science.org

73. Welsh RM, Seedhom MO. LCMV: Propagation, quantitation, and storage. Curr Protoc Microbiol [Internet]. 2008 [cited 2022 Nov 25];CHAPTER(SUPPL. 8):Unit. Available from: /pmc/articles/PMC3220596/

74. Lee KJ, Novella IS, Teng MN, Oldstone MBA, De JC, Torre LA. NP and L Proteins of Lymphocytic Choriomeningitis Virus (LCMV) Are Sufficient for Efficient Transcription and Replication of LCMV Genomic RNA Analogs. J Virol [Internet]. 2000 Apr 15 [cited 2022 Oct 16];74(8):3470–7. Available from: https://journals.asm.org/journal/jvi

75. Buchmeier' And MJ, Oldstone MBA. Protein Structure of Lymphocytic Choriomeningitis Virus: Evidence for a Cell-Associated Precursor of the Virion Glycopeptides. Virology. 99:111–20.

76. Bocharov G, Argilaguet J, Meyerhans A. Understanding Experimental LCMV Infection of Mice: The Role of Mathematical Models. J Immunol Res. 2015;2015.

77. Oldstone MBA, Ware BC, Horton LE, Welch MJ, Aiolfi R, Zarpellon A, et al. Lymphocytic choriomeningitis virus Clone 13 infection causes either persistence or acute death dependent on IFN-1, cytotoxic T lymphocytes (CTLs), and host genetics. Proc Natl Acad Sci U S A [Internet]. 2018 Aug 14 [cited 2023 Apr 15];115(33):E7814–23. Available from: https://www.pnas.org/doi/abs/10.1073/pnas.1804674115

78. Zhou X, Ramachandran S, Mann M, Popkin DL. Role of Lymphocytic Choriomeningitis Virus (LCMV) in Understanding Viral Immunology: Past, Present and Future. Viruses [Internet]. 2012;4:2650–69. Available from: www.mdpi.com/journal/viruses

79. Salvato M, Borrow P, Shimomaye E, Oldstone MBA. Molecular basis of viral persistence: a single amino acid change in the glycoprotein of lymphocytic choriomeningitis virus is associated with suppression of the antiviral cytotoxic T-lymphocyte response and establishment of persistence. J Virol [Internet]. 1991 Apr [cited 2023 Mar 28];65(4):1863–9. Available from: https://journals.asm.org/journal/jvi

80. Salvato M, Shimomaye E, Southern P, Oldstone MBA. Virus-lymphocyte interactions IV. Molecular characterization of LCMV Armstrong (CTL+) small genomic segment and that of its variant, clone 13 (CTL−). Virology. 1988 Jun 1;164(2):517–22.

81. Cao W, Henry MD, Borrow P, Yamada H, Elder JH, Ravkov E V., et al. Identification of α-dystroglycan as a receptor for lymphocytic choriomeningitis virus and Lassa fever virus. Science (80-) [Internet]. 1998 Dec 11 [cited 2023 Mar 27];282(5396):2079–81. Available from: https://www-science-org.uml.idm.oclc.org/doi/10.1126/science.282.5396.2079

82. Van Den Berg TK, Van Der Ende M, D6pp EA, Kraal G, Dijkstra CD. Localization of (31 Integrins and Their Extracellular Ligands in Human Lymphoid Tissues. Am Journtal Pathol. 1993;143(4).

83. Author A-D, Kunz S, Sevilla N, Mcgavern DB, Campbell KP, Oldstone MBA. Molecular Analysis of the Interaction of LCMV with Its Cellular Receptor. Source J Cell Biol [Internet]. 2001 [cited 2023 Mar 28];155(2):301–10. Available from: http://www.jcb.org/cgi/doi/10.1083/jcb.200104103

84. Sevilla N, Kunz S, Mcgavern D, Oldstone MBA. Infection of Dendritic Cells by Lymphocytic Choriomeningitis Virus.

85. Smelt SC, Borrow P, Kunz S, Cao W, Tishon A, Lewicki H, et al. Differences in Affinity of Binding of Lymphocytic Choriomeningitis Virus Strains to the Cellular Receptor α-Dystroglycan Correlate with Viral Tropism and Disease Kinetics. J Virol [Internet]. 2001 Jan [cited 2023 Mar 28];75(1):448. Available from: /pmc/articles/PMC113937/

86. Bergthaler A, Flatz L, Hegazy AN, Johnson S, Horvath E, Löhning M, et al. Viral replicative capacity is the primary determinant of lymphocytic choriomeningitis virus persistence and immunosuppression. Proc Natl Acad Sci U S A [Internet]. 2010 Dec 14 [cited 2023 Mar 28];107(50):21641–6. Available from: www.pnas.org/cgi/doi/10.1073/pnas.1011998107

87. Sevilla N, Kunz S, Holz A, Lewicki H, Homann D, Yamada H, et al. Immunosuppression and Resultant Viral Persistence by Specific Viral Targeting of Dendritic Cells. J Exp Med © [Internet]. 2000 [cited 2023 Mar 28];192(9). Available from: http://www.jem.org/cgi/content/full/192/9/1249

88. Steinman RM, Pack M, Inaba K, Stcimnan RM, Maggie *, Kapfnoba' P'. Dendritic cells in the T-cell areas of lymphoid organs Authors' addresses. Immunol Rev [Internet]. 1997 [cited 2023 Mar 28];156:25–37. Available from: https://onlinelibrary.wiley.com/doi/10.1111/j.1600-065X.1997.tb00956.x

89. Mueller SN, Matloubian M, Clemens DM, Sharpe AH, Freeman GJ, Gangappa S, et al. Viral targeting of fibroblastic reticular cells contributes to immunosuppression and persistence during chronic infection. Proc Natl Acad Sci U S A [Internet]. 2007 Sep 25 [cited 2023 Mar 28];104(39):15430–5. Available from: www.pnas.org/cgi/content/full/

90. Bajénoff M, Egen JG, Koo LY, Laugier JP, Brau F, Glaichenhaus N, et al. Stromal Cell Networks Regulate Lymphocyte Entry, Migration, and Territoriality in Lymph Nodes. Immunity [Internet]. 2006 Dec 1 [cited 2023 Mar 28];25(6):989–1001. Available from: http://www.cell.com/article/S1074761306004833/fulltext

91. Kakaradov B, Arsenio J, Widjaja CE, He Z, Aigner S, Metz PJ, et al. Early transcriptional and epigenetic regulation of CD8 + T cell differentiation revealed by single-cell RNA-seq. [cited 2023 Mar 2]; Available from: http://www.nature.com/authors/editorial_policies/license.html#terms

92. Zhao M, Kiernan CH, Stairiker CJ, Hope JL, Leon LG, van Meurs M, et al. Rapid in vitro generation of bona fide exhausted CD8+ T cells is accompanied by Tcf7 promotor methylation. PLoS Pathog [Internet]. 2020 Jun 1 [cited 2023 Jun 21];16(6). Available from: /pmc/articles/PMC7340326/

93. Beltra J-C, Bourbonnais S, Bédard N, Charpentier T, Boulangé M, Michaud E, et al. IL2Rβ-dependent signals drive terminal exhaustion and suppress memory development during chronic viral infection. [cited 2023 May 10]; Available from: www.pnas.org/cgi/doi/10.1073/pnas.1604256113

94. Chang JT, Palanivel VR, Kinjyo I, Schambach F, Intlekofer AM, Banerjee A, et al. Asymmetric T lymphocyte division in the initiation of adaptive immune responses. Science (80-) [Internet]. 2007 Mar 23 [cited 2022 Nov 14];315(5819):1687–91. Available from: https://www-science-org.uml.idm.oclc.org/doi/10.1126/science.1139393

95. Welsh RM. Cytotoxic cells induced during lymphocytic choriomeningitis virus infection of mice. I. Characterization of natural killer cell induction. J Exp Med [Internet]. 1978 Jul 1 [cited 2023 Mar 28];148(1):163–81. Available from: http://rupress.org/jem/article-pdf/148/1/163/1089302/163.pdf

96. Kaech SM, Cui W. Transcriptional control of effector and memory CD8 + T cell differentiation. Nat Publ Gr [Internet]. 2012 [cited 2023 Mar 15];12:749. Available from: www.nature.com/reviews/immunol

97. McLane LM, Abdel-Hakeem MS, Wherry EJ. CD8 T Cell Exhaustion During Chronic Viral Infection and Cancer. Annu Rev Immunol [Internet]. 2019 Apr 26 [cited 2022 Oct 25];37:457–95. Available from: https://pubmed.ncbi.nlm.nih.gov/30676822/

98. Terr I, Orrantia A, Vitall J, Zenarruzabeitia O, Borrego F. CFSE dilution to study human T and NK cell proliferation in vitro. [cited 2023 Feb 22]; Available from: https://doi.org/10.1016/bs.mie.2019.05.020

99. Nath PR, Pal-Nath D, Kaur S, Gangaplara A, Meyer TJ, Cam MC, et al. Loss of CD47 alters CD8+ T cell activation in vitro and immunodynamics in mice. Oncoimmunology [Internet]. 2022 [cited 2023 Mar 28];11(1). Available from: /pmc/articles/PMC9467551/

100. Rodrigues LS, Barreto AS, Bomfim LGS, Gomes MC, Ferreira NLC, da Cruz GS, et al. Multifunctional, TNF-α and IFN-γ-Secreting CD4 and CD8 T Cells and CD8High T Cells Are Associated With the Cure of Human Visceral Leishmaniasis. Front Immunol. 2021 Oct 28;12:4433.

101. Abdel-Hakeem MS, Manne S, Beltra JC, Stelekati E, Chen Z, Nzingha K, et al. Epigenetic scarring of exhausted T cells hinders memory differentiation upon eliminating chronic antigenic stimulation. Nat Immunol [Internet]. 2021 Aug 1 [cited 2023 Mar 29];22(8):1008–20. Available from: https://go-gale-com.uml.idm.oclc.org/ps/i.do?p=HRCA&sw=w&issn=15292908&v=2.1&it=r&id=GALE%7CA669695616&sid=googleScholar&linkaccess=fulltext

102. Tsui C, Kretschmer L, Rapelius S, Gabriel SS, Chisanga D, Knöpper K, et al. MYB orchestrates T cell exhaustion and response to checkpoint inhibition. Nat 2022 6097926 [Internet]. 2022 Aug 17 [cited 2023 Mar 29];609(7926):354–60. Available from: https://www-nature-

com.uml.idm.oclc.org/articles/s41586-022-05105-1

103. Cornish GH, Sinclair L V, Cantrell DA. Differential regulation of T-cell growth by IL-2 and IL-15. 2006;

104. Kuchroo VK, Anderson AC, Petrovas C. Coinhibitory receptors and CD8 T cell exhaustion in chronic infections. Curr Opin HIV AIDS. 2014;9(5):439–45.

105. MacAl M, Lewis GM, Kunz S, Flavell R, Harker JA, Zúñiga EI. Plasmacytoid dendritic cells are productively infected and activated through TLR-7 early after arenavirus infection. Cell Host Microbe [Internet]. 2012 Jun 14 [cited 2023 Mar 29];11(6):617–30. Available from: http://www.cell.com/article/S1931312812001643/fulltext

106. Teijaro JR, Ng C, Lee AM, Sullivan BM, Sheehan KCF, Welch M, et al. Persistent LCMV infection is controlled by blockade of type I interferon signaling. Science (80-) [Internet]. 2013 Apr 12 [cited 2023 Mar 29];340(6129):207–11. Available from: https://www-science-org.uml.idm.oclc.org/doi/10.1126/science.1235214

107. Borrow P, Evans CF, Oldstone MB. Virus-induced immunosuppression: immune system-mediated destruction of virus-infected dendritic cells results in generalized immune suppression. J Virol [Internet]. 1995 Feb [cited 2023 Mar 29];69(2):1059. Available from: /pmc/articles/PMC188677/?report=abstract

108. Baldacci Amici P Bonola E Betto G Fogliani E Refatti EA, Fooolt A, Agraria Milano J. Gene Action in the X-chromosome of the Mouse (Mus musculus L.). Nat 1961 1904773 [Internet]. 1961 [cited 2023 Mar 29];190(4773):372–3. Available from: https://www-nature-com.uml.idm.oclc.org/articles/190372a0

109. Berletch JB, Yang F, Xu J, Carrel L, Disteche CM. Genes that escape from X inactivation. Hum Genet [Internet]. 2011 Aug 1 [cited 2023 Mar 29];130(2):237–46. Available from: https://go-gale-com.uml.idm.oclc.org/ps/i.do?p=HRCA&sw=w&issn=03406717&v=2.1&it=r&id=GALE%7CA364958255&sid=googleScholar&linkaccess=fulltext

110. Berletch JB, Ma W, Yang F, Shendure J, Noble WS, Disteche CM, et al. Escape from X inactivation varies in mouse tissues. PLoS Genet [Internet]. 2015 Mar 1 [cited 2023 Mar 29];11(3). Available from: https://go-gale-com.uml.idm.oclc.org/ps/i.do?p=HRCA&sw=w&issn=15537390&v=2.1&it=r&id=GALE%7CA418465206&sid=googleScholar&linkaccess=fulltext

111. Carrel L, Willard HF. Heterogeneous gene expression from the inactive X chromosome: An X-linked gene that escapes X inactivation in some human cell lines but is inactivated in others. Proc Natl Acad Sci [Internet]. 1999 Jun 22 [cited 2023 Mar 29];96(13):7364–9. Available from: https://www-pnas-org.uml.idm.oclc.org/doi/abs/10.1073/pnas.96.13.7364

112. Bennett-Baker PE, Wilkowski J, Burke DT. Age-Associated Activation of Epigenetically Repressed Genes in the Mouse. [cited 2023 Mar 29]; Available from: https://academic.oup.com/genetics/article/165/4/2055/6050503

113. Loetscher M, Loetscher P, Brass N, Meese E, Moser B. Lymphocyte-specific chemokine receptor CXCR3: regulation, chemokine binding and gene localization. [cited 2023 Mar 16]; Available from: https://onlinelibrary.wiley.com/doi/10.1002/

114. Barbi J, Oghumu S, Lezama-Davila CM, Satoskar AR. IFN-γ and STAT1 are required for efficient induction of CXC chemokine receptor 3 (CXCR3) on CD4+ but not CD8+ T cells. Blood [Internet]. 2007 Sep 15 [cited 2023 Mar 16];110(6):2215–6. Available from:

https://ashpublications-org.uml.idm.oclc.org/blood/article/110/6/2215/24181/IFN-and-STAT1-are-required-for-efficient-induction

115. Hewagama A, Gorelik G, Patel D, Liyanarachchi P, Joseph McCune W, Somers E, et al. Overexpression of X-Linked genes in T cells from women with lupus. J Autoimmun. 2013 Mar 1;41:60–71.

116. Heil F, Hemmi H, Hochrein H, Ampenberger F, Kirschning C, Akira S, et al. Species-Specific Recognition of Single-Stranded RNA via Toll-like Receptor 7 and 8. New Ser. 2004;303(5663):1526–9.

117. Beignon A-S, Mckenna K, Skoberne M, Manches O, Dasilva I, Kavanagh DG, et al. Endocytosis of HIV-1 activates plasmacytoid dendritic cells via Toll-like receptor-viral RNA interactions. J Clin Invest [Internet]. 2005 [cited 2023 Mar 29];115. Available from: http://www.jci.org

118. Berghöfer B, Frommer T, Haley G, Fink L, Bein G, Hackstein H. TLR7 Ligands Induce Higher IFN-α Production in Females. J Immunol. 2006;177(4):2088–96.

119. Meier A, Chang JJ, Chan ES, Pollard RB, Sidhu HK, Kulkarni S, et al. Sex differences in the Toll-like receptor-mediated response of plasmacytoid dendritic cells to HIV-1. Nat Med [Internet]. 2009 Aug 1 [cited 2023 Feb 25];15(8):955–61. Available from: https://go-gale-com.uml.idm.oclc.org/ps/i.do?p=HRCA&sw=w&issn=10788956&v=2.1&it=r&id=GALE%7CA206465151&sid=googleScholar&linkaccess=fulltext

120. Sodora DL, Gettie A, Miller CJ, Marx PA. Vaginal transmission of SIV: Assessing infectivity and hormonal influences in macaques inoculated with cell-free and cell-associated viral stocks. AIDS Res Hum Retroviruses. 1998;14(SUPPL. 1).

121. Smith SM, Mefford M, Sodora D, Klase Z, Singh M, Alexander N, et al. Topical estrogen protects against SIV vaginal transmission without evidence of systemic effect. AIDS [Internet]. 2004 Aug 20 [cited 2023 Mar 29];18(12):1637–43. Available from: https://journals.lww.com/aidsonline/Fulltext/2004/08200/Topical_estrogen_protects_against_SIV_vaginal.4.aspx

122. Guan X, Polesso F, Wang C, Sehrawat A, Hawkins RM, Murray SE, et al. Androgen receptor activity in T cells limits checkpoint blockade efficacy. Nat 2022 6067915 [Internet]. 2022 Mar 23 [cited 2023 Mar 31];606(7915):791–6. Available from: https://www-nature-com.uml.idm.oclc.org/articles/s41586-022-04522-6

123. Mohammad I, Starskaia I, Nagy T, Guo J, Yatkin E, Väänänen K, et al. Estrogen receptor contributes to T cell–mediated autoimmune inflammation by promoting T cell activation and proliferation. Sci Signal [Internet]. 2018 Apr 17 [cited 2023 Mar 26];11(526):9415. Available from: https://www.science.org

124. Kovats S, McClelland EE, Huber SA, Fijak M, Schwinge dschwinge D, Christoph Schramm ukede, et al. The Effects of Androgens on T Cells: Clues to Female Predominance in Autoimmune Liver Diseases? Front Immunol | www.frontiersin.org [Internet]. 2020 [cited 2023 Mar 27];1:1567. Available from: www.frontiersin.org

125. Fuentes N, Cabello N, Nicoleau M, Chroneos ZC, Silveyra P. Modulation of the lung inflammatory response to ozone by the estrous cycle. Physiol Rep. 2019 Mar 1;7(5).

126. Ajayi AF, Akhigbe RE. Staging of the estrous cycle and induction of estrus in experimental rodents: an update. Fertil Res Pract. 2020;6(1):1–15.